

The analysis of natural gemstones and their synthetic counterparts using analytical spectroscopy methods

Raabell Shah

A thesis submitted in partial fulfilment of the requirements of
Edinburgh Napier University, for the award of Master of
Science by Research.

May 2012

Declaration

It is hereby declared that this thesis and the research work upon which it is based were conducted by the author, Raabell Shah

Raabell Shah

CONTENTS

Acknowledgements	3
Preface	3
<u>List of Abbreviations</u>	3
<u>List of Tables</u>	3
<u>List of Figures</u>	3
Abstract	3
TABLE OF CONTENTS	3
<u>Appendix A</u>	138
<u>Appendix B</u>	140
<u>Appendix C</u>	144
<u>Appendix D</u>	3

Acknowledgements

It would not have been possible to write this thesis without the help and support of the kind people around me, to only some of whom it is possible to give particular mention here. Firstly, I would like to thank my principal supervisor Mrs Nicole Payton for her personal support, input and great patience at all stages throughout this project. The good advice, support and guidance of my second supervisor, Dr. Kevin Smith, has been invaluable on both an academic and a personal level, for which I am extremely grateful. I would like to thank Dr Brian Jackson of the National Museum of Scotland for providing me with the necessary gemstones and materials to conduct this research to its full potential; not to mention his advice and unsurpassed knowledge of gemology. I am also thankful to Dr Susanna Kirk for her time, generosity and help. A sincere thank you to all my fellow postgraduate students in The Office and friends elsewhere for their support and encouragement, especially to Lauren O'Connor for her invaluable discussions and contributions. Above all, I would like to thank my family who have given me their constant and unconditional support throughout, as always, for which my mere expression of thanks likewise does not suffice.

unreserved

Preface

The need for continued research into Forensic Gemology is considerable, especially considering the paucity of substantial academic works on the subject. There remain a vast number of areas of uncertainty that warrant further detailed study. This thesis seeks to address only a limited range of the most important of these issues and is therefore focussed upon principal studies of selected natural and synthetic major commercial gemstones. The reason that this thesis deals only with these areas is one of space: in the opinion of the present author, it would not have been desirable within the confines of this MSc research thesis, in addition to the work that has been undertaken, to address in sufficient depth all of the major unresolved issues concerning proper identification of this particular group of gemstones. Instead, the focus has been to deliver a comprehensive study of the problems under discussion, and it is hoped that this in return provides a level of unity to the work as a whole and that this study will represent a major step forward in understanding the nature and chemistry of natural gemstones and their synthetic counterparts.

List of Abbreviations

Al ₂ O ₃	Aluminium Oxide
Be	Beryllium
Be ₃ Al ₂ (SiO ₃) ₆	Beryllium Aluminium Silicate
C-axis	Crystallographic axis
Ca ₂ Al ₃ (SiO ₄)	Tsavorite
Ca ₃ Fe ₂ (SiO ₄) ₃	Andradite
CCD	Charged Coupled Device
CO ₂	Carbon Dioxide
cps	Counts Per Second
Cr	Chromium
Cr ₂ O ₃	Chromium Oxide
Fe	Iron
FeO	Iron Oxide
FTC	Federal Trade Commission
H ₂ O	Water
IGA	International Coloured Gemstone Association
IR	Infra-red
MgO	Magnesium Oxide
Na ₂ O	Sodium Oxide
OH ⁻	Hydroxide
Ti	Titanium
SEM/EDX	Scanning Electron Microscopy/Energy Dispersive X-Ray spectroscopy

Si	Silicon
SiO ₂	Silicon Dioxide
SITC	Standard International Trade Classification
SNR	Signal to Noise Ratio
SOP	Standard Operating Procedure
UN	United Nations
USGS	United States Geological Survey
V	Vanadium
V ₂ O ₃	Vanadium Oxide

List of Tables

Table 1.1: Differentiation between alpha (α) and gamma (γ) aluminium oxide	7
Table 1.2: Liquid crystal growth methods and properties	17
Table 1.3: Laboratory Created Gemstone Production Methods and Dates (adapted from Olson, 2001)	18
Table 3.1: A list of all the types of gemstones for analysis	48
Table 3.2: stones for SEM/EDX analysis	49
Table 3.3: specifications comparison of the DXR and TruScan Raman spectrometers	55
Table 3.4: specifications for sampling measures	57
Table 4.1: Data of each sample spot, taken from three separate areas of each ruby table facet	79
Table 4.2: Overall averages of SEM/EDX analysis results of the 2.98ct Burma, Afghanistan, and 4.63ct and 1.76ct Verneuil rubies respectively	80
Table 4.3: “schist-type”, “non-schist-type”, and synthetic origin determination of emeralds	97
Table 4.4: Data of each sample spot, taken from three separate areas of each emerald table facet	102
Table 4.5: Overall averages of SEM/EDX analysis results of 0.58ct Russia, 0.69ct Pakistan, 1.04ct Russian flux and 0.92ct Biron hydrothermal emeralds	103

List of Figures

- Figure 1.1:** Raman spectra between the 3500cm⁻¹ to 3700cm⁻¹ region depicting water peaks in natural and synthetic emeralds, respectively (Shelementiev and Serov, 2011) 11
- Figure 1.2:** (a) flux-grown emerald and (b) hydrothermally-grown emerald showing typical inclusions and properties of these types of stones (Shelementiev and Serov, 2011) 12
- Figure 1.3:** Diagram of the flame fusion apparatus (Read, 2005) 21
- Figure 1.4:** (a) a verneuil boule shown whole with a crack running down the middle, and (b) shown parted into two pieces 22
- Figure 1.5:** Diagram of the crystal pulling apparatus (Read, 2005) 23
- Figure 1.6:** Diagram of the hydrothermal process (www.alexandrite.net) 24
- Figure 1.7:** Diagram of the flux method (Read, 2005) 26
- Figure 1.8:** Diagram of the zone melting process. Zone refining method used by Kyocera (left). Floating zone method used by Seiko (right) (Read, 2005) 28
- Figure 2.1:** Retrieved from University of Cambridge (2007), a quantum diagram of Rayleigh and Raman light scattering depicts the basic processes which occur for one vibration 32
- Figure 2.2:** TruScan™ logic tree illustrating system logic of the DecisionEngine™ software for material identity verification (Ahura TruScan™ Manual, 2010) 39
- Figure 2.3:** diagram of the main components of a scanning electron microscope: electron column, scanning system, detector(s), display, vacuum system and electronics controls, all depicting a typical sample analysis process (Thomas and Steven, 2009) 43
- Figure 2.4:** schematic representation of an energy-dispersive spectrometer (Goldstein *et al.* 1981) 45
- Figure 2.5:** simplified SEM/EDX schematic of the overall analysis process (www2.rgu.ac.uk) 46

Figure 3.1: Pictures of the Raman instrument. (a) the overall view of the Raman spectroscopy. (b) with the doors open, a view of the microscope and sample stage	50
Figure 3.2: gemstone mounted on a glass slide with “Blu-Tack” both upright (a) and sideways (b) at a 90° angle	51
Figure 3.3: Front and back views of the Ahura TruScan™ unit depicting the controls and accessories (ahurascientific.com)	52
Figure 3.4: Battery compartment area; also the access area for the memory card (CF Slot) (ahurascientific.com)	53
Figure 3.5: Diagram depicting the TruScan with attached nose cone performing Raman analysis on the gemstone; the red dot being the laser beam hitting the surface (adapted from ahurascientific.com)	53
Figure 3.6: nose and nose cone configurations, showing the measurement of the laser focal point with and without the nose cone attached	54
Figure 3.7: stone attached to the barrel-shaped nose cone for analysis using Sellotape	54
Figure 3.8: size comparison of DXR bench top Raman spectrometer and TruScan handheld Raman spectrometer	55
Figure 4.1a: Afghanistan ruby spectrum	59
Figure 4.1b: Afghanistan ruby	59
Figure 4.2a: 2.98ct Burma (Myanmar) ruby spectrum	60
Figure 4.2b: 2.98ct Burma (Myanmar) ruby with visible calcite inclusions	60
Figure 4.3a: 2.95ct Sri Lanka sapphire spectrum	61
Figure 4.3b: 2.95ct Sri Lanka sapphire	61
Figure 4.4a: group spectrum of Chatham synthetic stones analysed from the top	62
Figure 4.4b: group spectrum of Chatham synthetic stones analysed from the side	63

Figure 4.4c: Close up of a 3.54ct Chatham ruby and 2.58ct sapphire respectively, depicting their distinguishing peaks	63
Figure 4.5a: 1.24ct synthetic flux Kashan ruby spectrum	64
Figure 4.5b: 1.24ct synthetic flux Kashan ruby	64
Figure 4.5c: 1.52ct synthetic Kashan ruby spectrum	65
Figure 4.5d: 1.52ct synthetic Kashan ruby	65
Figure 4.6a: 1.00ct synthetic Knischka flux ruby spectrum	66
Figure 4.6b: 1.00ct synthetic Knischka flux ruby	66
Figure 4.7a: 5.50ct synthetic hydrothermal Lechleitner Ruby	67
Figure 4.7b: 8.70ct synthetic hydrothermal Lechleitner sapphire	67
Figure 4.8a: group spectrum of a ruby and sapphire Czochralski pulled gemstone respectively	68
Figures 4.8b and 4.8c: (b) 0.79ct Czochralski pulled synthetic ruby and (c) 1.87ct Czochralski pulled synthetic sapphire	68
Figure 4.9: synthetic Seiko floating zone ruby	69
Figure 4.10a: 9.57ct blue synthetic Kyocera zone crystal sapphire spectrum	69
Figure 4.10b: 9.57ct blue synthetic Kyocera zone crystal sapphire	70
Figure 4.11a: 24.75ct synthetic Verneuil ruby spectrum	70
Figure 4.11b: 24.75ct synthetic Verneuil ruby	71
Figure 4.12a: 11.54ct pink synthetic Verneuil sapphire spectrum	71
Figure 4.12b: 11.54ct pink synthetic Verneuil sapphire	71
Figure 4.13a: group spectrum of a 2.95ct light blue natural Sri Lankan sapphire and an 11.54ct pink synthetic Verneuil sapphire	72
Figure 4.13b: 2.95ct Blue Sri Lanka sapphire	72
Figure 4.14a: clear surface spectrum of 2.58ct pink red zone refined Inamori	

Kyocera star ruby	73
Figures 4.14b and 4.14c: 2.58ct pink red zone refined Inamori Kyocera star ruby cabochon and a piece from the original boule showing the frosted (b) and clear (c) surfaces from two different angles	73
Figure 4.15a: clear surface spectrum of 4.36ct blue hydrothermal part crystal Sapphire	74
Figures 4.15b and 4.15c: 4.36ct blue hydrothermal part crystal sapphire with both a smooth (b) and frosted (c) surface	74
Figure 4.16: DXR Raman comparison between frosted surfaces of a blue 4.36ct hydrothermal part crystal sapphire (above) and a pink red 2.58ct zone refined Inamori Kyocera star ruby (below)	75
Figure 4.17: spectrum of 0.79ct pulled Czochralski ruby	76
Figure 4.18: 0.68ct Red Hydrothermal Synthetic Ruby comparison spectrum	76
Figure 4.19: 1.00ct Red Ruby Knischka Flux comparison spectrum	77
Figure 4.20: 2.58ct Pink Red Star Ruby Zone Refined Inamori Kyocera comparison spectrum	77
Figure 4.21: 1.24ct Red Kashan Flux Ruby comparison spectrum	78
Figure 4.22a: Graph depicting the average difference in concentration of Cr_2O_3 and Fe_2O_3 in natural and synthetic rubies	80
Figure 4.22b: from left to right- 2.98ct Burma, Afghanistan, 4.36ct Verneuil and 1.76ct Verneuil rubies	80
Figure 4.23a: 0.58ct Russia Emerald spectrum	83
Figure 4.23b: 0.58ct Russia emerald	83
Figure 4.24a: 0.27ct Muzo, Colombia emerald spectrum	83
Figure 4.24b: 0.27ct Muzo, Colombia emerald with visible solid inclusions	84
Figure 4.25a: 0.76ct Columbia Emerald spectrum	84

Figure 4.25b: 0.76ct light green Columbia emerald	84
Figure 4.26a: 0.69ct Green Swat, Pakistan Emerald spectrum	85
Figure 4.26b: 0.69ct light green Swat, Pakistan emerald	85
Figure 4.27a: spectrum of a green stone labelled as 0.25ct Pakistan Emerald	86
Figure 4.27b: dark green stone labelled as a 0.25ct Pakistan Emerald	86
Figure 4.27c: comparison of a 0.25ct green stone labelled as Pakistan emerald (above) and a green grossular garnet (below)	87
Figure 4.28: 0.23ct Mellit, Germany two piece emerald set with rough and polished surfaces	88
Figure 4.29a: 0.5ct Chatham synthetic flux emerald spectrum	89
Figure 4.29b: broad twin peak situated in the 1500-1800cm ⁻¹ region in the 0.5ct Chatham synthetic flux emerald	90
Figure 4.29c: 0.5ct Chatham synthetic flux emerald, visibly clear with a glassy Appearance	90
Figure 4.30a: 0.36ct Russian Synthetic Flux Emerald spectrum	91
Figure 4.30b: broad twin peak situated in 1500-1800cm ⁻¹ region in a 0.36ct Russian synthetic flux emerald	91
Figure 4.30c: 0.36ct Russian Synthetic Flux Emerald, a visibly clear stone with a glassy appearance	92
Figure 4.31a: 0.92ct Biron synthetic emerald	93
Figure 4.31b: 0.92ct Biron synthetic emerald inclusion	93
Figure 4.31c: the 2300cm ⁻¹ to 3400cm ⁻¹ region in the Biron emerald showing peaks at 2453cm ⁻¹ , 2817cm ⁻¹ and 3374cm ⁻¹ respectively	94
Figure 4.31d: 0.92ct synthetic hydrothermal Biron emerald, showing colour	

Zoning	94
Figure 4.32a: 0.61ct unknown origin emerald spectrum	95
Figure 4.32b: 0.61ct unknown origin emerald with a glassy appearance, showing solid inclusions	96
Figure 4.33a: 1.02ct unknown origin emerald spectrum	96
Figure 4.33b: 1.02ct unknown origin emerald, showing visible dark solid inclusions	97
Figure 4.34a: DXR and TruScan comparison spectrum of the 7.43ct unknown origin natural emerald	99
Figure 4.34b: 7.43ct unknown origin natural emerald with cracks on the surface and light and dark solid inclusions occurring throughout the stone	99
Figure 4.35a: DXR and TruScan comparison spectrum of the 1.13ct Colombia Emerald	100
Figure 4.35b: 1.13ct Colombia emerald	100
Figure 4.36: DXR and TruScan comparison spectrum of the 0.69ct Swat, Pakistan emerald	101
Figure 4.37: DXR and TruScan comparison spectrum of the 0.92ct synthetic hydrothermal Biron emerald	101
Figure 4.38a: Graph depicting the average difference in concentration of Na ₂ O and MgO in natural and synthetic emeralds	103
Figure 4.38b: from left to right: 0.58ct Russian, 0.69ct Pakistan, 1.04ct Russian flux and 0.92ct Biron hydrothermal emeralds	103
Figure 4.39a: a 2.24ct natural red spinel spectrum from Sri Lanka	107
Figure 4.39b: a natural spinel spectrum taken from the Handbook of Minerals Raman Spectra (2012). <i>NB: the x-axis is reversed to the analytical spectra</i>	108

Figure 4.39c: 2.24ct natural red spinel from Sri Lanka	108
Figure 4.40a: a group spectrum of red, blue and grey spinels of the same origin but of different colours	109
Figure 4.40b: 2.24ct red, 1.20ct blue and 1.44ct grey spinels of natural origin	109
Figure 4.41a: depicting a 1.20ct natural cobalt blue spinel (red spectrum) with defined peaks and a synthetic blue spinel (blue spectrum) exhibiting broad fluorescence in the spectrum	110
Figure 4.41b: pale blue synthetic spinel	110
Figure 4.42a: spectrum of a 1.22ct gemstone of unknown origin labelled as Spinel	111
Figure 4.42b: a typical glass spectrum, acquired using a glass vial	111
Figure 4.42c: 1.22ct gemstone of unknown origin, labelled as spinel to be spinel	112
Figure 4.43a: spectrum of a 1.30ct unknown origin dark blue stone, considered to be spinel	112
Figure 4.43b: 1.30ct unknown origin dark blue stone, considered to be spinel	112
Figure 4.44a: unknown origin royal blue stone, alleged to be spinel	113
Figure 4.44b: top spectrum of a blue synthetic Chatham flux sapphire and below showing the unknown origin royal blue stone purported to be spinel	113
Figure 4.45: from left to right: the unknown origin royal blue spinel, 2.58ct Chatham flux sapphire and 2.95ct Sri Lanka sapphire	114
Figure 4.46: Raman spectrum depicting a 2.24ct Spinel of Sri Lankan origin analysed with both the bench top and handheld instrument	115
Figure 5.1: handheld spectrum of 12.58ct quartz treated 'mystic quartz'	120

Figure 5.2: handheld Raman spectroscopy covered with black opaque object

121

Abstract

Prompted by the increasing number, sophistication and quality of laboratory-grown gemstones; gemology has evolved into an individual science, incorporating the likes of biology and chemistry into its discipline. Synthetic gem materials are commonly encountered today in the jewellery industry and are becoming increasingly difficult to distinguish from their natural counterparts. A new approach is needed towards identification as traditional methods have shown to produce inconclusive results. The focus of this research is directed to some of the major commercial gemstones; ruby, sapphire, emerald and spinel to ensure the integrity of the international gemstone market.

Raman spectroscopy makes for a useful analytical tool for the study of gemstones as it requires a small amount of material and short measurement times, no sample preparation and is non-destructive. For this work, a review of a laboratory Raman spectrometer equipped with 532nm and 780nm lasers respectively, and a portable Raman system with a 785nm laser applied in the gemology field is provided. Many examples are given of the use of Raman spectroscopy as an identification tool; primarily focussing on natural versus synthetic gems and the various types of synthetics produced using different manufacturing methods. Repetitive measurements conducted under an identical instrumental operation confirm the reliability of the results as Raman bands are found at correct wavenumber positions within a $\pm 5\text{cm}^{-1}$ parameter compared to reference values in literature.

Results of the laboratory Raman spectrometer show the instrument is capable of origin determination of gems of the same colour and for differentiating between natural and synthetic gemstones. A choice of two lasers proved useful as emerald analysis was only possible with the 532nm laser.

The portable Raman system was able to distinguish between the different types of stones; however it proved less sensitive than the laboratory instrument as it could not distinguish between natural and synthetic gemstones.

TABLE OF CONTENTS

CHAPTER	TITLE	PAGE NUMBER
CHAPTER 1		
1	Introduction	1
1.1	Gemology	2
1.2	Forensic Gemology	2
1.3	Gemstones	3
1.4	Synthetic Gemstones	3
1.5	Gemstone Legal and Ethical Requirements	4
1.6	Gemstone Trade	5
1.7	Alternative Investments: Investing in Jewellery	6
1.8	Major Commercial Gemstones	7
1.8.1	Corundum: Ruby and Sapphire	7
1.8.1.1	Natural vs. Synthetic Corundum	7
1.8.2	Beryl: Emerald	8
1.8.2.1	Origin Determination	9
1.8.2.2	Chemical Composition: minor and trace elements	9
1.8.2.3	Water in Emeralds	10
1.8.2.4	Synthetic Features & Properties	12
1.8.2.5	Synthetic Production	12
1.8.3	Spinel	14
1.8.3.1	Spinel Group	14
1.8.3.2	Source and Occurrence	15
1.8.3.3	Synthetic Spinel	15
1.8.3.3.1	<i>Flame Fusion</i>	15
1.8.3.3.2	<i>Flux-melt</i>	16
1.8.3.3.3	<i>Pulling</i>	16
1.9	Synthetic Manufacturing Methods	16
1.10	Synthetic Gemstone Types and their Characteristic Properties	19
1.11	Flame Fusion (Verneuil) Method	21
1.11.1	<i>Properties of Verneuil Stones</i>	22

1.11.2	Advantages	22
1.11.3	Disadvantages	22
1.12	Crystal Pulling (Czochralski) Method	23
1.12.1	Properties of Pulled Crystals	23
1.12.2	Advantages	23
1.12.3	Disadvantages	24
1.13	Hydrothermal Method	24
1.13.1	Properties of Hydrothermal Stones	25
1.13.2	Advantages	25
1.13.3	Disadvantages	25
1.14	Flux Growth Method	25
1.14.1	Properties of Flux Growth Stones	27
1.14.2	Advantages	27
1.14.3	Disadvantages	27
1.15	Zone Growth	27
1.16	Lattice Defects	28
1.17	Crystal Orientation	29
1.18	Spectral Intensities and Wavenumber Shifts	29
1.19	Aims and Objectives	30
CHAPTER 2		
2	Analytical Methods	31
2.1	Raman Spectroscopy	31
2.1.1	Basic Theory: The Raman Effect	31
2.1.2	Applications of Raman Spectroscopy	34
2.1.3	Advantages and Disadvantages of Raman Spectroscopy	34
2.2	Ahura TruScan™ Handheld Raman Spectrometer	36
2.2.1	Applications	37
2.2.2	Advantages and Disadvantages	37
2.2.3	Basic Theory	38
2.2.4	<i>Origins of Raman spectra</i>	40
2.3	Scanning Electron Microscopy coupled with Energy Dispersive X-Ray spectroscopy	41

2.3.1	Scanning Electron Microscopy	41
2.3.1.1	Basic Theory	42
2.3.2	Energy Dispersive X-Ray spectroscopy	43
2.3.2.1	Basic Theory	44
2.3.2.2	<i>Advantages and Disadvantages</i>	45
2.3.2.3	<i>Qualitative Analysis</i>	47
2.3.2.4	<i>Quantitative Analysis</i>	47
CHAPTER 3		
3	Experiment	48
3.1	Materials for Raman spectroscopy	48
3.2	Materials for SEM/EDX	49
3.3	Analytical Instruments	49
3.3.1	DXR Raman spectrometer Instrument	49
3.3.1.1	<i>Method of Analysis using a Standard Operating Procedure (SOP)</i>	50
3.3.1.2	<i>Method Development for Analysis of Gemstones using Raman Spectroscopy</i>	50
3.3.2	Ahura TruScan™ Handheld Raman Spectrometer	52
3.3.2.1	Product Specifications	52
3.3.2.2	Instrument	52
3.3.2.3	Method	53
3.3.3	Scanning Electron Microscopy coupled with Energy Dispersive X-Ray spectroscopy	56
3.3.3.1	<i>Sample Preparation</i>	56
3.3.3.2	Method	56
3.3.3.3	<i>Method Development</i>	57
CHAPTER 4		
4	Results and Discussion	58
4.1	<i>Interpretation of Raman spectra</i>	58
4.2	<i>Surface analysis of gemstones</i>	58
4.3	Corundum	59
4.3.1	<u><i>Natural Corundum</i></u>	59
4.3.2	<u><i>Synthetic Corundum</i></u>	60

4.3.2.1	<i>Chatham stones</i>	60
4.3.2.2	<i>Kashan stones</i>	64
4.3.2.3	<i>Knischka Stones</i>	66
4.3.2.4	<i>Lechleitner stones</i>	67
4.3.2.5	<i>Czochralski stones</i>	68
4.3.2.6	<i>Seiko™ and Kyocera™ stones</i>	69
4.3.2.7	<i>Verneuil stones</i>	70
4.3.2.8	<i>Frosted Surfaces of Gemstones</i>	73
4.3.3	<i>TruScan™ Handheld Raman spectroscopy</i>	75
4.3.4	<i>SEM/EDX Analysis</i>	79
4.3.4.1	<i>Ruby</i>	79
4.3.4.2	<i>Sapphire</i>	81
4.4	<i>Emerald</i>	82
4.4.1	<u><i>Natural Emerald</i></u>	82
4.4.2	<u><i>Synthetic Emerald</i></u>	89
4.4.2.1	<i>Flux Emeralds</i>	89
4.4.2.2	<i>Hydrothermal Emeralds</i>	92
4.4.2.3	<i>Unknown Origin Emeralds</i>	95
4.4.3	<i>TruScan™ Handheld Raman spectroscopy</i>	98
4.4.4	<i>SEM/EDX Analysis</i>	102
4.5	<i>Spinel</i>	107
4.5.1	<u><i>Natural Origin Spinel</i></u>	107
4.5.2	<u><i>Synthetic Origin Spinel</i></u>	109
4.5.3	<u><i>Unknown Origin Spinel</i></u>	111
4.5.4	<i>TruScan™ handheld Raman spectroscopy</i>	115
CHAPTER 5		
5	<i>Conclusion</i>	117
5.1	<u><i>DXR Raman spectroscopy</i></u>	117
5.1	<u><i>Ahura TruScan™ Raman spectroscopy</i></u>	118
CHAPTER 6		
6	<i>Further work</i>	123
CHAPTER 7		
7	<i>References</i>	125

1 Introduction

For many centuries gemstones have been noted in history as being the object of status, respect and desire in most cultures. Although from time to time there are new natural gemstone occurrences, the major commercial gems such as diamond, emerald, ruby and sapphire remain in high demand due to their formidable attributes of beauty, durability and rarity. With natural resources depleting and consumer demand ever growing, many gemologists and researchers have resorted to synthetically producing these highly prized gemstones. Over the years synthesis methods have been finely tuned; producing stones which are looking more and more like their natural counterparts. This has become a concern in the gemological world as identification of these synthetics is becoming increasingly difficult through traditional, conventional testing methods. This study is an attempt to uncover the distinguishing features of gemstones of natural and synthetic flame fusion, flux and hydrothermal origin. Furthermore, the desired technique to be used for analysis will be Raman spectroscopy; both being applied in bench top and handheld form. There is a notable lack of published information on the use of Raman spectroscopy as a means of an identification tool for natural and synthetic gemstones. This is primarily due to Raman spectroscopy being in its infancy as a means of use in a gemological context. It seems probable that research similar in nature to this paper is likely to lie hidden amongst files in top gemological laboratories around the world. Such laboratories tend to issue short origin reports from time to time with little relevant information provided. This is one of the primary motives for undertaking this study, so as to provide a more in-depth, detailed and informative view on gemstone origin, formation and production. The principle aim of current gemological research is to determine if Raman spectroscopy methods are useful for distinguishing between different types of stone in order to keep the integrity of the international gemstone market intact, and to reduce fraud and theft of precious and valuable natural gemstones. Currently, gemstones are sent to laboratories for identification. This is not only costly, but time-consuming and potentially unsafe as these stones are transported to and from laboratories by mail. The use of a portable, handheld Raman spectroscope would reduce and to a certain degree eliminate the need for laboratory based testing as analysis could conveniently be

conducted on-site at mine locations and the surrounding areas or jewellery stores.

1.1 Gemology

Gemology is the ever-developing science of gemstones. As most gemstones happen to be minerals, gemology is therefore related to mineralogy, a branch of geology. At the heart of gemology lies gemstone identification. This is aided with the involvement of chemistry and physics both of which help provide information on chemical, physical (optical and structural) and crystalline properties of gems. By obtaining information regarding certain characteristics, it is possible to determine the state of origin and thereby authenticate whether a gem is natural or synthetic. Being able to conclude whether a stone is natural or synthetic, and of the latter, the possible method of synthesis is important as even different synthetically produced stones have varying commercial values. The growth of this science has been prompted and propelled in recent years by the increasing number and sophistication of laboratory-grown gemstones and of the applied treatments and enhancements to natural gemstones. Production of man-made gemstones began to increase in the 1970s and by the 1980s had expanded so much that they were being commercially produced. The 1990s saw a rise and development of sophistication in the number of gemstone treatments and enhancement methods being applied (Fritsch and Rondeau, 2009). This is the reason why gemology has taken a more multidisciplinary approach in evolving from a trade practice to a recognised science by incorporating elements of chemistry, biology (work on pearls, amber, coral etc.), materials physics and spectroscopy into its mainframe structure.

1.2 Forensic Gemology

Forensic gemology is the newly formed observational science branch of gemology. Where simple gemology looks at gemstones on a basic fundamental level; forensic gemology takes matters further and looks at gemstones beyond traditional measures. For this it requires the use of highly technical instrumentation to conduct certain tasks. As evolving technology has greatly enhanced the quality of synthetic gemstone produce, it is at times difficult and even impossible to distinguish between natural and synthetic by some established analytical techniques. This is where the forensic analytical tool

Raman spectroscopy is particularly useful in distinguishing between different types of gemstone; as was established by previous research by the author.

The roll of forensic gemology in society is that of providing general information to sellers and consumers alike. Substantially, the importance of this science is to avoid frauds and to protect the consumer; mainly to provide litigation support which often involves the appraisal of lost or stolen jewellery, especially in cases involving major commercial gemstones like ruby and sapphire.

1.3 Gemstones

Gemstones do not have a single, precise definition. Coloured gemstones, unlike diamond, are not a single commodity. Instead they comprise of a category that includes many different types of precious and semi-precious gemstones, with different sources and different values. According to the United Nations Standard International Trade Classification (SITC) system, gemstones are defined as: all precious and semi-precious stones (whether or not they have been worked or graded) excluding: all categories of diamonds; all precious stones composed of non-mineral, organic materials (i.e. fossilised tree resins, pearls, ivory, corals, and lignite); and all precious stones made of synthetic or reconstructed materials (unstats.un.org). Primarily, there are three types of gemstone materials which one should take into consideration: natural gemstones, artificial gemstones and synthetic gemstones. Natural gemstones are produced in the Earth of which many are generally enhanced by some form of gemstone treatment. Artificial refers to imitation gems which are simulants of natural stones, made entirely or partially by man. Synthetic stones are crystallised or recrystallized materials whose manufacturing method is completely or partially caused by man. They have the same physical and chemical composition and optical properties as natural stones but are laboratory grown (www.cibjo.org). For the purpose of this paper, concentration and direction will mainly be focussed on synthetic gemstones.

1.4 Synthetic Gemstones

Attempts for gemstone synthesis first began in the mid-1800s with success prematurely arriving in the form of the Geneva ruby in 1885; but it was only in the early 19th century by French chemist A.V. Verneuil that the first successful gemstones of good quality were synthesised (Nassau, 2009). As technology

has evolved over the years so have the production methods that now top class synthetics are being produced. This poses a threat to gemologists around the world as synthetic production is so advanced that basic routine examination methods do not provide a satisfactory diagnosis on their own, and at times are proving futile in distinguishing between natural and synthetic stones as a definitive difference cannot be found (O'Donoghue, 1997). The main importance for distinguishing between the two types of stone derives from the mammoth differences in rarity and commercial value. In comparison to synthetics, natural gems form over a considerably long period of time and tend to be millions of years old whereas the longest synthetic gems take to grow may be up to a year (Gaft *et al*, 2005). As such, synthetics do not possess the rare aesthetic qualities that are found in natural gems. Commercially, there is a huge price difference between the two gem types. The price of synthetic gems depends on the type of production method used. The price for low cost flame fusion synthetic rubies can range from less than £1 to £5 per carat. Luxury synthetic rubies produced from the flux method range between £100 and £1000 per carat depending on how excellent the quality of the stone is. Natural rubies can approximately be priced from £20,000 per carat to £50,000 per carat depending on the quality of the stone and natural sapphires at an even higher rate (Nassau, 2009). In addition, a gemstones economic value also depends upon its surface planarity, colour and degree of purity; that is to say the level of inclusions and the lattice order on how stable the stone is (Bersani and Lottici, 2010). Therefore, to be able to distinguish between natural and synthetic stones is a great necessity.

1.5 Gemstone Legal and Ethical Requirements

The United States Federal Trade Commission (FTC) which regulates and guides the gem and jewellery trade has produced a Jewellery Guide which all buyers and sellers of jewellery must follow. The guide provides information on how to label and describe jewels and jewellery products non-deceptively and on how to disclose material information to all consumers. The FTC is very specific in prohibiting the use of the terms "gem" or "gemstone" unless the item in question is wholly and exclusively the work of nature; it must be 100% natural. All other products must have an affixed adjective which is clear and concise in

its meaning and understanding and thereby indicates their man-made status. The following terms have been commissioned for describing a true synthetic: Lab-grown, Laboratory-grown, Lab-created, and Laboratory-created. The FTC also allows "trade names" to be used, such as Chatham-Created or Gilson-Created (www.ftc.gov). Other descriptive terminology for a man-made gemstone is variable from place to place, such as "synthetic", "cultured", "man-made" or "reconstituted" which implies that the product in question has not originated in nature. Such information has to be legally disclosed to the consumer with all honesty so as to not overprice and sell gems by deception. Unfortunately, many suppliers in developing/third world countries do not conform to these rules and regulations; making it easier for synthetic stones to enter the natural gemstone trade.

1.6 Gemstone Trade

In accordance with the United States Geological Survey (USGS) report, the United States of America (USA) currently dominates the gemstone market, as imported gemstones into the country make up 99% of their domestic consumption. In 2010, the world demand for gem-quality diamonds was \$50 Billion of which 35% was of the USA alone (www.geology.com). The estimated total for the USA was approximately \$18 Billion, an increase of about 42% on the previous year. The market for non-diamond gemstones was estimated to be around \$1 Billion, an increase of 21% on the previous year. Interestingly, the USA accounts for less than 1% of the total global gemstone production. Due to the lack of home production, up to 50% of the annual gem mining total is imported thus making the country the world's leading gemstone market today and for the foreseeable future (minerals.usgs.gov). Unlike the De Beers Company which controls the stock of diamonds; the non-diamond [coloured gemstone](#) world fortunately has no cartel to maintain prices at a high level. There are however many forces which try to influence market demand and perceived value. According to the International Coloured Gemstone Association (ICA), the "traditional gemstones" of red [ruby](#), green [emerald](#) and [blue sapphire](#) command a premium price in the market due to "their ever-lasting appeal and distinguished history through time." Even though in today's market most of these stones are enhanced or treated in some way, the label "[precious](#)" stone

adds a substantial premium to the price (gemstone.org). The price of coloured gemstones per carat tends to fluctuate at a far greater rate than diamonds as it is generally influenced by market supply and demand, therefore if a particular stone increases in popularity then so does its rarity which then has a knock-on effect on the price (minerals.usgs.gov).

1.7 Alternative Investments: Investing in Jewellery

In the economic climate of today, consumers are investing less in the stock market and instead are turning to the gemstone market as a means of preserving or increasing their wealth. Coloured gemstones are considered as one of the largest investment opportunities today and one of the least known, making it an exclusive commodity. These stones are considered to be among some of the safest, secure investments available today as they are a hedge against negative economic fluctuations in the stock market, currency and real estate. These hard assets have increased in price on average 15% each year since 1949 and have never gone down in value on a wholesale level in the past 35 years (www.rareandpreciousgems.com). It has become common for those in the statement jewellery trade to find consumers building investment portfolios which are mainly based on the major commercial gemstones. The most sought after stones other than diamonds are Colombian emeralds, Kashmir sapphires and Burmese rubies as these localities are purported to provide the best quality stones of those particular types. Collectors and connoisseurs are readily buying and building portfolios with primary criteria in mind, the first and foremost being conditions that gemstones are of a rare size, exceptional quality and preferably unenhanced in colour. Over the years, jewellery has not only maintained but also increased its value, as recent record sales of gemstones have been made at various prestigious auction houses, namely Doyle's, Sotheby's and Christies (Lapin, 2010). As the number of investors in the high end jewellery market increases, so do the prices of these coveted rare gems as they are not becoming more readily available. Some consumers are even going to the extent of sourcing stones directly from mine sights and local outlets near mines so as to buy these natural products first hand. The trouble many of these consumers tend to find is the sale of counterfeit gemstones to them occurring near these mines as many devious sellers import synthetics or imitations to sell from the surrounding mining areas (Lanford and Lanford, 2012). This type of trickery has

long been in practice in many countries. It therefore becomes more evident that there is a much higher need for origin determination on or near location as a lot more money is at stake than ever before.

1.8 Major Commercial Gemstones

This study will be focussing on ruby, sapphire, emerald and spinel gemstones; all which comprise a large portion of the major commercial gemstone group.

1.8.1 Corundum: Ruby and Sapphire

Corundum is a crystalline rock-forming mineral of aluminium oxide (Al_2O_3). It is allochromatic (white in its natural state) but can become coloured by different colouring impurities; the main dopants being chromium and iron. Red corundum is known as ruby and is coloured by chromium; all other colours of corundum are termed as sapphires and are coloured mainly by iron amongst many other dopants.

1.8.1.1 Natural vs. Synthetic Corundum

One of the studies being performed in this paper will be looking at synthetic corundum. In order to understand the nature of synthetic stones and why they differ, it is important to understand and know the differences between natural and synthetic corundum. All forms of corundum are composed of aluminium oxide (Al_2O_3). The following table distinguishes between the two crystalline forms of natural (α) and synthetic (γ) alumina.

Table 1.1: Differentiation between alpha (α) and gamma (γ) aluminium oxide

	Alpha (α)	Gamma (γ)
Form	Alpha (α) Aluminium Oxide: $\alpha\text{-Al}_2\text{O}_3$	Gamma (γ) Aluminium Oxide: $\gamma\text{-Al}_2\text{O}_3$
Crystal Structure	Monocrystalline: single crystal homogenous form where the crystal lattice is unbroken and continuous	Polycrystalline: many different crystals of heterogeneous form, varying in size and orientation throughout the structure

	throughout the structure	
Crystal System	Hexagonal	Cubic
Mohs Scale Hardness	9	8
Transformation	-	Transforms to the alpha form at high temperatures (1150°C+) by a nucleation and growth process, preceded by an incubation time (Dynys and Halloran, 1982; Jellinek and Fankuchen, 1948).

1.8.2 Beryl: Emerald

Emerald is a green mineral variety belonging to the beryl family with the chemical composition of beryllium aluminium silicate $\text{Be}_3\text{Al}_2(\text{SiO}_3)_6$. Other beryl minerals are aquamarine, heliodor and morganite amongst many more. Emerald is allochromatic (naturally white in its pure state) but garners its colour from trace concentrations of chromium (Cr^{3+}) and/or vanadium (V^{3+}) by substituting small amounts in the aluminium (Al^{3+}) position by crystal field energy reaction (Morosin, 1972). In accordance with the Confédération Internationale de la Bijouterie, Joaillerie et Orfèvrerie (CIBJO) regulations, also known as the World Jewellery Confederation, only Cr-containing green beryl can be labelled as emerald. Schwartz and Schmetzer (2002) defined emeralds as: “yellowish green, green or bluish green, natural or synthetic beryls, which reveal distinct Cr and/or V absorption bands in the red and blue-violet ranges of their absorption spectra.” Green stones void of chromium are simply labelled as green beryl and command a much lower price than their chromium-included counterparts. Like all other gemstones, emerald is graded based upon four elementary factors: colour, clarity, carat and cut. Emerald can have the tendency to be highly included thus generally having poor toughness and hence requiring special care. Despite its included nature, emerald remains a much sought after gem as it is considered to be amongst the most valuable due to its striking deep grass-green colour and rarity.

1.8.2.1 Origin Determination

Provenance and origin identification of emeralds using Raman spectroscopy has been conducted by various authors (Hagemann *et al*, 1990; Moroz *et al*, 2000) whereby comparisons of single-crystal Raman spectra are done between natural emeralds of different deposits and synthetics. Huong and Häger (2010) focussed on one of the main Raman peaks which shift between the regions of 1067 cm^{-1} to about 1072 cm^{-1} . They concluded the peak shifts to shorter wavenumbers in the region of $1068\text{-}1070\text{ cm}^{-1}$ in “non-schist-type” emeralds whilst the peak shifts to longer wavenumbers in the region of $1069\text{-}1072\text{ cm}^{-1}$ in “schist-type” emeralds. The authors also determined the peak wavenumbers to approximately be around $1067\text{-}1068\text{ cm}^{-1}$ in synthetic emeralds. Furthermore, they believe that the features of Raman bands in the region of $1067\text{-}1072\text{ cm}^{-1}$ depends on the concentration of silicon in each sample; hence they have assigned the band to Si-O bonding vibrations. Confirmation of the assignment of this band to Si-O vibrations has also been concluded by Adams and Gardner (1974) and Charoy *et al*. (1996). However, in contrast, Kim *et al*. (1974) and Moroz *et al*. (2000) have assigned the bands as Be-O bonding vibrations. Nonetheless, through their research using chemical and elemental analysis methods, Huong and Häger (2010) showed that samples with a high silicon content had low band positions, whereas, in comparison; samples with a low silicon content had high band positions. Here, they have put forward their justification for band assignment based on this silicon correlation to band positioning; demonstrating that band position is affected by silicon concentration in emeralds. They also stated that they did not find such a correlation between beryllium concentration and band position data. This leads the reader to much debate upon the assignment of the band as all authors have provided firm reasoning behind their choice of assignment. For now, the assignment remains quite a controversial discussion in literature.

1.8.2.2 Chemical Composition: minor and trace elements

Staatz *et al* (1965), Hänni (1982), Schraeder (1983) and Stockton (1984) have all conducted studies based on the chemical composition of emeralds, especially focussing on the amounts of minor and trace elements. Many of the emeralds analysed from different localities showed individual compositions with

extreme differences between them. In a study by Hänni (1982), it was shown that concentrations of Cr_2O_3 , FeO , MgO and Na_2O in natural emeralds are much higher than those in synthetic emeralds; however, there was not a clear separation between natural emeralds from different localities. Groat *et al.* (2008) report magnesium to be the main substituent in emeralds from most localities. The authors also state that in most cases Cr_2O_3 content is much greater than that of V_2O_3 in emeralds with the exception of samples from the Muzo mine in Colombia, the Mohmund district in Pakistan, the Lened occurrence in Canada and Norway. Schraeder (1983) claimed to not only distinguish natural from synthetic emeralds but to also separate natural emeralds from different localities based on minor elements. Stockton (1984) suggested that Al_2O_3 and SiO_2 could be used to supply additional information regarding origin. Huong *et al* (2010) found that these two elements are shown to be in larger quantities in "non-schist-type" (e.g. pegmatitic - hydrothermal) emeralds than "schist-type" (e.g. mica-schist, gneissic etc.) emeralds and therefore can be indicative of geologic origin. They also found that synthetic emeralds contained almost ideal amounts of these to form good quality stones.

1.8.2.3 Water in Emeralds

Another important set of Raman bands to consider when distinguishing emeralds from one another are in the range from 3300cm^{-1} to 3800cm^{-1} (Shelementiev and Serov, 2011). In literature, these bands have unanimously been assigned to water vibrations from the water inclusions in emeralds (see figure 1.1). The exact positioning of these water bands vary slightly between natural emeralds of differing origins and synthetic hydrothermal origin. Huong *et al.* (2010) stated that natural emeralds contain two water peaks in this region at room temperature; one at approximately 3598cm^{-1} and another at 3608cm^{-1} . Huong *et al* (2010) have further distinguished the emeralds to two types of origin based upon the intensity ratio of the two peaks as "schist-type" and "non-schist-type". They stated that the intensity of band 3608cm^{-1} is higher than that of band 3598cm^{-1} in "non-schist-type" emeralds and, conversely; the intensity of band 3608cm^{-1} is lower than that of band 3598cm^{-1} in "schist-type" emeralds. They then proceeded to assign bands 3608cm^{-1} and 3598cm^{-1} to water type 1 (without alkali nearby) and water type 2 (with alkali nearby), respectively. Hydrothermal synthetic emeralds show only one Raman band at 3608cm^{-1}

whereas there are no water bands present in the spectra of flux synthetic emeralds. The two Raman peaks of water observed in the emerald spectra are associated with OH⁻ and H₂O occurring at various orientations by substitutions into the mineral structure (Johnson, 2006).

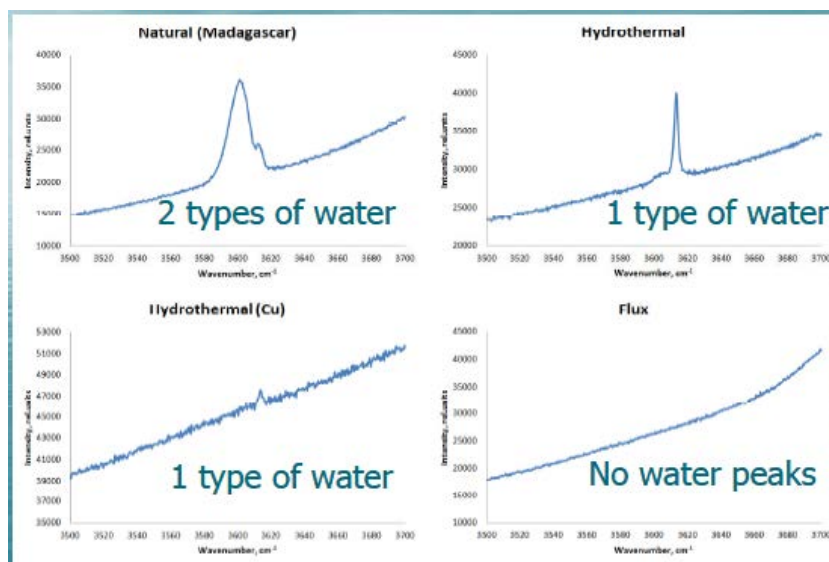


Figure 1.1: Raman spectra between the 3500cm⁻¹ to 3700cm⁻¹ region depicting water peaks in natural and synthetic emeralds, respectively (Shelementiev and Serov, 2011)

Hydrothermal synthetic emeralds contain water impurities because the growth process uses water and is quite similar to natural emerald formation processes. Arif *et al.* (1996) established that there were two components of water in emerald; channel water and inclusion water. Through conducting stable-isotopic investigations, the authors concluded that both waters had a different range of hydrogen isotopic composition, OH⁻ and H₂O with an outcome of the channel waters being distinctly isotopically heavier than the inclusion waters. There is a possibility that the higher intensity water band seen in Raman spectra could be assigned to the isotopically heavier channel waters and likewise, the lower intensity band to the inclusion waters. Determination of the amount of water in beryl can be difficult; however fluid composition studies by Giuliani *et al.* (1997) derived the following equation based on existing emerald experimental data: H₂O(in wt.%) = [0.84958 x Na₂O(in wt.%) + 0.8373.

1.8.2.4 Synthetic Features & Properties

In recent years, chemical composition, growth parameters and environment have continued to vary during the synthesis process used by synthetic emerald producers in order to replicate and obtain colours similar to those found in nature. These emeralds are generally more internally clean than natural emeralds; likewise they can also contain growth structures, cracks and inclusions. To the untrained eye, some of these features in synthetics can occasionally be mistaken for genuine emerald features; leading to misidentification. Flux emeralds tend to contain veil-like inclusions, as is seen in figure 1.2 (a) but more commonly contain metal inclusions. This happens by partial dissolution of the crucible occurring, causing flux and crucible particles (usually platinum) to be lodged inside the stone. Hydrothermal emeralds tend to be a lot clearer in appearance but usually have tell-tale signs of their undulating growth pattern as is seen in figure 1.2 (b).

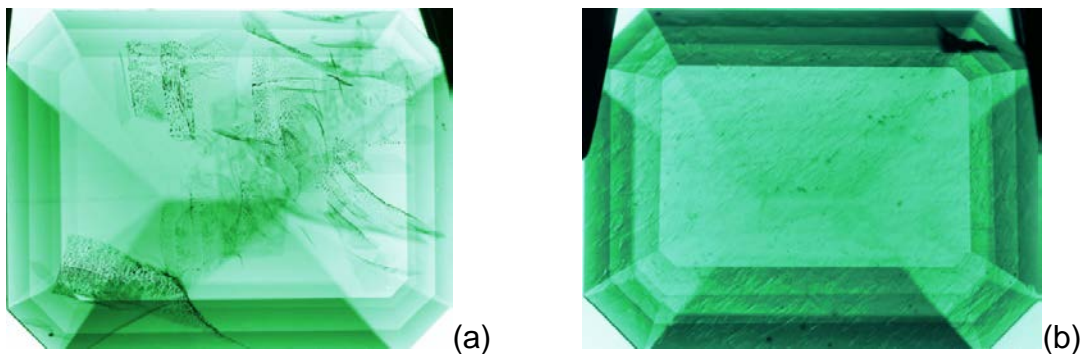


Figure 1.2: (a) flux-grown emerald and (b) hydrothermally-grown emerald showing typical inclusions and properties of these types of stones (Shelementiev and Serov, 2011)

1.8.2.5 Synthetic Production

Synthetic emeralds are produced by either the flux or hydrothermal method. Both of the growth methods share some similarities and have previously been confused with one another; the main difference between the two being the flux method using a crucible made of a metal with a high melting point; usually platinum, and the hydrothermal method using an autoclave (sealed pressure vessel) which usually has a gold lining. The properties of one or the other type of emerald depend on the growth method, colour controlling elements and

producer. The earliest report of emerald synthesis is by Ebelman (1848) who managed to form small hexagonal prisms by heating natural emerald powder in fused boric acid. The first successful small scale production of synthetic emerald was achieved by the German chemical company I.G. Farben-Industrie after a number of experiments between 1911-1942 (Flanigen *et al*, 1967). The emeralds were produced using a lithium polymolybdate flux in a platinum crucible; an isothermal diffusion process was used to combine beryllia (beryllium oxide), alumina (aluminium oxide) and silica (silicon dioxide) (O'Donoghue, 1983). The resulting emeralds were marketed under the trade name "Igemerald" (Flanigen *et al*, 1967). One of the most prominent synthetic gemstone manufacturers to date is the Chatham Company in San Francisco which has been producing synthetic (Chatham-created) gemstones since the 1940s. Although the actual process was not revealed it is believed Carroll Chatham produced the emeralds using self-nucleating crystals which were grown from a molten flux (Wood and Nassau, 1967). The process has culminated in the production of large, nearly flawless emeralds which at present leaves Chatham as the world leader in emerald synthesis. Emerald crystals have also been produced by the hydrothermal method on a commercial basis. The first fully synthetic hydrothermal emeralds were produced by Flanigen of the Linde Company, Division of Union Carbide, at Buffalo, New York in the 1960's who used two acid mineralizers which gave satisfactory emerald growth (Flanigen *et al*, 1967). Hydrothermal Biron emeralds were synthesised in Australia at the end of the 1970s. Chemical analysis by Kane and Liddicoat (1985) showed that the emeralds contain one type of water and the colouring agent vanadium, as well as lesser amounts of chromium. They discovered that the Biron synthetic is inert to ultraviolet radiation and can possess distinctive inclusions such as gold. These types of gold inclusions are normally incorporated into the stone through the growth process as the autoclave is lined with gold. The chemical composition of emerald as a silicate means that the simple flame fusion growth method cannot be carried out for technical reasons, hence why all synthetic emeralds have to be grown using the flux or hydrothermal method (Flanigen *et al*, 1967). In 1963 Gentile *et al* claimed they had after many unsuccessful attempts melted emerald congruently and created two boules using the flame fusion method. However, a study by Miller and Mercer (1965) showed emerald melts incongruently and so all attempts to

crystallise beryl from glass or a melt were unsuccessful. This therefore explains why all synthetic emerald produced today is either by the flux or hydrothermal method.

1.8.3 Spinel

Spinel has always been among the most beautiful and valuable gemstones. For many centuries, spinel was misidentified as corundum, mainly the ruby type as they have similar optical and physical properties and occur side by side within the same geological deposits (gemologyproject.com). Many of the world's most famous "rubies" are in fact red spinel. The Black Prince Ruby in the centre of the British Imperial State Crown and also the Timur Ruby in the British Crown Jewels have both only recently been identified as spinel (geo.utexas.edu). There are many theories behind the origin of the name spinel. It is possible that the name was derived from the ancient Greek term "spinos" meaning "sparkling", thus referring to the brilliance of the gem. It is also possible that the name comes from the Latin term "spina" meaning "little thorn" which is describing the octahedral "thorny" shape of the crystals (Krzemnicki, 2010).

1.8.3.1 Spinel Group

Mineralogically, like garnet and tourmaline, spinel belongs to a large group of minerals consisting of composite oxides of similar crystal structure (isomorphs). The general formulation of the group is $A^{2+}B_2^{3+}O_4^{2-}$ which crystallises in the cubic crystal system; whereby A can stand for either Mg^{2+} , Fe^{2+} , Mn^{2+} , Zn^{2+} , Ni^{2+} and B is either Al^{3+} , Fe^{3+} or Cr^{3+} (ssef.ch). Mineral members of this isomorphous group include spinel, gahnite, magnetite, chromite, hercynite and many others. There are three main isomorphous series; the spinel series (aluminium), the magnetite series (ferric iron) and the chromite series (chrome), all defined by the B^{3+} cation (gemologyproject.com). The spinel which we are concerned with is the gem type from the aluminium spinel series; magnesium aluminium spinel ($MgAl_2O_4$). The chemically pure form is naturally colourless; however trace amounts of colouring elements (chromophores) account for the wide range of possible colours. Chromium colours spinel red or pink, vanadium and iron

colour blue, violet, green and orange, whilst cobalt is rarely found in some vivid blue, violet and purple stones but to name a few (geo.utexas.edu). The same colouring dopants are present in different coloured corundum gemstones.

1.8.3.2 Source and Occurrence

Gem spinel mainly forms by the same processes and in the same rock type as corundum; the most common occurrence being in metamorphosed impure limestone (marble). It is also found as a primary mineral in mafic igneous rock. Magma that is relatively deficient in alkalis relative to aluminium will form corundum or may combine with magnesia to form spinel; hence why the two types of mineral are often found together (gemologyproject.com). The classical sources for spinel since ancient times have been the Mogok Gemstone Tract (Burma/Myanmar), Ceylon (Sri Lanka), Pamir (Tajikistan), Badakhshan (Afghanistan) and the Karakorum Range (Pakistan). Other recent areas for mining include Nigeria, South Africa, Kenya and Brazil (Krzemnicki, 2010).

1.8.3.3 Synthetic Spinel

1.8.3.3.1 Flame Fusion

Synthetic spinel was first produced accidentally in 1908 by A.V Verneuil using the flame fusion method when he was trying to synthesise ruby. It was not until the early 1930s that synthetic spinel had begun to be produced commercially. The ratio for common spinel of MgO to Al₂O₃ is 1:1. Synthesis through the Verneuil process changes this ratio by increasing the amount of Al₂O₃ in the mixture so the boules become stable. It was found that resulting boules produced by the 1:1 ratio were prone to fracturing and as a result no reasonably sized gemstones were able to be cut. As the addition of extra Al₂O₃ alters the chemical composition of the synthetic end product, it is strictly not a true synthetic; however it is generally accepted as being one. Synthetic spinels produced by this method often show a colour range from blue - light blue, green, and colourless. Red stones are generally not synthesised by this altered ratio; the few that are created tend to be extremely small in size and will show

curved striae like synthetic corundum (gemologyproject.com). As a consequence to the addition of extra Al_2O_3 , the crystal structure is slightly deformed resulting in the broadening of peaks in the Raman spectrum (Krzemnicki, 2008).

1.8.3.3.2 Flux-melt

First commercial production of flux-melt synthetic spinels occurred in the late 1980s; however they have been a rare breed up until the past few years, where in 2008 they became more prevalent in the gemstone market. This is largely a consequence of the increased value and interest in the natural red and blue spinels, therefore synthetic production is used in order to meet consumer demand. Unlike flame fusion spinels, the flux-melt variety form as good octahedral crystals, usually in saturated red colours, occasionally blue and are very difficult to distinguish from natural spinels using traditional gemological methods (Krzemnicki, 2008).

1.8.3.3.3 Pulling

The production of synthetic spinel using the Czochralski pulling method was developed in 2007, producing red to pink coloured spinels but is rarely ever used for spinel formation (gemologyproject.com).

1.9 Synthetic Manufacturing Methods

Synthetic gemstones can be produced by a range of several different growth methods. The three different types are solid growth (solid \rightarrow crystal e.g. skull melting, zone heating), vapour growth (vapour \rightarrow crystal e.g. Chemical Vapour Deposition (CVD)) and liquid growth (liquid \rightarrow crystal). The most common method of synthetic gemstone production is liquid growth which can be further categorised into two classes: liquid melt growth and liquid solution growth as shown in Table 1.2 (Nassau, 2009a; Oishi, 2003; Read, 2005; Shigley, 2000). In the production of melt crystals, powdered material is heated to a molten state and manipulated to solidify into a crystalline form. Crystal production from

solution sees aluminium oxide and chromium dissolved in a suitable flux material and manipulated to precipitate into a crystalline form (Elwell, 1979).

Table 1.2: Liquid crystal growth methods and properties

	Melt	Solution
Components	Crystallisation from a melt with approximately the same chemical composition as the crystal being grown	Crystallisation from a fluid of different composition, in addition to those contained in the crystal
Growth Rate	Rapid -Flame Fusion: 1-2 hours -Pulling: 1-8 weeks depending on crystal size	Slow and difficult Flux: between 2 months-1 year depending on crystal size
Crystal Properties	-large crystals -commercially highly important as very cost effective	-crystal growth at lower temperatures -crystals grown with well-developed faces
Crystal Type	-low cost, commercial mass production crystals (Flame Fusion) -high-optical quality laser crystals (Pulling)	-luxury synthetic crystals -niche production for price-restricted markets
Method	-Flame Fusion -Pulling -Zone Growth	-Flux -Hydrothermal
Additional Chemicals:	-Flame Fusion: oxygen-hydrogen torch to melt basic powder components -Pulling: an electrical heating mechanism	-Flux: Lithium Oxide (Li_2O), Molybdenum Oxide (MoO_3), or Lead Fluoride (PbF_2) as a solvent for the nutrient -Hydrothermal: an aqueous (water-based) solution of Sodium Carbonate (Na_2CO_3) acting as a solvent

Types of Stones Produced	-Chatham (Flame Fusion)	-Chatham (Flux/Hydrothermal)
	-Kashan (Flame Fusion)	-Kashan (Flux)
	-Verneuil (Flame Fusion)	-Knischka (Flux)
	-Czochralski (Pulling)	-Ramaura (Flux)
	-Kyocera (Pulling/Zone Growth)	-Lechleitner (Hydrothermal)
	-Seiko (Zone Growth)	

The rate of crystal growth is critical to the quality of the finished product, and with regard to this factor the price of crystals is also variable. When crystals form rapidly the atoms in the structure are not given enough time to align into their correct positions which results in a high dislocation density. The faster the production method, the higher the dislocation; therefore, gemstones produced by melt techniques will have many more defects within their crystal lattices in comparison to gemstones produced by solution techniques. Having a high dislocation density results in light being distorted or lost when passing through the crystal; thus giving it a greasy, glassy appearance (www.ndt-ed.org, www.ramaura.com).

The following table outlines the different production methods and the dates when they were first implemented.

Table 1.3: Laboratory Created Gemstone Production Methods and Dates (adapted from Olson, 2001)

Gemstone	Production method	Company/producer	Date of first production
Alexandrite	Flux	Creative Crystals Inc.	1970s.
“	Melt pulling	J.O. Crystal Co., Inc.	1990s.
“	“	Kyocera Corp.	1980s.
“	Zone melt	Seiko Corp.	“
Cubic zirconia	Skull melt	Various producers	1970s.
Emerald	Flux	Chatham Created Gems	1930s.

“	“	Gilson		1960s.
“	“	Kyocera Corp.		1970s.
“	“	Lennix		1980s.
“	“	Russia		“
“	“	Seiko Corp.		“
“	Hydrothermal	Biron Corp.		“
“	“	Lechleitner		1960s.
“	“	Regency		1980s.
“	“	Russia		“
Ruby	Flux	Chatham Gems	Created	1950s.
“	“	Douras		1990s.
“	“	J.O. Crystal Co., Inc.		1980s.
“	“	Kashan Created Ruby		1960s.
“	Melt pulling	Kyocera Corp.		1970s.
“	Verneuil	Various producers		1900s.
“	Zone melt	Seiko Corp.		1980s.
Sapphire	Flux	Chatham Gems	Created	1970s.
“	Melt pulling	Kyocera Corp.		1980s.
“	Verneuil	Various producers		1900s.
“	Zone melt	Seiko Corp.		1980s.
Star ruby	Melt pulling	Kyocera Corp.		“
“	“	Nakazumi Crystals Co.	Earth	“
“	Verneuil	Linde Air Co.	Products	1940s.
Star sapphire	“	“		“

1.10 Synthetic Gemstone Types and their Characteristic Properties

-*Verneuil*: can show needle-like inclusions of strings of minute gas bubbles in sapphires (O'Donoghue, 2006). Common characteristics are curved growth bands/lines (striations) and gas bubbles which are either grouped together in a 'cloud' or are separately spaced with tadpole-like characteristics as seen in older Verneuil production stones (Read, 2005). Generally gas bubbles tend to

be large and well-rounded and randomly distributed within the crystals (O'Donoghue, 1997).

-*Czochralski*: stones can show concentric colour zoning from core to rim (O'Donoghue, 2006).

-*Kashan*: frequently contain solid flux characteristics of flattened 'paint splashes' or 'footprints', also contain fine pinpoint inclusions which look like 'rain' (O'Donoghue, 2006). Stones produced of lesser quality usually contain coarse mesh-like networks of flux-filled whitish negative crystals (Read, 2005).

-*Chatham*: characteristic flux and platinum inclusions, usually occurring from fragments of the crucible (O'Donoghue, 2006). Common characteristics are curved growth lines (striations) and gas bubbles which are either grouped together in a 'cloud' or are separately with tadpole-like characteristics seen in older Verneuil production stones (Read, 2005)

-*Knischka*: generally have negative crystal inclusions terminating in long crystalline tubes, may also contain black distorted hexagonal platelets of silver and platinum (fragments chipped off from the crucible wall). The main diagnostic feature for Knischka rubies are liquid inclusions containing gas bubbles which are known as two-phase inclusions (Read, 2005).

-*Ramaura*: generally tend to be inclusion-free but can at times contain 'comet-like' inclusions with tails and feathers of white and orange-yellow flux, where white flux is characteristic of earlier produced Ramaura stones (Read, 2005). The flux can at times be grouped in a way so as to imitate fingerprint inclusions in natural rubies. When tilted some stones may show colour zoning. A variety of crystallographic orientations will be present due to the crystals formed by high-temperature flux growth by spontaneous nucleation (O'Donoghue, 2005).

-*Lechleitner*: may have Verneuil-type growth features and inclusions characteristic of flux growth. Curved colour banding can be seen in orange and yellow synthetic sapphires and curved striae have been observed in many stones (O'Donoghue, 2006). Flux inclusions cause haziness in stones, whilst white flux residues cause transparent to opaque wispy veils to form (Read, 2005). Dichroism (two different colours in two different optical planes) can be seen in some stones (O'Donoghue, 2005).

Although these characteristics are seen in synthetic stones, they can imitate natural inclusions to a certain degree; another reason why mistakes can be made by traditional testing methods.

1.11 Flame Fusion (Verneuil) Method

The flame fusion process also known as the Verneuil method was first developed in 1902 by French chemist August Verneuil. A breakthrough in the science of gemology, the method produced the world's first commercially successful synthetic gemstones. The apparatus is a furnace with a vertical oxyhydrogen torch through which finely powdered alumina doped with impurities is transported in a stream of pure oxygen until it travels to the hydrogen input at the point of combustion (Thomas, 2008). For the production of rubies, chromium (Cr^{3+}) dopants are used, whereas a wide range of dopants are used for different coloured sapphires, the most common being a combination of iron (Fe^{2+}) and titanium (Ti^{4+}) to produce blue sapphires. The powders melt into minute droplets of aluminium and fall onto a rotating ceramic pedestal located in a circular firebrick chamber where they form a small puddle on the seed crystal (Read, 2005).

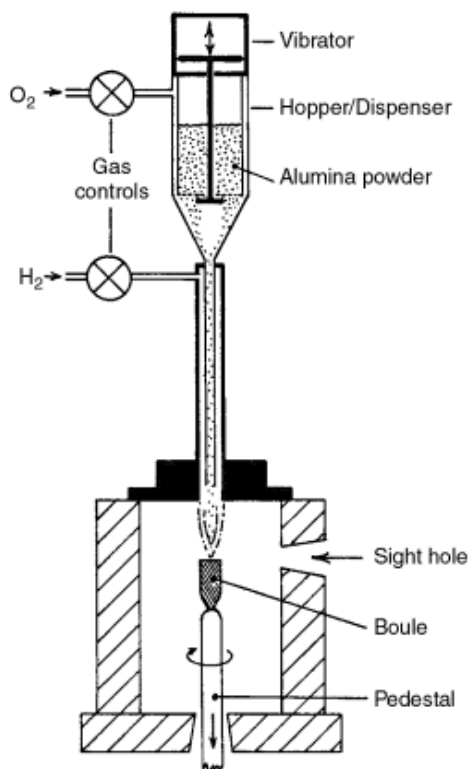


Figure 1.3: Diagram of the flame fusion apparatus (Read, 2005)

As they fall, the molecules promptly cool which results in them not being able to orient themselves properly. As the boule grows, the pedestal of the seed crystal is steadily lowered with the build-up of the crystal gradually taking place until it

is ready to be nipped off of its stem (Oishi, 2003). Internal stresses are commonly produced in boules due to the rapid growth and cooling they undergo. To relieve the stresses and to avoid the boule cracking, it is sawn parallel rather than at right angles to its length (Read, 2005).

1.11.1 Properties of Verneuil Stones

Flame fusion stones tend to have striations (curved growth lines) and curved colour banding which is easily seen on the surface of faceted gems. They usually also contain tadpole-like gas bubbles and minute gas bubble clouds however, they do not contain any solid inclusions (Read, 2005)

1.11.2 Advantages

Being a crucible-less technique, the produced boule is easily removed from the apparatus without any hindrance. Large crystals are readily made at higher temperatures than any other technique and crystal growth is rapid so synthetic gemstones can be easily mass-produced which makes the technique cost effective (Thomas, 2008)

1.11.3 Disadvantages

The boules can easily fracture and crack into pieces due to high levels of internal stresses; commonly known as parting of the boules (Oishi, 2003)

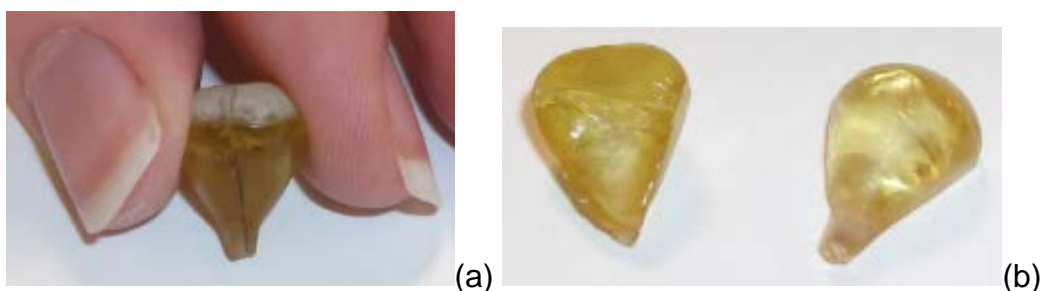


Figure 1.4: (a) a verneuil boule shown whole with a crack running down the middle, and (b) shown parted into two pieces

1.12 Crystal Pulling (Czochralski) Method

The crystal pulling technique was invented by Jan Czochralski in 1918 by perfecting the pulling process of synthetic crystals straight from the melt. A mixture of the constituents of the principle material with a suitable flux are placed in an iridium or platinum crucible and brought to a temperature just above its melting point.

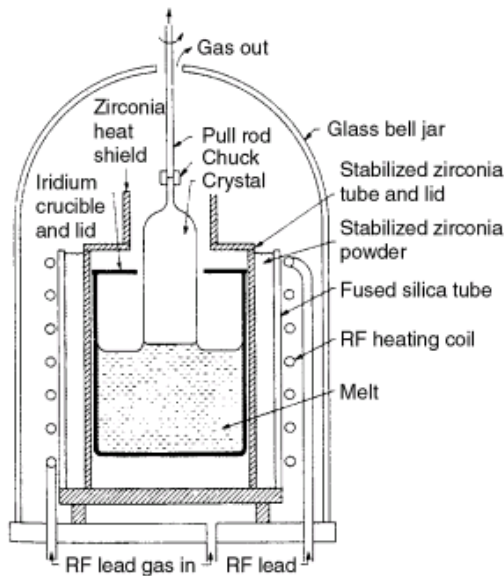


Figure 1.5: Diagram of the crystal pulling apparatus (Read, 2005)

A seed crystal is carefully lowered into the crucible until it makes slight contact with the melt. The rod holding the seed steadily lifts and rotates from the melt at a slow speed as the crystal forms. Constant temperature fluctuations within the melt help to increase the diameter of the crystals (Thomas, 2008).

1.12.1 Properties of Pulled Crystals

Czochralski stones are virtually inclusion-free, have no growth or colour banding yet may contain occasional elongated gas bubble (O'Donoghue, 1997)

1.12.2 Advantages

Production of large, dislocation-free crystals can be grown in many different orientations which can be achieved in a relatively short space of time. The separation of the crystal from the melt is not necessary; also, the compositional change in solid solution crystals can be minimised by pulling small crystals from large melts (Oishi, 2003).

1.12.3 Disadvantages

Highly advanced operator skills are necessary to conduct this production method successfully, atmosphere control of the system is complicated and equipment is highly expensive. Contamination of the melt may become an issue as a crucible is required for this technique (Oishi, 2003).

1.13 Hydrothermal Method

The first stones to be produced by the hydrothermal method were in Austria by Johann Lechleitner in the mid-1980s. Complete corundum crystals have been grown but as of yet have not entered the market in large quantities like ones produced by other methods (O'Donoghue, 1997).

Unlike other synthetic production techniques, the hydrothermal method grows crystals from an aqueous solution of the source material at high pressures and temperatures. The process uses an autoclave vessel typically lined with gold which raises the boiling point of water above its standard boiling point of 100°C to 400°C. At such a high temperature; the water in conjunction with the superheated steam act as a solvent for the many minerals (Read, 2005).

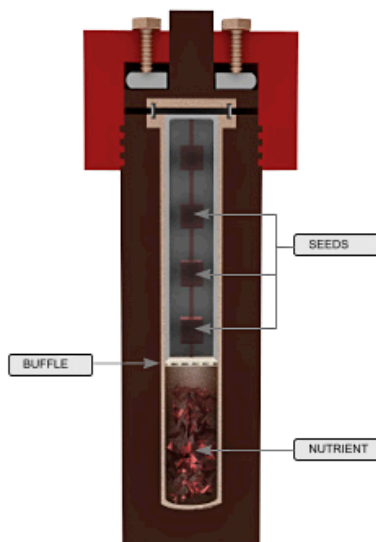


Figure 1.6: Diagram of the hydrothermal process (www.alexandrite.net)

As the autoclave base is heated to dissolve all the nutrients; the upper region containing the racks of seed crystals is cooled to speed up the deposition

process (Thomas, 2008). This method can basically be seen as a solution growth process by a temperature gradient transfer (Oishi, 2003).

1.13.1 Properties of Hydrothermal Stones

These stones may contain the same type of inclusions as seen in Verneuil stones; typical inclusions of white flux residues may produce feathers and wispy veils in the gemstones (Read, 2005).

1.13.2 Advantages

In comparison to the other techniques, hydrothermal synthesis requires modestly low temperatures and the grand thermal mass of the autoclave grant the use of inexpensive and uncomplicated furnaces and controllers. It is noted that autoclaves tend to be expensive but if handled and controlled properly, they have a long life which brings down the operation costs (Oishi, 2003).

1.13.3 Disadvantages

The one disadvantage of this technique is the possibility of OH⁻ or H₂O being incorporated into the crystals due to the nature of the production method (Oishi, 2003).

1.14 Flux Growth Method

In comparison to other methods, the flux growth method is a more recent arrival on the scene of crystal growth, coming into play after World War II, and was introduced by Carroll Chatham in 1958 (O'Donoghue, 2005). It is a solution growth technique which takes place at high temperatures and can either occur by spontaneous nucleation or growth on a seed crystal. The technique is used to grow single crystals of various melting compounds. The type of flux to be used is highly important as some fluxes produce block crystals whilst others will produce flat, bladed crystals (O'Donoghue, 2005). For the growth of corundum, constituent gem-forming chemicals of aluminium oxide and chosen impurities (Cr³⁺ for rubies, Fe²⁺ and Ti⁴⁺ for sapphires) are mixed with a suitable flux solvent (Nassau, 2009).

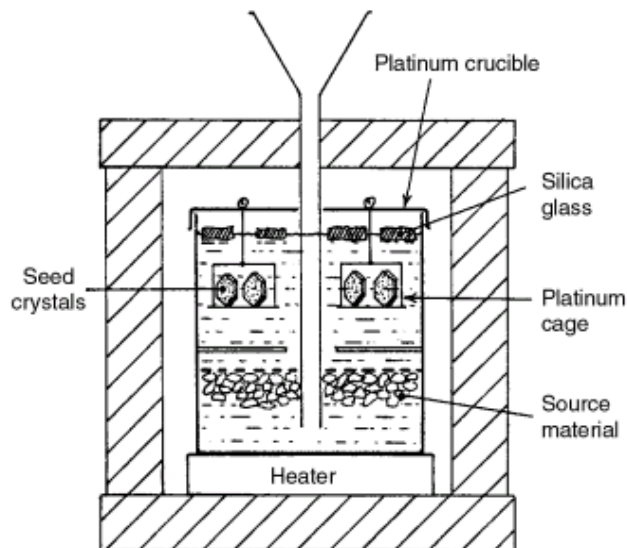


Figure 1.7: Diagram of the flux method (Read, 2005)

The mixture is then placed in a platinum or iridium crucible and melted at temperatures approximating 1300°C. Seed crystals are lowered into the solution and the temperature of the crucible is slowly reduced to a pre-set level approximating 1000°C (Nassau, 2009). Over a several-week period the solution becomes supersaturated; the synthetic crystals either precipitate out and grow on crystallographically oriented seeds or self-nucleate and grow along the slightly cooler crucible bottom, as is the case with Ramaura rubies. During the long process the growth materials are replenished regularly through the access funnel located at the top of the apparatus. Any unwanted flux is drained off via the hollow pedestal located at the bottom of the apparatus (Nassau, 2009; O'Donoghue, 2005; Read, 2005).

Overall, there are three flux techniques which one can choose from: Slow Cooling Technique, Flux Evaporation Technique and Temperature Gradient Technique. The slow cooling technique, as mentioned above, is the most common of the three, followed by flux evaporation, whereas the temperature gradient technique is suited for growing large crystals. Choosing a good flux is vital to how well the finished crystal product will form. Key characteristics of a good flux are that it should have a low melting point, be easily separated from the product, not form stable compounds with the reactants or create competing phases, and must not enter the crystals as inclusions (Fisk and Remeika, 1989).

1.14.1 Properties of Flux Growth Stones

Stones grown by this method often contain flux or crucible residue within the formed crystals which tend to mimic the characteristics of solid or liquid inclusions in natural stones (O'Donoghue, 2006). Flux residues that become incorporated in the production process usually tend to be placed at the sides of faceted stones so the stones look inclusion-free when analysed through their table (O'Donoghue, 1997).

1.14.2 Advantages

Crystal growth at constant temperatures is achieved by using the flux evaporation technique. The method requires relatively simple equipment from which the crystals can grow into the solution free from thermal or mechanical strain (Oishi, 2003). Flux crystals tend to have a relatively lower degree of dislocation density compared to crystals produced by other methods as the process is much lengthier and only requires small amounts of materials (Pamplin, 1980; Oishi *et al*, 2004).

1.14.3 Disadvantages

Stones generally have a long growth period ranging from a few months to a year from which only relatively small crystals are grown. Fragments from the crucible wall may break off and become included in the finished product, resulting in interstitial or substitutional incorporation of flux ions into a crystal. Veil-like inclusions of undigested flux which may resemble congregations of liquid feathers/droplets may also be incorporated within a crystal (O'Donoghue, 2005; Oishi, 2003).

1.15 Zone Growth

Developed in the 1970's by Armenian scientist, Professor Bagdosarov, the zone growth method is not used quite as commonly as other production methods. The technique is very similar to the Crystal Pulling Czochralski method of production; the main difference being the direction of pull on the crystal. In the pulling method the crystal is pulled vertically instead of horizontally, as is the opposite in zone growth. The method uses slow-melting techniques and a

tungsten dish which is pulled under a heating element over a period of time. The length of time of crystal growth is dependent on the volume of the dish being used and the materials being crystallised (O'Donoghue and Joyner, 2002).

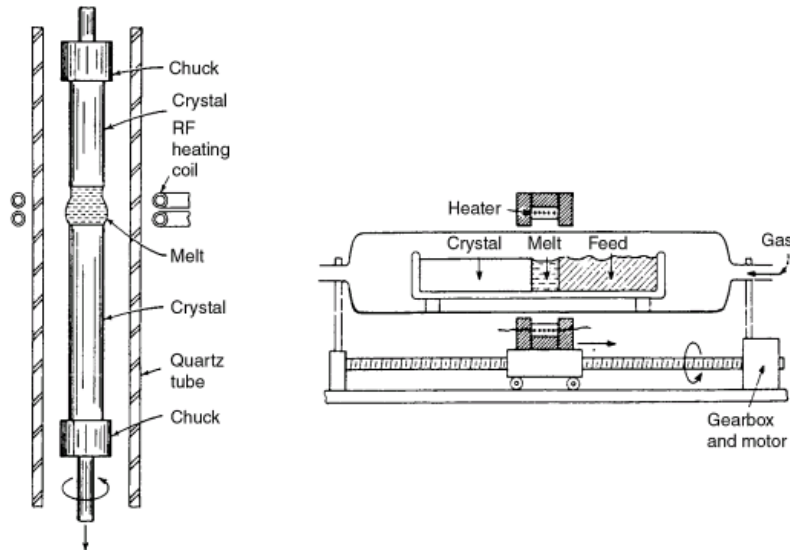


Figure 1.8: Diagram of the zone melting process. Zone refining method used by Kyocera (left). Floating zone method used by Seiko (right) (Read, 2005).

1.16 Lattice Defects

When viewed in perspective, powdered aluminium oxide is essentially being mixed and fused with various amounts of dopants; the amount of dopant dependent on the type and depth of colour to produce and type of growth method used. The faster the formation process of a gem, the higher the dislocation density and therefore the greater the lattice distortion. In rapid formation, the unit cells; regular repeating material portions; are unable to align properly resulting in structural disorder imperfection from misalignment, causing irregularity of the periodic repetition pattern. As a result, in lattice distortion where Al_2O_3 is not lined uniformly, the spaces are filled by the dopant. However due to the dopants large ionic size and metastable character it does not always fit into the crystal lattice properly. This may account for some of the large variations in band intensities and wavenumber shifts. However it has not been completely proved that all wavenumber variations in relation to chemical substitution are linear. It is noted that compositions in synthetic chemical systems may be crystallographically imperfect due to the desired composition

not being achieved because of experimental issues and as a result the lattice will form in an unstable manner (Smith, 2008).

1.17 Crystal Orientation

Gemstones are often cut depending on their crystal habit, crystalline system and symmetry, therefore a gems main surface edges are generally related to the crystallographic axis (C-axis). Thereby it is known to be common for one or more peaks to be absent from a Raman spectrum depending on particular orientations of the gem in question (Huong, 1996). For crystals with symmetric geometry (cubic system), orientation of the crystal will not significantly affect the outcome of the Raman spectrum. Crystals with asymmetric geometry (all non-cubic) will yield different spectra when analysed from different angles. This is because laser interaction is dependent upon the light beams angle of incidence in relation to the minerals crystal lattice and polarisation of the incident beam (Hope *et al*, 2001).

1.18 Spectral Intensities and Wavenumber Shifts

The wavenumber position in different gemstone samples is mostly *constant*, with the exception of regular experimental uncertainty. In contrast; spectral relative intensity of a given Raman band is ever changing due to varying physical structure and chemical composition of gemstones. This is due to one or more chemical elements being substituted by another. Where this occurs; modifications in bond angles and lengths cause changes in bond energies. This in turn can result in wavenumber shifts occurring in quite a few Raman bands. Furthermore it should be noted that wavenumber shifts are independent of crystal orientation and of exciting laser wavelength. It is observed that synthetic stones produced by different growth methods may have additional bands of varying wavenumbers and intensities correlating with the type of growth method used. Therefore, depending on the time taken for a gem to grow, wavenumber shifts may also be observed (Smith, 2008). It is imperative to know and understand what lattice defects and crystal orientations within gemstones are and what effect they may have on the resulting spectrum produced by Raman analysis. This is due to Raman frequencies/wavenumbers varying according to two basic factors: the weights of the atoms at the ends of a bond, and the strength of the bond between them. Ultimately, a spectrum displays information

regarding the bond order between two atoms, therefore lattice defects and geometry symmetry may influence wavenumber shifts and intensities.

1.19 Aims and Objectives

As technology evolves and enhances the production methods of gemstones; it has become more and more difficult to distinguish natural from synthetic stones, and to discriminate different gemological materials from one another based upon the various types of synthetic production methods. The aim of this study is to differentiate between the different types of natural and synthetic stones being produced by determining their natural origin and/or their original method of production respectively. The technique to be employed in detecting these differences is the highly desirable Raman spectroscopy, as its ideal characteristics; including being quick and non-destructive make it a powerful tool for the investigation of chemical and structural properties of gemstones. For this, both a bench top and handheld Raman spectrometer will be used. The quality of results from both these instruments will be compared in order to establish their suitability and effectiveness of each instrument. As gemstone identification and verification is now required efficiently and in many cases 'on-the-spot', the handheld Raman spectrometer will be used to test its capabilities as a portable, on-site detection device to provide fast and accurate results to sellers, consumers and officials in the field. It will also be tested for its ease of use for a person with a non-scientific background to determine its operational and interpretive difficulty. There is a great need for such research to be conducted as there is very little literature for the use of bench top Raman spectroscopy as an application method for the analysis and identification of gemstones. It is also noted that as of yet, there is no literature present specifically for the application of handheld Raman spectroscopy to gemstone analysis. The core of this study will mainly be with these methods of analysis, however, Scanning Electron Microscopy coupled with Energy Dispersive X-ray spectroscopy (SEM/EDX) was chosen for brief use during this study. This analytical technique will primarily be used as a means of validation/verification of the Raman spectroscopy results and the theories behind any conclusions drawn from those results.

2 Analytical Methods

2.1 Raman Spectroscopy

The phenomenon of light scattering first came to attention in an article in Nature entitled 'Molecular Diffraction of Light' by C.V. Raman (1922), the first of a series of collaborations with his fellow scientists. This article led to the discovery of Raman light scattering where the findings were published in Nature six years later in another paper by C.V. Raman and K.S. Krishnan (1928) entitled 'A New Type of Secondary Radiation'. Other pioneers in this technique were Landsberg & Mandelstam (1928) and Hollaender & Williams (1931) who obtained some of the first ever spectra for minerals and silicate glasses (McMillan, 1989). Although Raman spectroscopy was discovered in 1928 in which the analysis of solid materials was almost immediate; a review by Griffith (1974) stated that the technique for structural studies and characterisation of minerals was still in its infancy, almost 50 years on since its discovery. Raman spectroscopy was initially applied to gemology around 30 years ago and was soon forgotten due to technical difficulties of the equipment. Only in the last decade has a renaissance occurred from which it has flourished, mainly due to upgraded equipment which has seen the instrumentation as a whole develop and become more compact and easier to use (Bersani and Lottici, 2010; Moffat *et al.*, 2004). It is with these developments that this technique has become an exceptionally useful tool in a number of sciences like gemology; and at the 15th Meeting of the International Association of Forensic Sciences (IAFS 1999) it was presented as an emerging technology for analysis in forensic science (Bartick, 2002). As is understood, Raman spectroscopy is in its infancy within both the forensic and gemological fraternities as it is often overshadowed by more established analytical methods of analysis.

2.1.1 Basic Theory: The Raman Effect

Raman spectroscopy is an analytical spectroscopic technique based upon the inelastic scattering of monochromatic light, typically from a laser in the visible, near infrared or near ultraviolet light region (Whittaker *et al.*, 2000). For research purposes of this paper, two light scattering forms should be understood; elastic and inelastic light respectively. Firstly, in the elastic scattering of light, the absorbed and emitted frequencies are equal to one another, i.e. there is no gain

or loss of energy. This type of elastic light scattering is termed Rayleigh scattering. The particles or molecules which scatter the light are much smaller than the wavelength of light. Rayleigh scattered light is always at the same wavelength as the excitation laser and is generally more intense than Raman scattered light. In the OMNIC software of the bench top instrument; notch filters automatically remove Rayleigh scattering along with stray laser radiation from the resulting spectrum.

The second form of light scattering, Raman scattering or the Raman Effect, is inelastic in nature; whereby the absorbed and emitted frequencies are unequal. The Raman Effect is a phenomenon found in the scattering of light in which a portion of the light undergoes a frequency change. It is possible to further distinguish between the two types of Raman scattering as the photons from the light source gain or lose energy during scattering and therefore decrease or increase in wavelength respectively (Amer, 2010). The concept of the energetics of the Rayleigh and Raman scattering processes are illustrated in Figure 2.1.

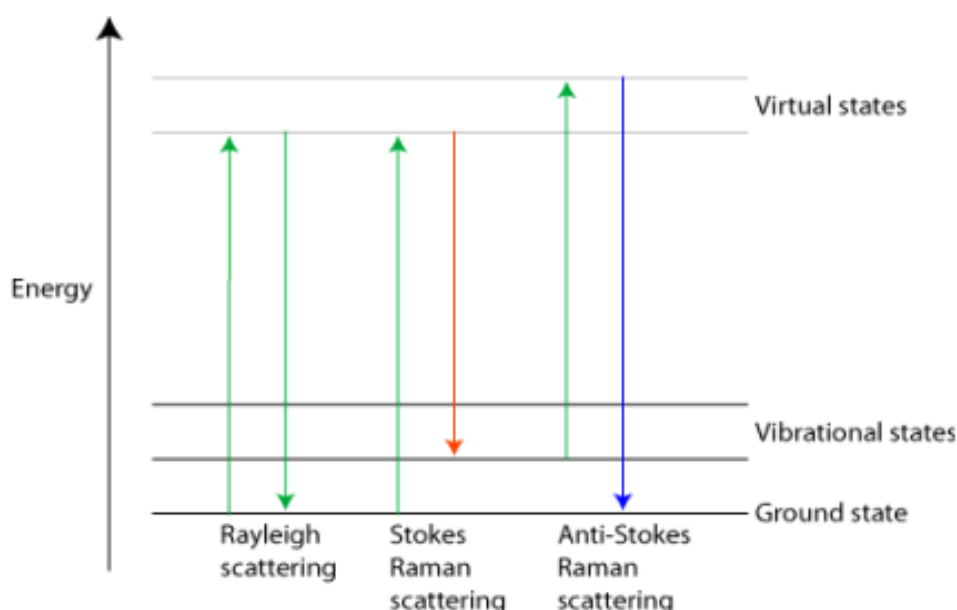


Figure 2.1: Retrieved from University of Cambridge (2007), a quantum diagram of Rayleigh and Raman light scattering depicts the basic processes which occur for one vibration.

From figure 2.1 it can be seen that Rayleigh scattering does not have any effect on the emitted light photon as the molecule descends from a “virtual” energy

state back to its original ground energy state, therefore no loss or gain of energy takes place. This will result in the scattered light having the same wavelength it began with (Amer, 2010). Raman scattering, whereby the light is scattered with lower energy is known as Stokes scattering and light scattered with higher energy is known as anti-Stokes scattering respectively. In Stokes scattering if the molecule is promoted to a virtual state from a ground state then returns back down to a vibrational state; the scattered photon will have lost energy and have acquired a longer wavelength. Anti-Stokes scattering occurs when the molecule is already in a vibrational state and once scattered makes a transition to the ground state. This results in the scattered photon gaining energy and therefore acquiring a shorter wavelength as can be seen in Figure 2.1. It is this change in energy of the photon leaving the molecule in relation to the original energy of the photon entering the molecule which Raman spectroscopy analyses. These Raman shifts occur due to the interaction of the photons with the molecules. This results in changes in the vibrational and rotational energies of chemical bonds within the molecules and in the vibrations of the crystal lattices. This acquired polarisability is linked to the directional attributes of chemical bonds in a molecule hence the relation to vibrational spectroscopy. (Hope *et al*, 2001). This then indicates that the Raman shift is directly proportional to the relative position of the electronic energy states in a molecule or atom (Amer, 2010). The Stokes and anti-Stokes scattered light is always shifted at an equal distance on both opposite sides of the Rayleigh scattered light. Consequently, the spectrum of wavelength of light is symmetrical; besides the differing intensities, whereby Stokes scattering is generally used due to its considerably higher intensity than anti-Stokes scattering (University of Cambridge, 2007). Raman selection rules apply for a molecule to be Raman active, which is to say that the molecule should possess anisotropic polarisability. Molecules interact with the electromagnetic radiation in Raman via the oscillating induced dipole moment; more accurately termed as the oscillating molecular polarisability. In order for a molecule to be Raman active, there must be a change in polarisability during the vibration (Mackenzie, 2011). The spectrum outputted by the software is usually shown as Raman intensity versus Raman shift, whereby Raman Intensity is the amount of photon per second and Raman Shift is the shift in frequency of the emitted photon (Jickells and Nergrusz, 2008).

2.1.2 Applications of Raman Spectroscopy

Raman spectroscopy is used to detect the vibrations occurring within molecules or atoms since vibrational information is specific for the chemical bonds in molecules. Hence it is used to provide information on both the physical forms and chemical structures of materials for identification purposes by their characteristic spectral patterns; also known as 'fingerprints' (Smith and Dent, 2005). The technique examines crystal lattice and molecular vibrations thus making it sensitive to the bonding, chemical environment, composition and crystalline structure of the sample matter or material. It concentrates on the polymer backbones, looking at the non-polar and symmetric vibrations within molecules. Such characteristics in relation to other techniques make it a superior method for clearly identifying matter in any physical form whether as an amorphous or crystalline solid, liquid, solution or gas (Smith and Clark, 2004). Raman spectroscopy is independent of the atomic mass of elements within materials therefore compounds containing light can be easily characterised. Even in polymorphs where solid chemical compounds have the same chemical composition yet exist in more than one crystalline form are clearly distinguished from one another (Hope *et al*, 2001). Sodo *et al.* (2003) concluded in their work that the spectral features of Raman allowed for a clear distinction between natural gemstones, their synthetic analogues including imitation gems. Under correct analytical conditions the technique was to an extent successfully applied and briefly used for both qualitative and quantitative analyses of molecular samples (McMillan, 1989).

2.1.3 Advantages and Disadvantages of Raman Spectroscopy

As with all techniques, Raman spectroscopy has its benefits and limitations which must be taken into account. Common known facts are that the testing technique is non-destructive and so leaves the sample invariant. It does not require any prior treatment or preparation of a sample is easy to use and time and cost efficient; having a high sensitivity at very fast acquisition times (Burke, 2001). It is applicable to large; non-uniform/odd shaped objects and mounted gems so there is no need to remove them from their setting (Jenkins and Larsen, 2004). Kiefert *et al* (2001) concluded that Raman spectroscopy was able to identify gemstone treatments such as crack and fissure filling and colour

enhancement for gemstones. As the technique is contactless and completely non-invasive; objects within a transparent medium can be analysed without the need for disassembling them. Water and glass are well documented as being weak Raman scatterers so spectra can be obtained for minerals immersed in water, in air or contained within glass-framed objects and also ones within a transparent medium such as plastic (Bartick, 2002; Hope *et al*, 2001; Smith and Clark, 2004). It has been noted that the technique has no issues of interference from atmospheric carbon dioxide (CO₂) or water (H₂O) (www.biotechprofiles.com). Minute volumes of material can be used since the Raman microscope objectives can focus the laser; a very narrow, highly monochromatic and coherent beam; down to a small diameter of 25µm. Raman spectra allow for the characterisation of both inorganic and organic compounds as it can cover a broad spectrum range from 50-3385cm⁻¹ in a single recording which is usually independent of the vibrational modes being studied (www.biotechprofiles.com; www.lambdasolutions.com).

For many years Raman spectroscopy was the technique which always complemented Infrared (IR) spectroscopy and lagged behind in research and use. In today's modern age much attention is being given to Raman spectroscopy. It has been well documented as not only being complementary to IR spectroscopy but now excelling beyond it with the number of advantages it has over the analytical technique.

It is known that most solid materials have their characteristic vibrational frequencies in the far-IR low-frequency ranges that are less than 400cm⁻¹. It is in this part of a spectrum where crystal lattice modes and vibrational bands of inorganic materials reside. However this region is not easily accessible by conventional means of IR spectroscopy. Where hydroxyl groups and water possess no problems for Raman; the opposite occurs within IR spectroscopy as they present very broad and strong absorptions in the IR region, thus completely swamping the spectra. Raman vibrational band widths are generally narrower than IR absorption band widths. This makes it easier to separate and distinguish multiple components in sample mixtures and to identify any characteristic features within the spectra. The fact that Raman easily accesses low frequency vibrations between 400-50 cm⁻¹ also makes it a highly desirable technique (Edwards and de Faria, 2004; Huong, 1996; Smith and Clark, 2004). Coupling the Raman instrument with a microscope allows the operator to direct

and focus the laser to a precise point on the sample they wish to analyse (Jickells and Nergusz, 2008).

As with all instruments there are always one or more objects which pose a disadvantage to any given technique. The principle disadvantage of Raman spectroscopy is the Raman scattering effect which is very weak; and as a result the detection of the scattered light needs highly optimised and sensitive instrumentation (Smith and Dent, 2005). The main problem in Raman spectroscopy is fluorescence which happens to be several magnitudes stronger than the weak Raman scattering (Burke, 2001). There are three possible features of cut and polished stones which may present fluorescence. These can either be the inclusions, matrix material, or the surface of a stone. Generally it is fluid inclusions which tend to be fluorescent in nature as many of them contain aromatic or cyclic hydrocarbons or fluorescent daughter materials. In some stones the matrix material it is made from may be the primary reason for the occurrence of fluorescence. Some examples of naturally fluorescing stones are feldspar, fluorite and occasionally quartz. Surfaces may become fluorescent if they contain remaining residue from some resins or epoxy which are used in the preparation of stones or when filling fissures and cracks, most commonly occurring in emeralds (Burke, 2001). When stones are mounted on glass slides, "Blu-Tack" is used to securely hold them in place. As quick and convenient as it is; "Blu-Tack" can present a real problem as it naturally exhibits high Raman fluorescence. This can cause the resulting spectrum of the stone being analysed to be completely overcome and suppressed (Kiefert *et al*, 2001). However, fluorescence may be overcome by continuous exposure of the sample under the laser beam. This may cause the fluorescence to sufficiently decay in order for a spectrum to be measured (Pelletier, 1999). One last disadvantage of Raman spectroscopy is the lack of readily available spectral libraries for mineral comparison. The lack of spectral libraries makes it difficult at times to ascertain the chemical nature of the analysed material which in turn makes it even more problematic when trying to categorise various unknown materials (Dele *et al*, 1997).

2.2 Ahura TruScan™ Handheld Raman Spectrometer

Developed in 2006, the Ahura TruScan™ Raman analyser by Ahura Scientific is a rugged handheld analytical instrument primarily used for rapid raw material identification (ahurascientific.com). Though the device was designed by Ahura Scientific Inc., the company was bought over in 2010 by Thermo Fisher Scientific Inc. (www.spectroscopyeurope.com). The Ahura TruScan™ user manual defines the instrument as light and portable, easily applied in the field and easy sampling as non-contact analysis is possible which reduces contamination of the sample, thus improving safety. This instrument was used throughout the study and the results were compared to those acquired by the DXR Raman spectrometer.

2.2.1 Applications

Apart from its main purpose for raw material identification, the TruScan analyser conducts inspection of intermediate and final products by examining their chemical composition and carries out process troubleshooting and counterfeit identification. It has been shown to ably identify polymers and explosives and also having potential to be applied to body fluid identification. It also examines coatings, dyes, and fillers to create unique spectra known as chemical 'fingerprints'. It can also identify aqueous solutions and components of solid/liquid combinations by use of its mixture analysis software. As it is a non-contact technique, it greatly reduces, and to an extent, eliminates potential exposure to highly potent active pharmaceutical ingredients (APIs) and hazardous chemicals. This is due to the device being able to conduct point-and-shoot analysis through glass containers, plastic bags, clear gel caps and blister packs. (ahurascientific.com).

2.2.2 Advantages and Disadvantages

The main advantage of the Ahura TruScan™ Raman analyser is that it is portable; therefore it can be used in clean, internal laboratory settings but also in most external places in unpredictable settings. The battery life of five hours

allows for ample analysis time in field deployment situations and a quick switch to an external mains supply through a wall plug transformer is easily done. With the device mostly being non-contact, it greatly reduces the risk of cross-contamination between samples and sample contamination in general. Clear onscreen Pass/Fail results make the handheld Raman fast to use for scientists who require quick results and easy to use for non-scientific people as it eliminates the need for spectral interpretation by trained and qualified personnel.

The main disadvantage is that the spectrometer has a shortened spectral range of 250cm^{-1} to 2875cm^{-1} in comparison to the bench top spectral range of 50cm^{-1} to 3385cm^{-1} . Having a full spectral range is a key factor in differentiating between compounds of similar chemical nature and molecular structure as it provides more complete data which allows for a better validation and verification process. Another disadvantage of the instrument is that the user has no control over the depth of focussing of the laser on the sample, i.e. the user cannot be selective and choose to focus on or below the surface of a gemstone, hence why it is imperative that a clear surface of the gemstone is chosen for analysis so as to avoid false data acquisition.

2.2.3 Basic Theory

TruScan uses a laser wavelength of 785nm on a sample to acquire a Raman measurement. The built-in software which provides a PASS/FAIL result by analysing the spectra is a patent-pending package called DecisionEngine™. The basic theory behind this operating software is stated as for use in detection and identification instruments. This is done using light sources and light detectors for detecting and identifying chemical and biological substances (www.trademarks.justia.com). The software has been designed to provide probabilistic material identification and mixture analysis and to eliminate false material identification. It does this by comparing the sample spectrum to the Discover library and saved methods by which, if there is no significant Raman discrepancy then a PASS result is reported; if there are discrepancies present then a FAIL result is reported. This is based upon the acquired Raman spectrum having a p-value of 0.05 or greater in order to pass a method, thus

meaning the sample spectrum should have a 95% significant match to a stored spectrum. A p-value between 0.001 and 0.05 are at moderate risk of passing the identification method as the sample has similar characteristics to the method, but not enough to confidently assign the sample to one correctly. Samples between these values, also known as risk materials are failed by the software as they could potentially produce false positives. (Ahura TruScan Manual, 2010).

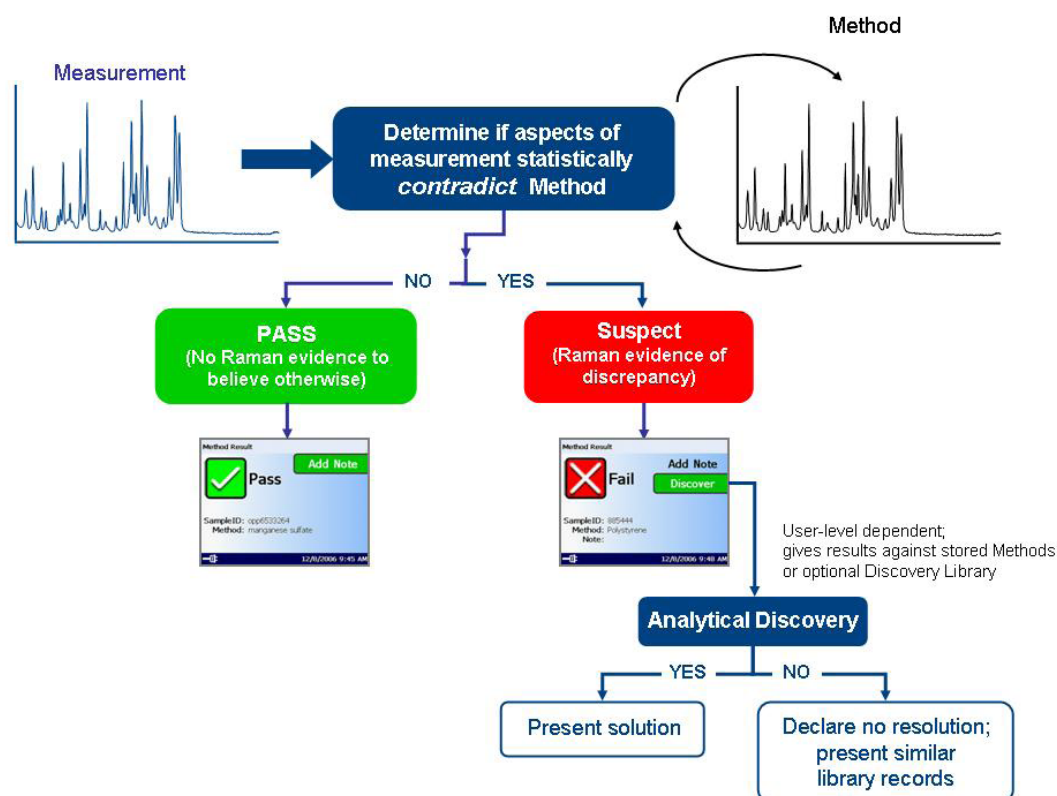


Figure 2.2: TruScan™ logic tree illustrating system logic of the DecisionEngine™ software for material identity verification (Ahura TruScan™ Manual, 2010)

The logic tree in figure 2.2 is illustrating TruScan’s system logic of the *Discover* software. When the TruScan™ presents a “FAIL” result, it gives the option to investigate the material in question so as to establish its identity. This is done by selecting the *Discover* option on the fail screen, whereby DecisionEngine™ compares the measured Raman data with the methods and active signatures

stored in the unit. These methods and active signatures stem from the optional factory Discovery Library and/or the methods and active signatures developed by the user.

2.2.4 Origins of Raman spectra

It is understood that less energy is needed to bend a bond than to stretch it, based on the rationale of the required effort to move the atoms relative to one another. Accordingly, the notion that stretching absorptions of vibrating chemical bonds occur at higher wavenumbers (frequencies) than corresponding bending or bond deformation vibrations is readily accepted. For this possibility it is understood that frequency and energy are proportionally related. Strong intensity bands are considered to be of long-chain structures that may or may not be linear and are attributed to crystallinity and a high degree of regularity; in contrast, weak intensity bands are considered to be indicative of chain branching. The molecular symmetry and bond order of a molecule can have a large impact on the spectrum. Additional bands can be observed due to additional functional groups being added to a basic backbone structure, forming a more complex molecule. These are either directly associated with the fundamental vibrations of the functional groups or indirectly related to interactions which occur amongst the basic substructure or component functional groups (Coates, 2000). Interactions like these can be severe; resulting in overwhelming distortions in the appearance of the spectrum. Spurious bands occurring in a spectrum can also be due to surface contaminants which may possibly be removed by cleaning of the sample. Common contaminants may be oil residue on the surface of the sample from previous testing methods or inclusions of the matrix which the sample originated from. In many cases it is important to know what type of matrix a sample has originated from as the matrix may have a strong Raman spectrum of its own which can overwhelm or mask the sample spectrum.

Identification of the gemstones was based in their characteristic Raman peaks utilizing online searchable databases such as the RUFF™ Project (Downs, 2006), aistRIO-DB Raman Spectra Database of Minerals and Inorganic Materials (RASMIN) (2012) and the University of Siena Department of Science

(2003) as well as consulting previous analyses conducted by Shah (2010). Tables of the main, characteristic vibrations of each stone type can be found in Appendix D.

2.3 Scanning Electron Microscopy coupled with Energy Dispersive X-Ray spectroscopy

Distinguishing natural gemstones from their synthetic counterparts by assessing their chemical properties has been performed by a number of researchers (Hänni, 1982; Schraeder, 1983; Stockton, 1984). The theory behind chemical discrimination between natural and synthetic gemstones is based on the premise that natural stones may contain some non-essential chemical elements in their crystal compound. These elements may not be found in synthetics as they are strictly not needed for the formation of the stones. Likewise, some elements used in the synthetic manufacture process which may be contaminated during production are most likely to be found in larger quantities in synthetic rather than natural stones (Stockton, 1984). Depending on their formation process and provenance; gemstones exude different colours and qualities. These varying factors could be contributed to the formation conditions of each stone, especially the trace elements (colour-inducing chromophores) responsible for colour incorporation. Consequently, it can be theoretically presumed that natural and synthetic discrimination in relation to their geological location and formation can be assisted by conducting chemical analyses of the gemstones. For this study, SEM/EDX will be briefly employed to determine the type and amount of chemical properties in natural and synthetic stones. The rationale for using this method is solely as a confirmatory/validation technique for any results and conclusions drawn from Raman analysis.

2.3.1 Scanning Electron Microscopy

Scanning Electron Microscopy (SEM) is a widely used technique employed to image the surface of samples. It is also a well suited tool for the examination of structures and crystal orientation on a micrometer or sub-micrometer scale. It provides outstanding image resolution, unique image contrast and a large depth

of field and focus on the surface of the desired specimen (www.mos.org). The principles and applications of scanning electron microscopy to electrochemical power sources are explained. The general features of an SEM are (1) generation and focusing of the electron beam over the samples, (2) interactions between electrons and atoms in the sample producing the analytical signals, (3) detection and recording modes, and (4) image reconstruction from secondary or backscattered electrons (Marassi and Nobili, 2009).

2.3.1.1 Basic Theory

The fundamental apparatus is a type of electron microscope which consists of an electron gun and two or more electromagnetic lenses operating in vacuum. The use of 30kV as the acceleration voltage in the SEM beam was considered routine in the 1980s. In recent times, there has been a diverging trend with advantages of lower beam energies in the SEM becoming apparent; with operation typically occurring between 5-10kV or even lower for some analyses (Garratt-Reed and Bell, 2003). For each kV of voltage applied, each electron has 1 keV of energy. Adjusting the kV allows the assignation of a specific amount of energy to each electron (Sprawls, 1995). For routine analysis the electron gun generates free electrons and accelerates these electrons to energies in the range of 1-40 keV. The focused, finely collimated electron beam is processed into a small probe and scanned in a raster across the solid surface of the specimen. Interactions between the beam and the sample result in the emission of electrons and photons as the electrons penetrate the surface. The ending product of the electron beam collision with the surface topology (physical features) of the sample is a clear image of the surface (Ebnesajjad and Ebnesajjad, 2006).

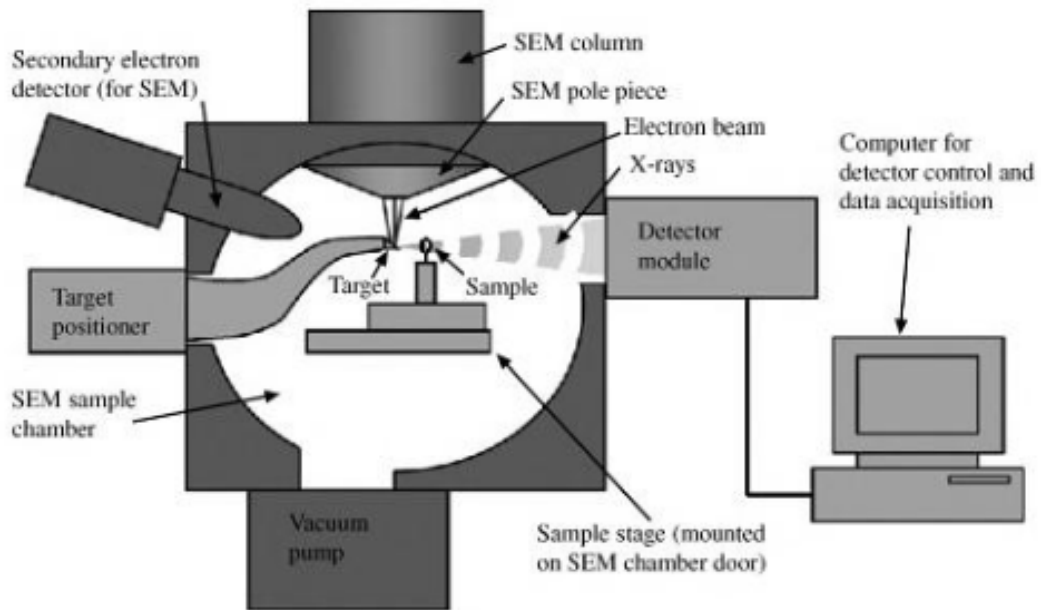


Figure 2.3: diagram of the main components of a scanning electron microscope: electron column, scanning system, detector(s), display, vacuum system and electronics controls, all depicting a typical sample analysis process (Thomas and Steven, 2009)

Variation in the characteristics of a specimen, such as composition or topography, determines the strength of resulting emissions of signals, which can differ from sample to sample. The intensity of the display cathode ray tube is directly modulated by these signals. The electron beam of the SEM and the display cathode ray tube are scanned synchronously resulting in a two-dimensional image of the sample being projected (Ebnesajjad, 2010). The SEM shows very detailed three-dimensional images at much higher magnifications than is possible with a light microscope. The images created without light waves are rendered black and white.

2.3.2 Energy Dispersive X-Ray spectroscopy

Energy Dispersive X-Ray analysis (EDX), also referred to as EDS and EDAX, is an x-ray technique used to identify the elemental composition or chemical characterisation of a sample, right down to the size of the sample being a few cubic micrometers. The atoms on the surface of a sample are excited by the SEM electron beam, emitting x-rays with specific wavelengths which are

characteristic of the atomic structure of the elements (Ebnesajjad and Ebnesajjad, 2006). It is these x-rays that are analysed by the EDX spectrometer, yielding the composition of the atoms on the sample surface. The x-rays are produced from shell transitions caused by interactions between the beam and the sample. EDX detectors were initially developed in the 1960s for nuclear applications. Application of these detectors to analysis of the SEM occurred around 1970 and was an immediate success. By 1980, manufacturers had adapted their SEMs to accept EDX detectors all whilst designing newer models to improve their performance as microanalytical tools; with vacuum improvement being a priority. The difference in x-ray detectors used in the 1970s to those used today lie in the technical detail. These details include highly improved resolution, sensitivity to soft x-rays, and the predictability of characteristics and collection. Due to these improvements, EDX analysis in the electron microscope has become an indispensable tool in a wide range of applications efficiency (Garratt-Reed and Bell, 2003). Energy dispersive spectroscopy is introduced to illustrate the potential of this technique for qualitative and quantitative elemental chemical analysis of natural and synthetic gemstones.

2.3.2.1 Basic Theory

Energy dispersive x-ray spectrometers employ pulse height analysis. Characteristic x-rays are generated at or near the surface of a sample when an electron beam strikes it; typically from an SEM. These characteristic x-rays are used to identify the chemical composition and measure the abundance of elements in a sample. A solid state semiconductor detector is used to accumulate x-rays at all wavelengths which are produced from the samples so the EDX spectrum with identified peaks can be recorded. This is done by giving output pulses proportional in height to the x-ray photon energy which is used in conjunction with a pulse height analyser, typically a multichannel type. This type of detector is used because of its enhanced energy resolution. Incident x-ray photons cause ionization in the detector, producing an electrical charge which is amplified by a sensitive preamplifier located close to the detector. Both detector and preamplifier are cooled with liquid nitrogen which is used to minimise

electronic noise. For this, Si(Li) or Si drift detectors (SDD) are commonly in use. Ideally, the surface of the sample needs to be flat and smooth as the sample may produce artifacts in the EDX spectrum due to non-uniform absorption and blockage of x-rays (Thomas and Steven, 2009).

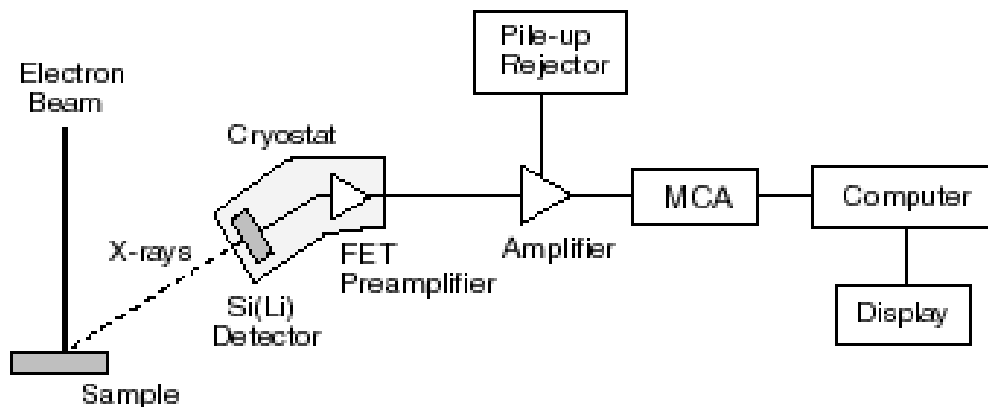


Figure 2.4: schematic representation of an energy-dispersive spectrometer (Goldstein *et al.* 1981)

2.3.2.2 Advantages and Disadvantages

SEM has rapid, high-resolution imaging and can do quick elemental identification of a sample. It also possesses a good depth of field and is a versatile platform which supports many other tools. Only a small sample size of a few cubic micrometers is required for analysis and the humidity and temperature within the chamber can be adjusted to suit the specimen. EDX is capable of quick “first look” analysis, is versatile, inexpensive and widely available. It can also be quantitative for flat, polished, homogeneous samples; making it ideal for cut gemstone analysis. Being a Windows based system allows for ease of use of the equipment. The limitations of SEM analysis begin with the need for the sample to require vacuum compatibility. The size of the sample may also be an issue for larger samples as size restrictions of the chamber may require cutting of the sample. With EDX analysis the limitations are mainly based on the sample as samples that are not flat, polished and homogeneous will only acquire semi-quantification. There is also a limited

sensitivity for low-z elements (e.g. Li, Be, B) as they possess a higher electron density. It is possible for minor components of a sample to be misidentified or omitted unless a systematic approach to elemental identification is used. These can include the consideration of X-ray line families, spectral artifacts, escape peaks, sum peaks, and overlaps. Several methods may be employed to resolve overlaps with the most common being to increase the live time count and/or the processing time of the pulse processor to improve spectral resolution. Like SEM, size restrictions and vacuum compatibility apply (www.eaglabs.com; www.nd.edu). Another limitation specific to the instrument is that the operator must have knowledge of the composition of the sample in question. This is due to the operator needing to manually input the desired elements they believe to be present within the sample into the machines software. The analysis process will only look for those particular elements highlighted and will then provide a percentage of each of those elements, if present, within the sample.

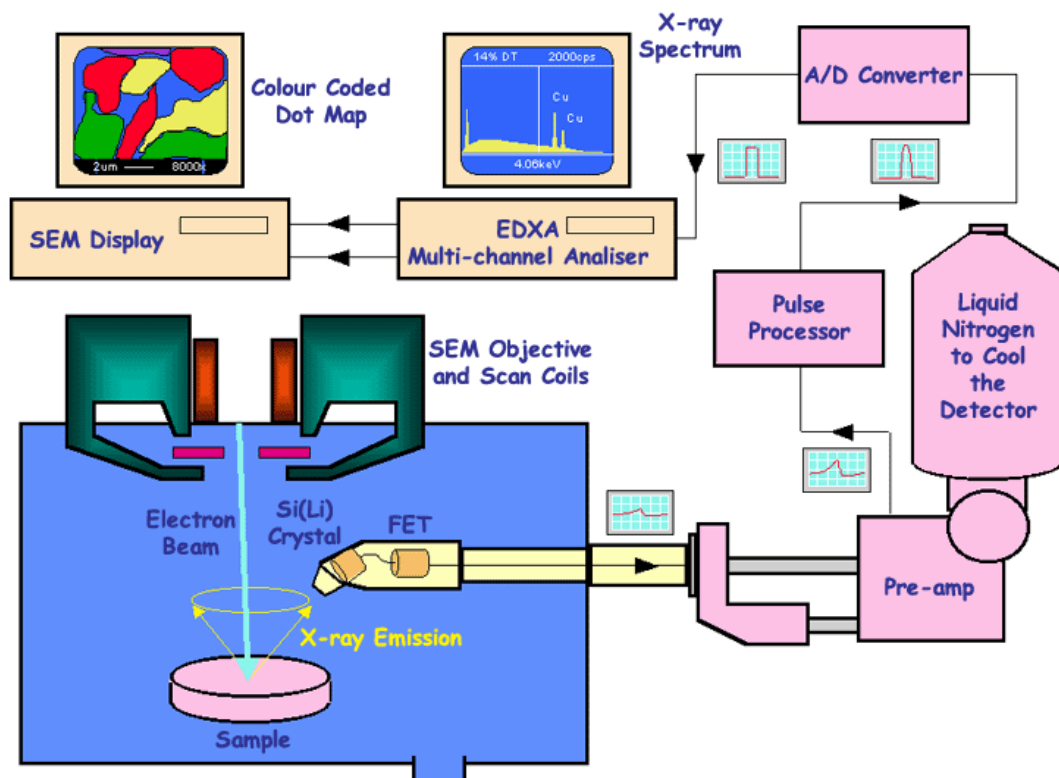


Figure 2.5: simplified SEM/EDX schematic of the overall analysis process (www2.rgu.ac.uk)

2.3.2.3 Qualitative Analysis

For qualitative analysis the sample x-ray energy values from the EDX spectrum are compared to known characteristic x-ray energy values to determine the presence of an element in a sample. Atomic numbers of elements ranging from beryllium to uranium can be detected. The minimum detection limits vary depending on the element and sample matrix. For this study, 0.05%wt is the absolute borderline limit for element detection.

2.3.2.4 Quantitative Analysis

Results can be obtained quantitatively from the relative x-ray counts at the characteristic energy levels for the sample constituents. Semi-quantitative results can be readily obtained without standards by using mathematical corrections based on the analysis parameters and the sample composition. Ultimately, the accuracy of standardless analysis depends on the sample composition. Greater accuracy of the results would be obtained if known standards are used which have similar structures and compositions to that of the unknown samples.

3 Experiment

3.1 Materials for Raman spectroscopy

The gemstones for Raman spectroscopy analysis were obtained from Dr. Brian Jackson; Research Curator of Mineralogy at the National Museum of Scotland.

Table 3.1: A list of all the types of gemstones for analysis

	Ruby	Sapphire	Emerald	Spinel
Natural	3	4	14	8
Chatham	1	4	1	
Kashan	5	0		
Knischka	3	0		
Ramaura	1	0		
Verneuil	0	5		
Linde Star	1	0		
Czochralski	1	6		
Russian Flux			1	
Lechleitner	5	9	1	
HST	4	5		
Kyocera	1	1		
Seiko	1	0		
Coated	0	1		
Biron			1	
Lennix			1	
Unknown Synthetic Production				7

Unknown Origin	3	1	3	5
TOTAL	26	32	22	20

A glass slide (measuring 75mmx25mmx1mm) and a pea-sized amount of Blu-Tack were used to firmly mount each stone in place.

3.2 Materials for SEM/EDX

A total of 12 stones were analysed; four rubies, four sapphires and four emeralds.

Table 3.2: stones for SEM/EDX analysis

Stone Type	Natural	Synthetic
Ruby	1. Ruby Afghanistan	3. 4.63ct Verneuil Ruby
	2. 2.98ct Burma Ruby	4. 1.76ct Verneuil Ruby
Sapphire	1. 2.95ct Sri Lanka Sapphire	3. 3.52ct Verneuil Sapphire
	2. 1.55ct	4. 2.58ct Chatham Sapphire
Emerald	1. 0.58ct Russia Emerald	3. 1.04ct Russia Flux Emerald
	2. 0.69ct Pakistan Emerald	4. 0.92 Biron Hyd. Emerald

3.3 Analytical Instruments

3.3.1 DXR Raman spectrometer Instrument

Raman spectra were obtained with a Thermo Scientific DXR Raman Microscope and DXR SmartRaman™ Spectrometer. Using the DXR Raman; the Smart background tool was used to supply a background reading for each sample collection. Samples were then excited by either a 532nm or the 780nm (I) emission line of a low-power, externally stabilised diode laser. The aperture size and power of the laser spot on the surface of a sample was either a 25µm or 50µm pinhole at 10mW or 14mW of power respectively. A microscope objective with 10x magnification was used at all times. The spectrometer operated with an applied spectral range between 100cm⁻¹ to 3385cm⁻¹. A

consistent exposure time of a one minute time period was applied to each sample spectrum, allowing for a signal to noise ratio (SNR) of 100:1, unless otherwise stated.

All spectra collected were saved and stored on a PC linked to the Thermo Scientific DXR Raman using the OMNIC 8 Raman dispersive software. The spectra obtained are displayed as collected and not subject to data manipulation.

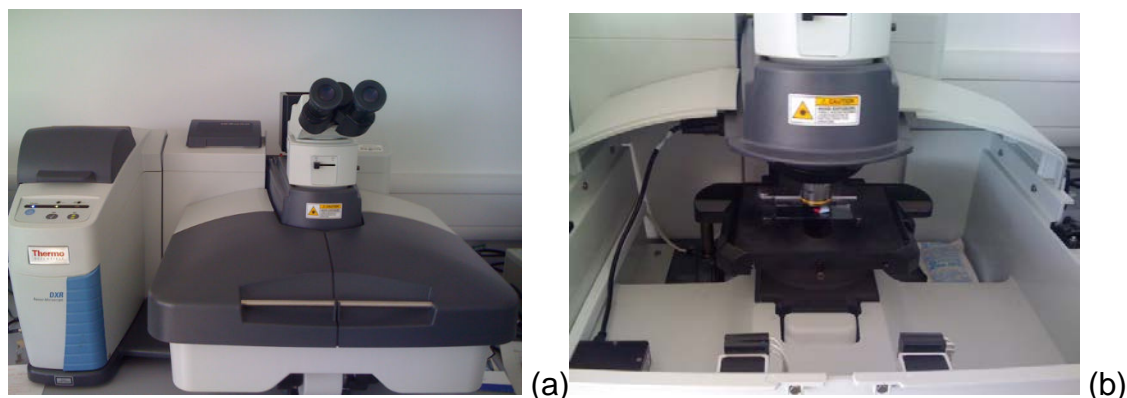


Figure 3.1: Pictures of the Raman instrument. (a) the overall view of the Raman spectroscope. (b) with the doors open, a view of the microscope and sample stage.

3.3.1.1 Method of Analysis using a Standard Operating Procedure (SOP)

Following on from previous work conducted in this field, the same favourable Raman spectroscopy settings were used again this time. A previous Raman SOP constructed by the author was used to maintain a high level of consistency throughout the experiment in order to obtain reliable results. A polystyrene standard was used to calibrate the system each time before all analysis sessions were conducted. The SOP for the DXR Raman spectrometer is available in Appendix A.

3.3.1.2 Method Development for Analysis of Gemstones using Raman Spectroscopy

Previous analysis of gemstone samples was carried out by mounting the gemstone on a standard glass microscope slide with "Blu-Tack". The slide

would then be placed into the Raman spectrometer stage and the laser beam focused on the table of the gemstone using the microscope. Although this method has previously been successful; some papers had stated that the optical properties of gems change with different orientations. An example of this is in a paper by Huong (1999) whereby the author states that depending on its orientation a single crystal alone can give up to six different spectra. To test this theory, the gemstones are now mounted both upright and at a 90 degree angle thus exposing the smooth straight sides of the table and pavilion of the gem to the laser beam respectively; as is seen in figure 3.2. Analysis conducted in this manner will see the crystal C-axis (vertical crystallographic axis) parallel and perpendicular to the laser beam. As the laser is of a depolarised nature (the vibrations are not restricted wholly or partially to one direction) it is expected that there will not be significant differences, if any, in the spectra collected from the top and side orientations. It is noted that Raman shifts are reproducible to $\pm 5 \text{ cm}^{-1}$. This has been established in previous works by Shah (2010); by conducting repetition analyses thrice per stone on different areas of the table facet and then calculating the average shift in the peak number.

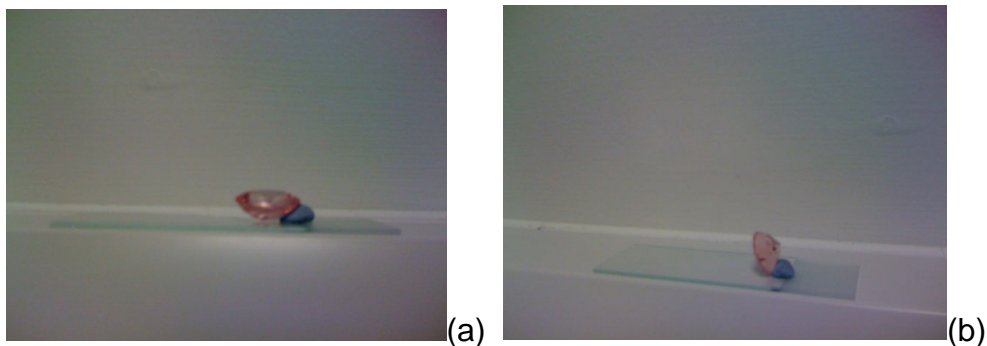


Figure 3.2: gemstone mounted on a glass slide with “Blu-Tack” both upright (a) and sideways (b) at a 90° angle

3.3.2 Ahura TruScan™ Handheld Raman Spectrometer

3.3.2.1 Product Specifications

The handheld Raman spectrometer varies greatly in many aspects in comparison to a conventional bench top Raman's specifications. It weighs less than four pounds (1.8kg) and has a rugged design; making it ideal for use in harsh external conditions. Its rechargeable battery has an approximate longevity time span of 5 hours when disconnected from a mains supply. The device has a built-in, Class 3B, 785nm laser with a maximum laser output power of 300mW which is auto-adjusted by the spectrometer, an automatic exposure feature and a spectral range of 250cm^{-1} to 2875cm^{-1} (ahurascientific.com).

3.3.2.2 Instrument

Gemstones from the National Museum of Scotland (NMS) were analysed using the handheld Ahura TruScan™ Raman spectrometer.

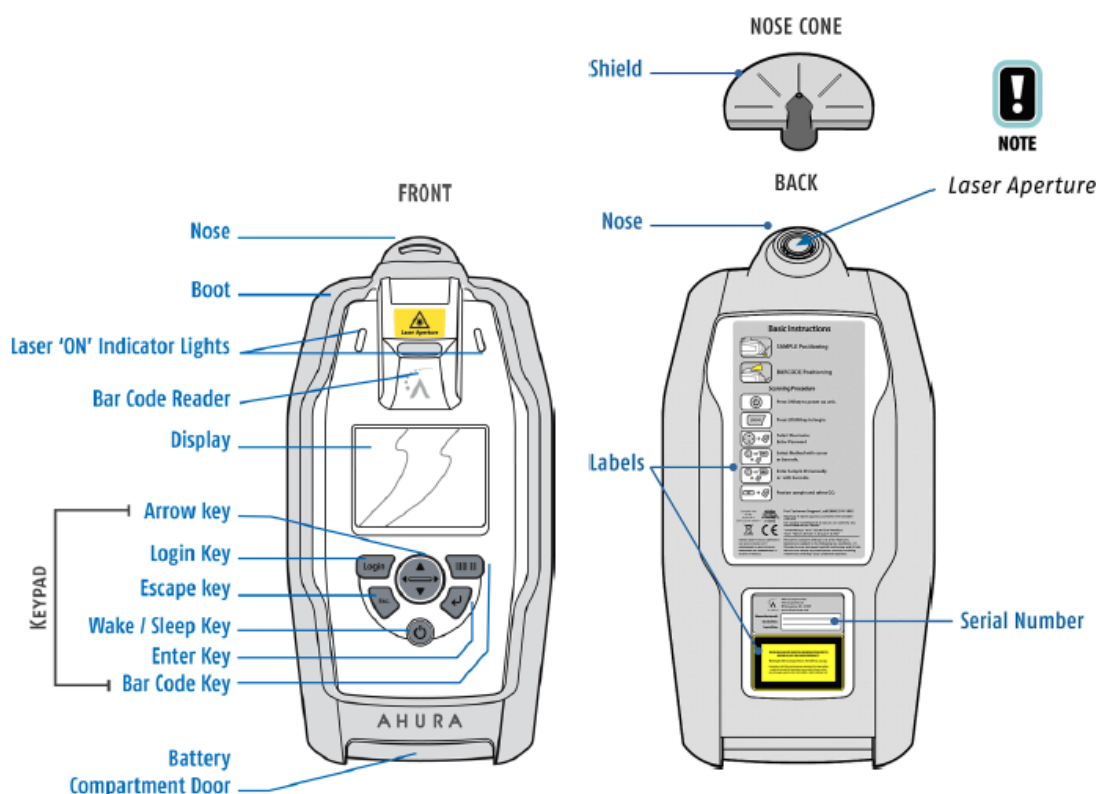


Figure 3.3: Front and back views of the Ahura TruScan™ unit depicting the controls and accessories (ahurascientific.com)

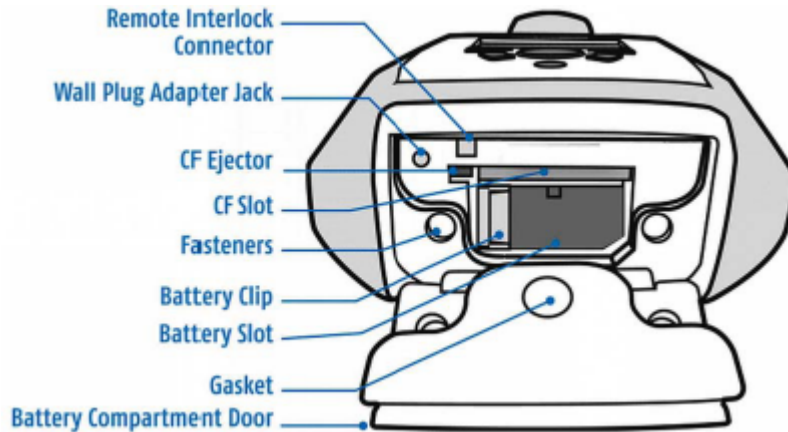


Figure 3.4: Battery compartment area; also the access area for the memory card (CF Slot) (ahurascientific.com)

3.3.2.3 Method

As Raman spectroscopy is an optical analysis technique, it does not require direct contact with the sample. Upon analysis, the Ahura TruScan™ instrument emits light at a single focused wavelength, then collects the light scattered by the sample, thus creating a unique molecular fingerprint. The focal point occurs at the end of the nose cone and onto the surface of the gemstone. The fingerprint made by the sample indicates its composition, which is then automatically compared to the on-board, integrated library.

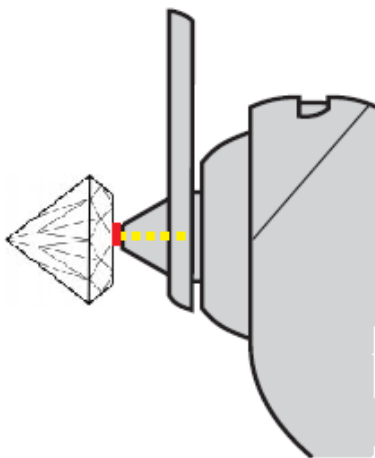


Figure 3.5: Diagram depicting the TruScan with attached nose cone performing Raman analysis on the gemstone; the red dot being the laser beam hitting the surface (adapted from ahurascientific.com).

After consulting the Ahura TruScan™ manual and through laborious trial and error sessions, it became evident that the barrel-shaped nose cone was needed for gemstone analysis, as this particular cone helped yield the best spectra. It is imperative that the laser is placed at the right focal point in order for it to be effective. The focal point of the laser without the nose cone is 18mm, whilst with the nose cone it is 3mm. *NB: The nose cone does not change the position of the focal point. Its only purpose is to help manually position the unit so that the focal point is in the correct place when a point-and-shoot scan is performed.*

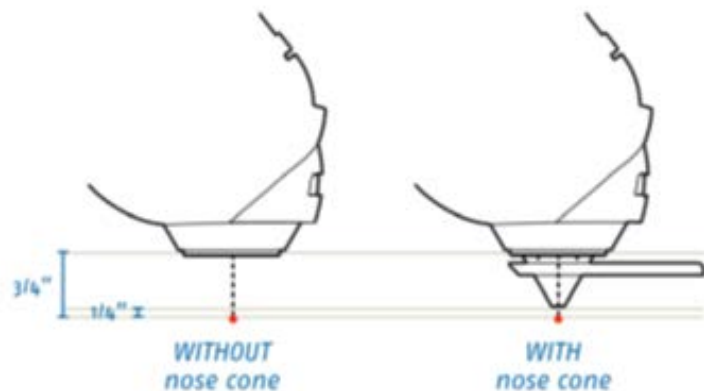


Figure 3.6: nose and nose cone configurations, showing the measurement of the laser focal point with and without the nose cone attached



Figure 3.7: stone attached to the barrel-shaped nose cone for analysis using sellotape

The stones had to be analysed in the manner as seen in figure 3.7 in order to acquire good spectral results. The point-and-shoot method was provisionally applied at the initial stages of the studies and was established that either a

Raman spectrum was unattainable or illegible due to a lack of Raman peaks. Therefore, this method of attaching the stone directly to the nose using sellotape was developed. Not only is analysis easier this way but clearer spectra with more detail are obtained.

The following figure depicts both the bench top and handheld Raman spectrometers side by side, showing the size difference between the two. Table 3.2 outlines the different operational specifications for each device.



Figure 3.8: size comparison of DXR bench top Raman spectrometer and TruScan handheld Raman spectrometer

Table 3.3: specifications comparison of the DXR and TruScan Raman spectrometers

Specifications	DXR	TruScan
Raman spectral range	50cm ⁻¹ -3385cm ⁻¹	250cm ⁻¹ -2875cm ⁻¹
Laser excitation wavelength	532nm/780nm	785nm
Laser power output	10mW/14mW	300mW

3.3.3 Scanning Electron Microscopy coupled with Energy Dispersive X-Ray spectroscopy

3.3.3.1 Sample Preparation

Since the electron probe analyses only to a shallow depth, specimens should be well polished so that if there are any surface contaminants or there is surface roughness then this does not affect the results. Sample preparation is essentially as for reflected light microscopy, with the provision that only vacuum compatible materials must be used.

In principle, specimens of any size and shape (within reasonable limits) can be analysed. Holders are commonly provided for specimens of 25mm (1") diameter and for rectangular glass slides. Any acquired standards are either mounted individually in small mounts or in batches in normal sized mounts.

Many samples are electrically non-conducting and a conducting surface coat must be applied to provide a path for the incident electrons to flow to ground. The usual coating material is vacuum-evaporated carbon (~10nm thick). This has a minimal influence on X-ray intensities on account of its low atomic number, and (unlike gold, which is commonly used for SEM specimens) does not add unwanted peaks to the X-ray spectrum (micron.ucr.edu).

3.3.3.2 Method

Chemical analyses were conducted using Scanning Electron Microscopy coupled with Energy Dispersive X-Ray Spectroscopy (SEM/EDX) at the National Museum of Scotland. The machine had a CamScan microscope with a backscattered electron, secondary electron and absorbed emission detectors with a ThermoNoran EDX (LN2 cooled doped silicon X-ray detector). The detection limits of the machine are approximately 0.1 oxide %wt. for most elements; though quantification for elements around this measurement is difficult. *NB: Quantities below 0.5%wt are at trace level and quantities below 0.05%wt cannot be guaranteed as present as they are below the detection limit (bdl).*

3.3.3.3 Method Development

As this was the first time any analysis was conducted at NMS using the SEM/EDX; an SOP method had to be developed. The SOP was consulted throughout the analysis process in order to conduct identical analyses each time. This was done to ensure standard repeatability sampling measures were applied, which in turn would ensure the integrity of the results. The stones were examined using a CamScan MX2500 SEM in controlled pressure (Envac) mode. Elemental analysis was provided using a Noran Vantage EDX system and processed using Vista software. The specific conditions for analysis are listed in the table below:

Table 3.4: specifications for sampling measures

Specifications
20kV accelerating voltage
X50 magnification
4 quadrant fluorescence back scatter electron detector (BSC)
5.00 spot size
Fully open lower aperture
10Pa chamber pressure
Si(Li) energy dispersive X-ray analysis (EDX)
200x150µm analysis spot
90s counting time for EDX

4 Results and Discussion

Identification of the gemstones was based in their characteristic Raman peaks utilizing online searchable databases such as the RUFF™ Project (Downs, 2006), the RASMIN© project (2012) and the University of Siena Department of Science (2003) as well as consulting previous analyses conducted by Shah (2010).

4.1 Interpretation of Raman spectra

The vibrational spectrum of any given molecule is considered to be a distinctive physical property which is characteristic of that particular molecule. The Raman spectrum can be used, per se, as a type of fingerprint identification by comparison of an unknown sample to a known standard, to reference material in literature or to computer-based libraries and databases. For the most part, bending and stretching vibrations resulting in the presence of peaks are considered unique for each molecule. An important factor to be noted for successful interpretation of a spectrum is to understand that the basis of interpretation lies not solely on the *presence* of particular peaks within the spectrum but also on the *absence* of other significant peaks.

4.2 Surface analysis of gemstones

For this study the surface was analysed for all the gemstones using a 50µm aperture with the exception of emeralds whereby a 25µm aperture was applied. By analysing the surface and not going beneath it into the stone, it was made sure that only the spectra of the stones were being collected, so as to not gain false spectral results by focusing on any inclusions that may have been present.

4.3 Corundum

4.3.1 Natural Corundum

With the aim of deducing natural from synthetic stones; the surfaces of some natural corundum gemstones were analysed. This will provide an insight into what peaks are expected to be found in natural stones in comparison to those found in synthetics and of the overall spectral shape of the stones. By spectral shape; it is meant that the broadness and sharpness of the peaks should be taken into consideration as this can provide an insight and imply what type of stone is present.

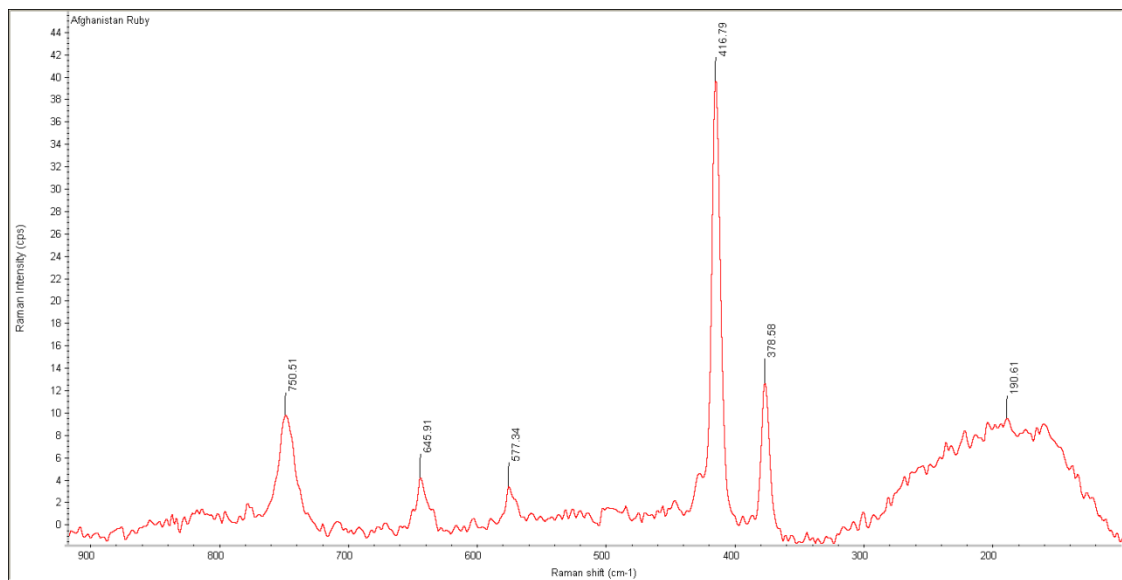


Figure 4.1a: Afghanistan ruby spectrum



Figure 4.1b: Afghanistan ruby

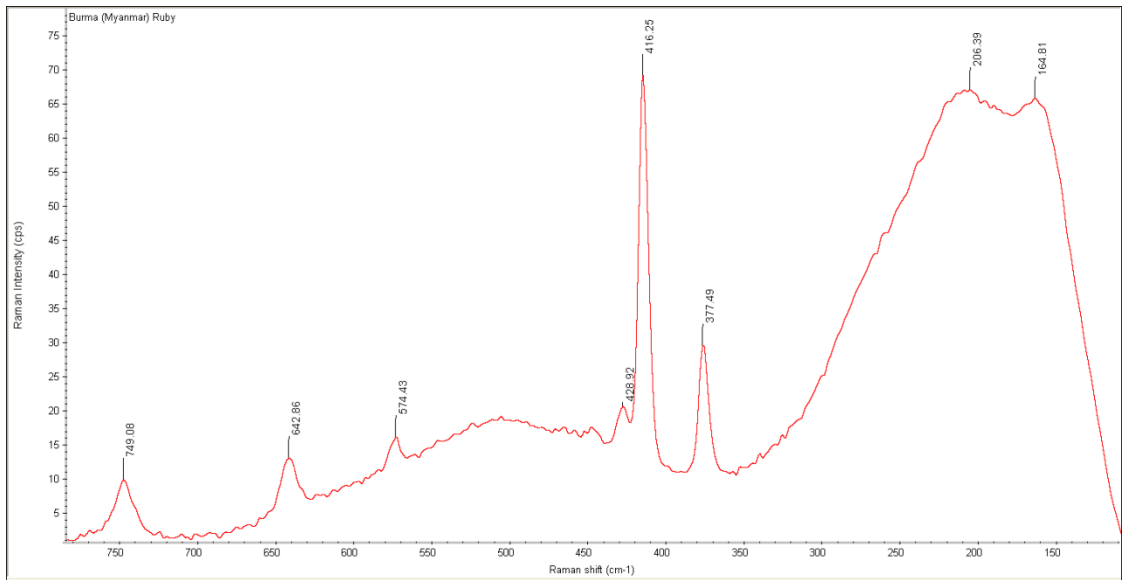


Figure 4.2a: 2.98ct Burma (Myanmar) ruby spectrum



Figure 4.2b: 2.98ct Burma (Myanmar) ruby with visible calcite inclusions

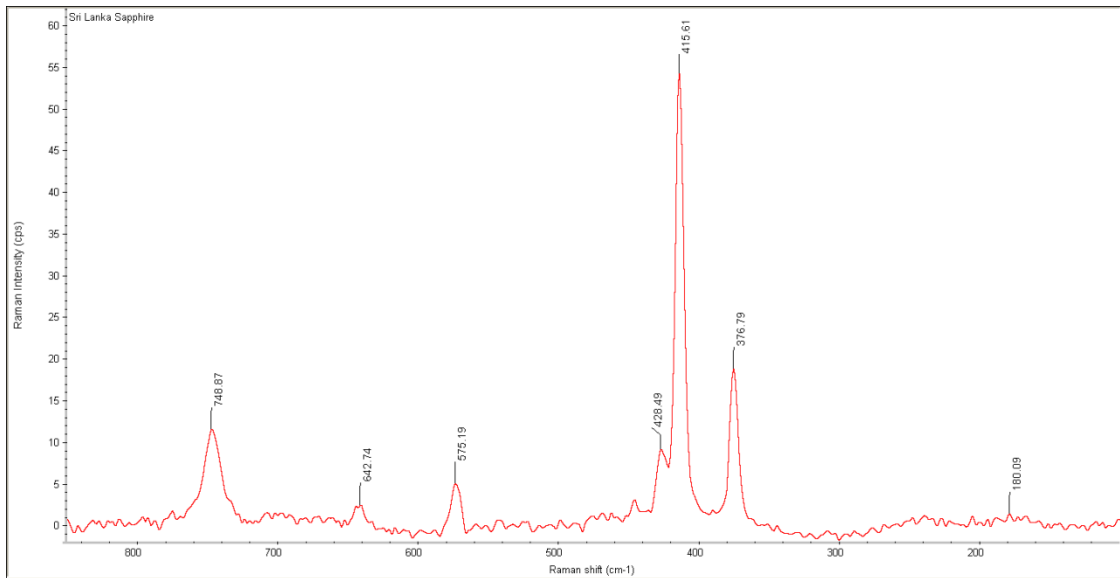


Figure 4.3a: 2.95ct Sri Lanka sapphire spectrum



Figure 4.3b: 2.95ct Sri Lanka sapphire

The spectra of the natural corundum primarily contain peaks at 378cm⁻¹, 417cm⁻¹, 575cm⁻¹, 645cm⁻¹ and 750cm⁻¹ respectively. Most of these peaks tend to be sharp and well defined, making it easier to interpret and label the spectra. The key feature to separating the spectrum of a natural ruby from a sapphire is a broad band occurring in ruby between 100cm⁻¹ and 350cm⁻¹; the remainder of the spectrum has a flat baseline like sapphire.

4.3.2 Synthetic Corundum

The following results are for all the synthetic ruby and sapphire stones made by various production methods; flux, hydrothermal, zone and flame fusion.

4.3.2.1 Chatham stones

The Chatham stones were all produced by the flux growth method. In the spectra below the first stone is a flux grown blue sapphire and is accompanied by four flux grown red rubies. During the time of analysis the first two rubies exuded fluorescence which was counteracted by automatic photobleaching of the sample by the Raman spectrometer.

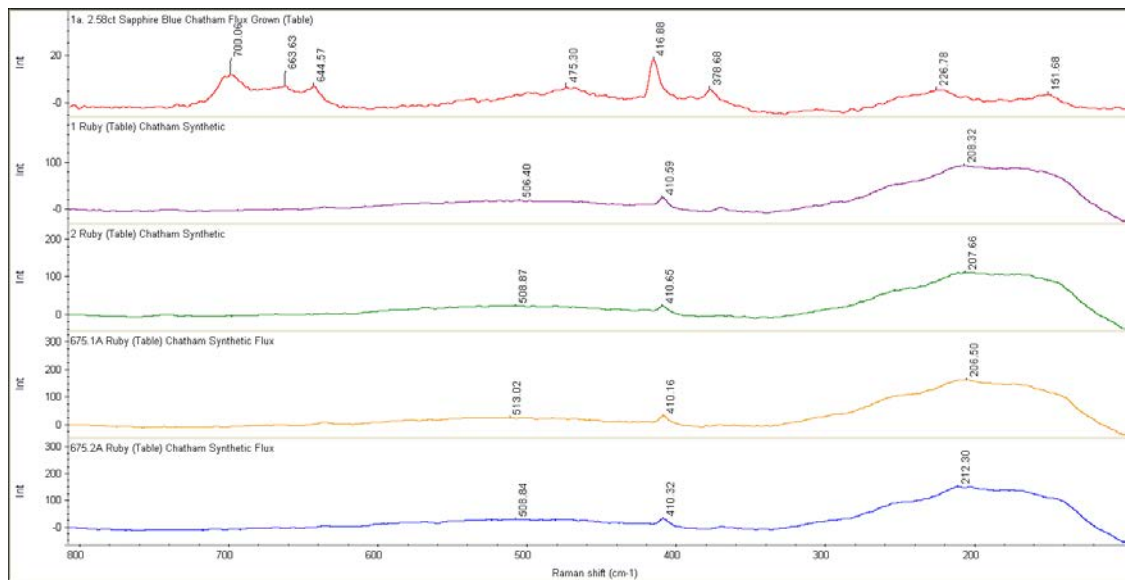


Figure 4.4a: group spectrum of Chatham synthetic stones analysed from the top

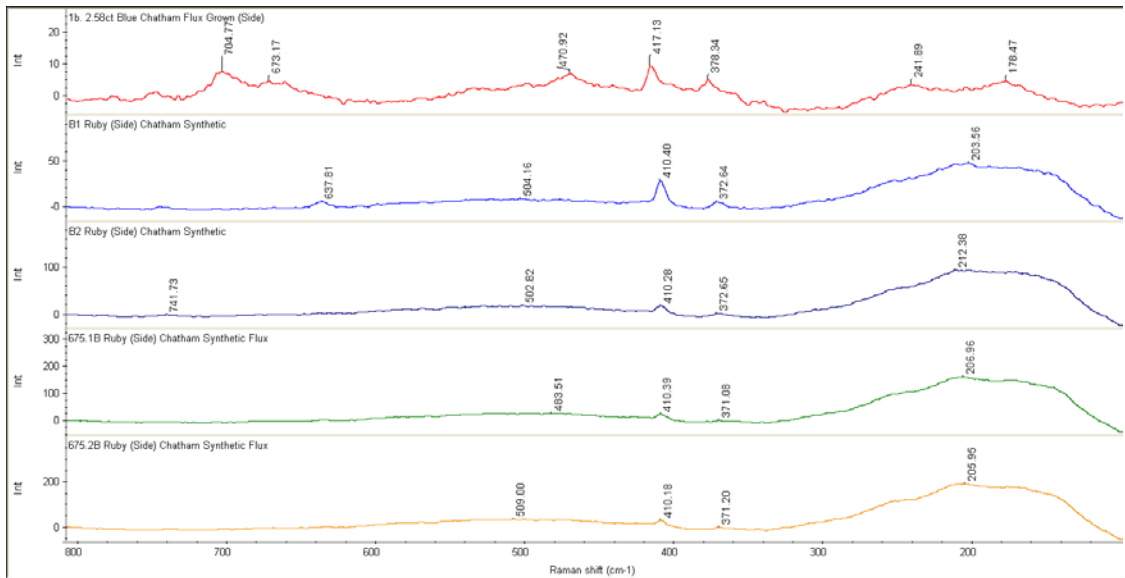


Figure 4.4b: group spectrum of Chatham synthetic stones analysed from the side

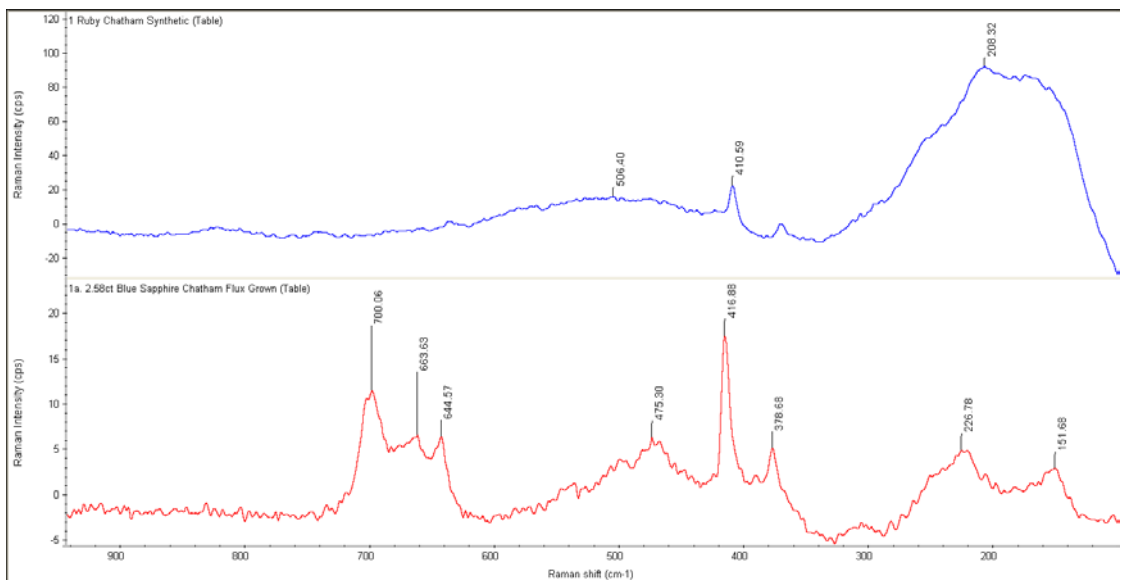


Figure 4.4c: Close up of a 3.54ct Chatham ruby and 2.58ct sapphire respectively, depicting their distinguishing peaks

The spectra depict the analysis of the stones from the top and side respectively. It can be seen that the spectra are roughly the same from both angles of the stone. It should be noted that there is an extra peak at 372cm^{-1} in all the Chatham rubies analysed from the side, which is missing from the top spectra. This could be due to anisotropy of the crystals, whereby the relative intensities of different Raman bands varies dramatically with the changing orientation of the ruby crystals.

4.3.2.2 Kashan stones

All the Kashan stones analysed were rubies. As previously noted; Kashan stones can be grown either by the flux or flame fusion method. It can be seen that figure 4.5a possess a completely different spectrum from figure 4.5c. In total five kashan labelled stones were analysed, of which three gave a spectrum like that of the 1.52ct stone who's production method is unknown and two stones gave a spectrum of the 1.24ct ruby which was labelled as being produced by the flux method.

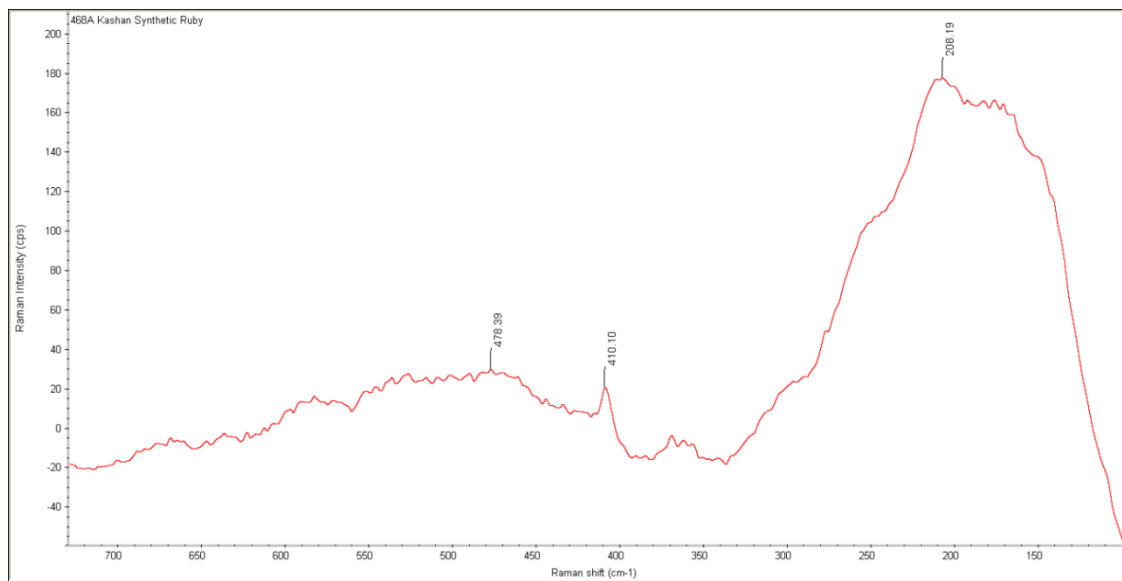


Figure 4.5a: 1.24ct synthetic flux Kashan ruby spectrum



Figure 4.5b: 1.24ct synthetic flux Kashan ruby

This 1.24ct ruby was the only stone which had a known production method; therefore it can be presumed that the latter two stones were grown using the

flux method whilst the other three were possibly created using the flame fusion method. The flux growth method outlined in chapter 1.14 states that there are three possible flux method variations from which rubies can be synthesised. It is possible that those three stones in question could have been synthesised by a different flux process. This would account for the complete difference in the spectra as it is observed that the production methods are likely to vary.

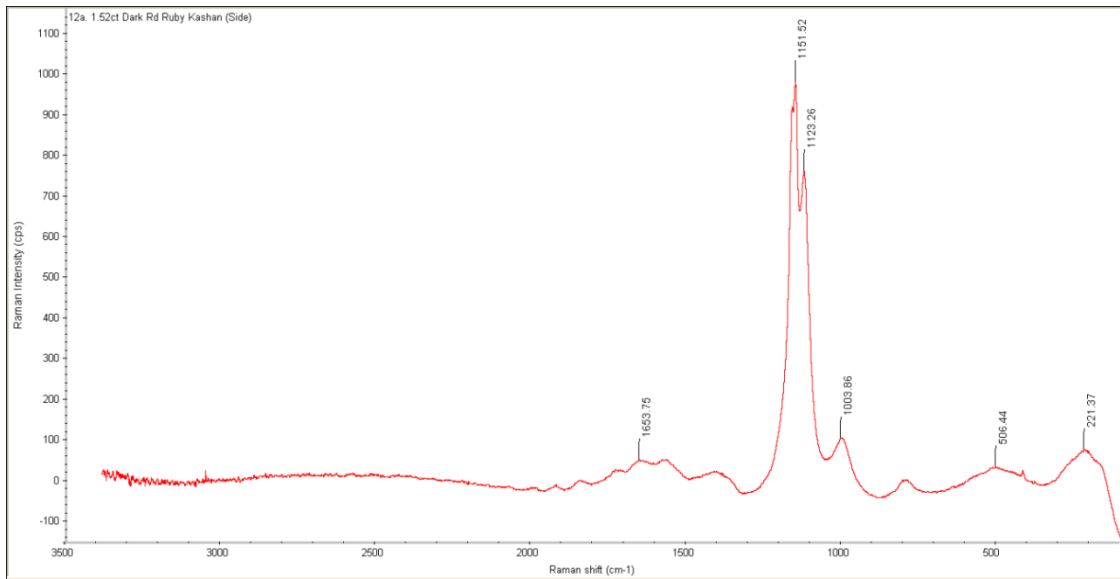


Figure 4.5c: 1.52ct synthetic Kashan ruby spectrum



Figure 4.5d: 1.52ct synthetic Kashan ruby

There is also a possibility that these stones with an unknown growth method could actually have been subjected to some form of treatment; as research has shown that heat treatment in particular can cause the lattice formation to drastically change. If this is the case then the Raman spectrum would be expected to be different.

4.3.2.3 Knischka Stones

Knischka stones are all produced by the flux growth method. In total, three Knischka rubies were subjected to analysis. Below is a spectrum representative of the flux rubies. All three stones possess spectra which are uniform in shape and lack peak numbers and that have characteristically shaped synthetic crystal spectra.

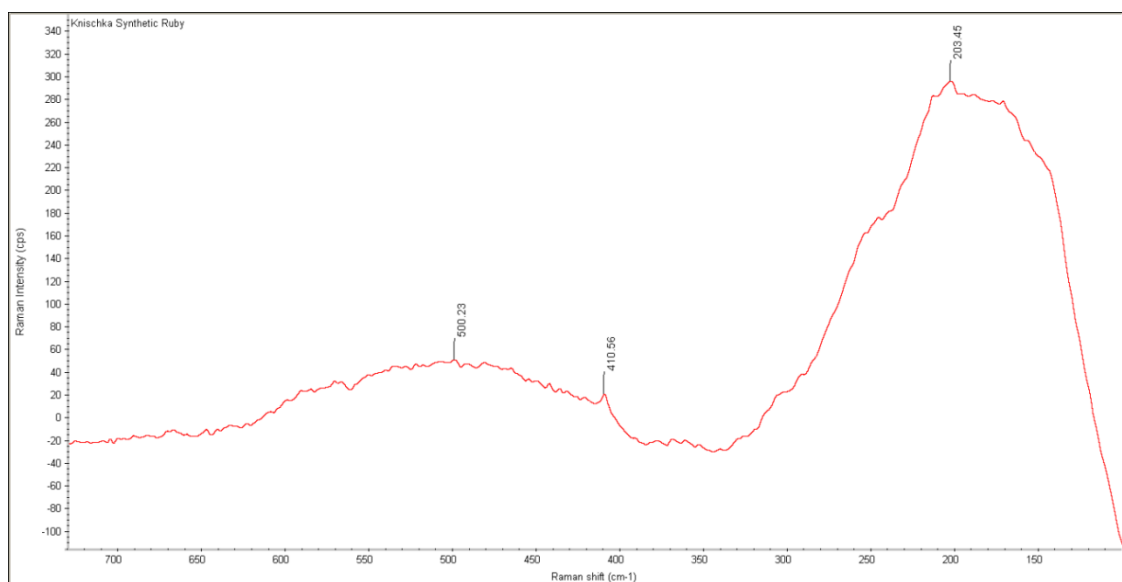


Figure 4.6a: 1.00ct synthetic Knischka flux ruby spectrum



Figure 4.6b: 1.00ct synthetic Knischka flux ruby

4.3.2.4 Lechleitner stones

All Lechleitner stones are grown by the hydrothermal method. In total five rubies and nine sapphires were analysed of which a representative spectrum of each is displayed below. Both the rubies and sapphires have very different spectra but share the same 410cm^{-1} peak which has a stronger intensity in the sapphires. There is a broad band in the 200cm^{-1} region, continuously throughout all the rubies which is absent from the sapphires as this is a characteristic ruby spectral pattern. The sapphires all have recurring peaks at 637cm^{-1} and 745cm^{-1} respectively. Like other synthetic rubies, these peaks do not appear in their spectrum.

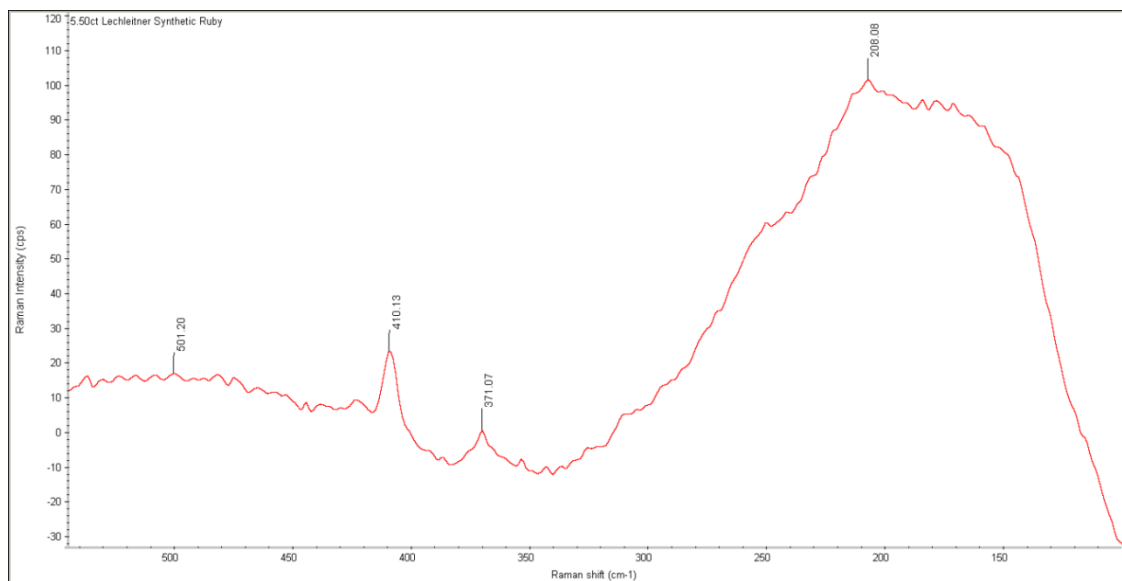


Figure 4.7a: 5.50ct synthetic hydrothermal Lechleitner Ruby

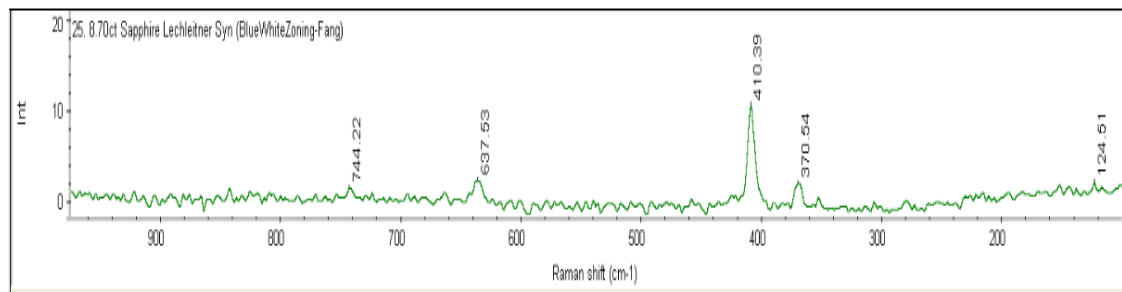


Figure 4.7b: 8.70ct synthetic hydrothermal Lechleitner sapphire

4.3.2.5 Czochralski stones

Czochralski stones are produced by the melt growth method of crystal pulling. Figures 4.8b and 4.8c depict a ruby and sapphire grown by this method. Once again the ruby has a distinct broad band in the 200cm^{-1} region, whilst the sapphire has individual strong intensity peaks. The peaks seen in the sapphire are similar to peaks noted in natural sapphire, especially the peak at 417cm^{-1} which occurs throughout natural corundum. It is maybe possible to believe that Raman spectroscopy cannot distinguish synthetic Czochralski sapphires from natural sapphires. The ruby spectrum is however extremely reminiscent of synthetic rubies of all types.

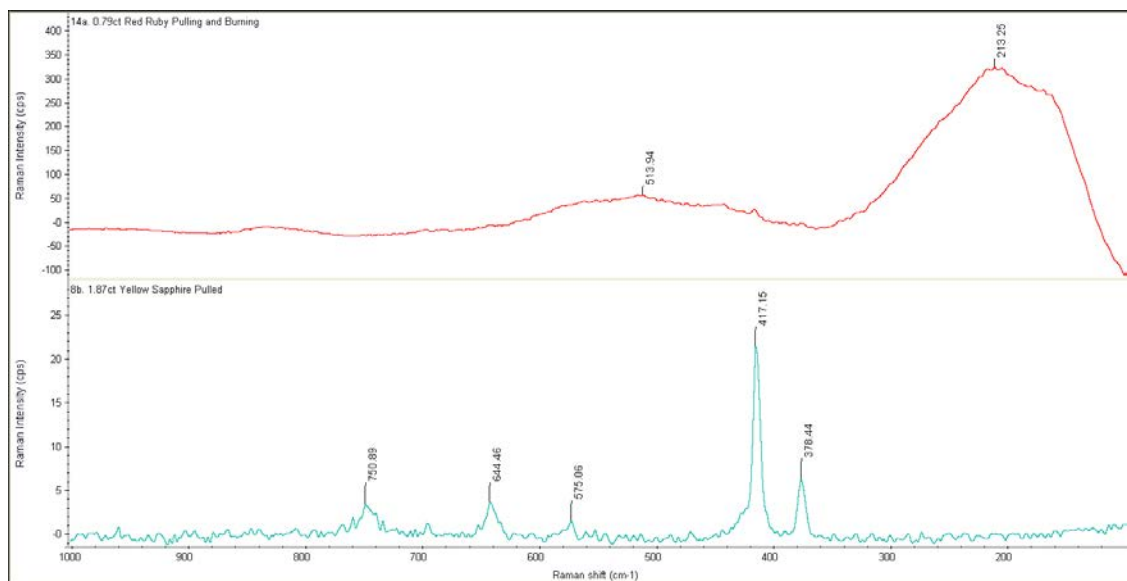


Figure 4.8a: group spectrum of a ruby and sapphire Czochralski pulled gemstone respectively



Figures 4.8b and 4.8c: (b) 0.79ct Czochralski pulled synthetic ruby and (c) 1.87ct Czochralski pulled synthetic sapphire

4.3.2.6 Seiko™ and Kyocera™ stones

All Seiko™ stones are grown using the floating zone method. Kyocera™ stones are generally grown using the zone refining method but are sometimes grown using the crystal pulling (Czochralski) method.

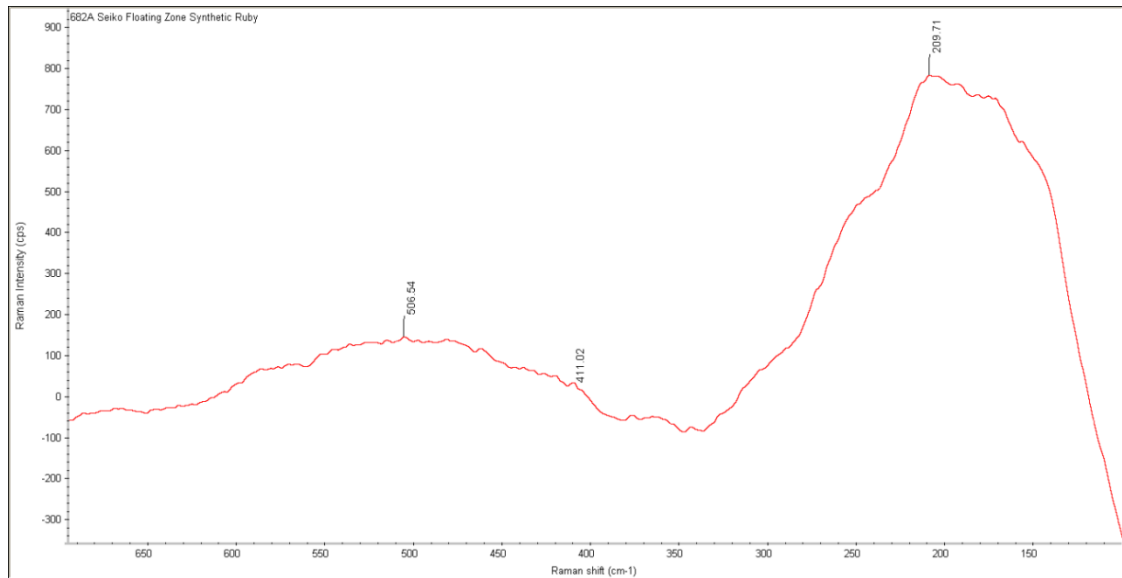


Figure 4.9: synthetic Seiko floating zone ruby

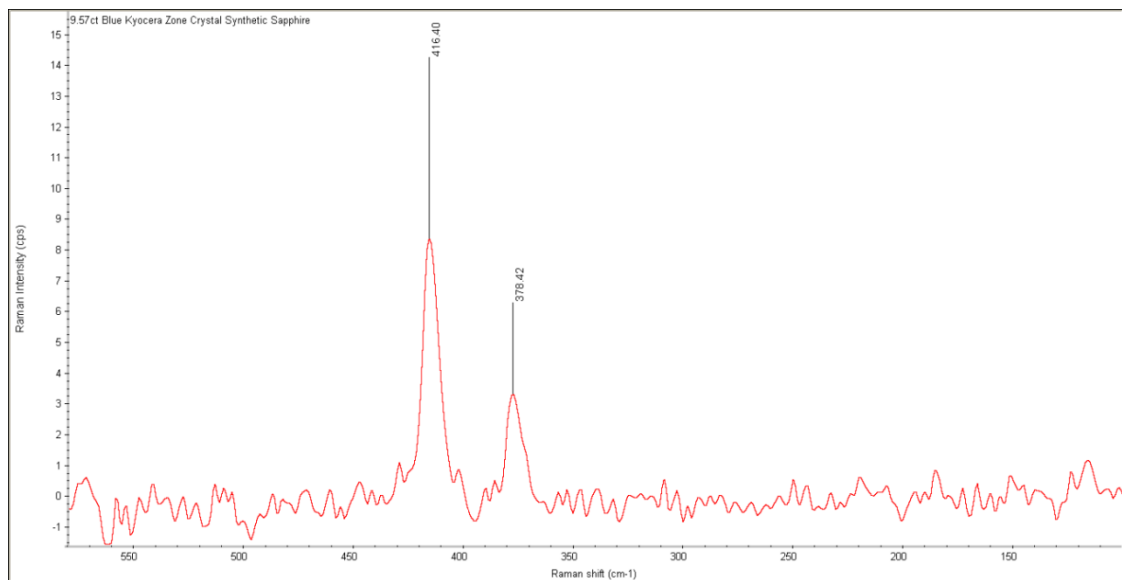


Figure 4.10a: 9.57ct blue synthetic Kyocera zone crystal sapphire spectrum



Figure 4.10b: 9.57ct blue synthetic Kyocera zone crystal sapphire

Again, the ruby spectrum is as expected for a synthetic stone. However, the zone sapphire has quite a bare spectrum only showing two peaks of which one is the characteristic sapphire peak at 416cm^{-1} . The lack of peaks observed could be due to the colour zoning in the sapphire which can be seen in figure 4.10b. The missing spectral peaks could be a result of the laser beam focussing on a clear area of the stone instead of a blue coloured area.

4.3.2.7 Verneuil stones

All seven ruby and 16 sapphire Verneuil stones were produced using the flame fusion method.

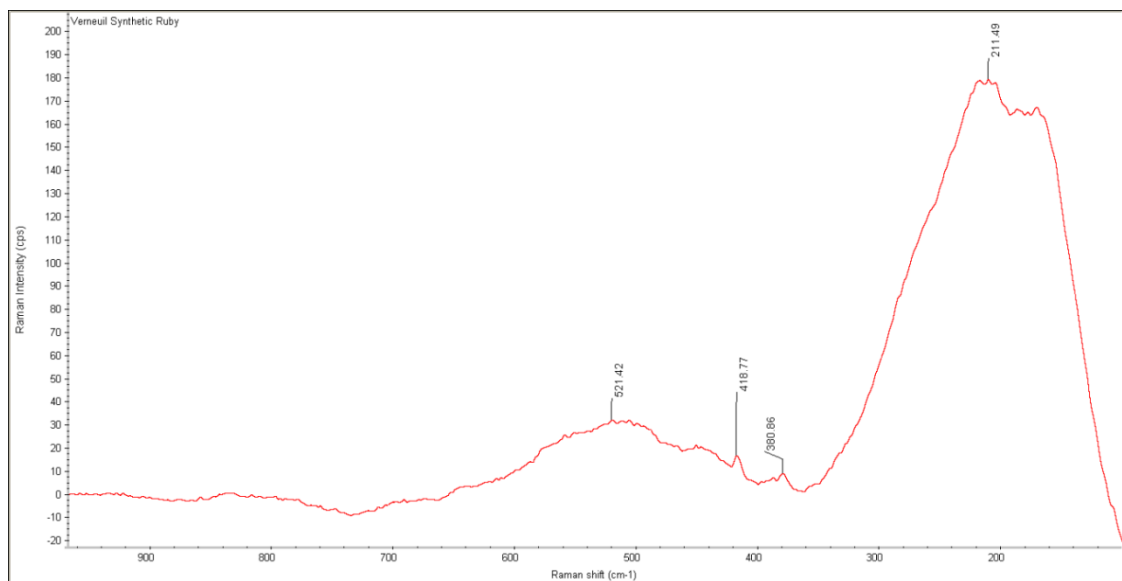


Figure 4.11a: 24.75ct synthetic Verneuil ruby spectrum



Figure 4.11b: 24.75ct synthetic Verneuil ruby

The Verneuil rubies are missing key Raman peaks between the regions of 500cm^{-1} to 800cm^{-1} which are seen in natural rubies. However, instead of 410cm^{-1} , they possess the peak at 418cm^{-1} ; the characteristic peak number present in natural ruby.

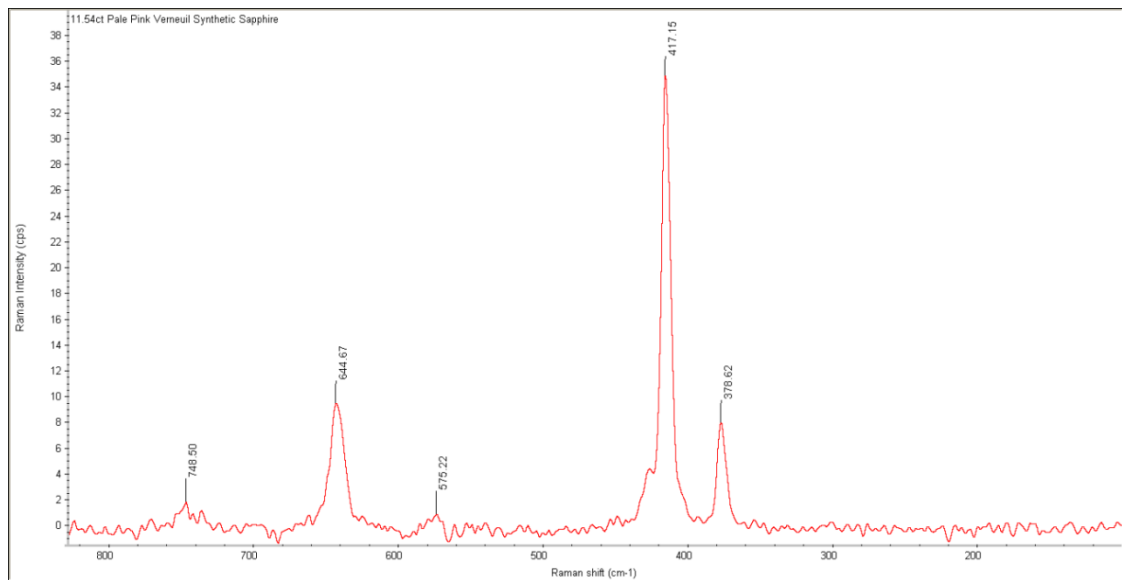


Figure 4.12a: 11.54ct pink synthetic Verneuil sapphire spectrum



Figure 4.12b: 11.54ct pink synthetic Verneuil sapphire

It was noted that all the sapphires had similar or same peak numbers and peak intensities for natural sapphire, particularly the Sri Lankan sapphires, as is seen in comparison in figure 4.13a. This leads to believe that Raman spectroscopy may not be able to distinguish natural from synthetic Verneuil sapphire produced by the flame fusion method. The same can be said for Verneuil ruby as it possesses Raman peaks in with the measurements of natural ruby. It has extensively been noted in literature that Verneuil stones are the easiest of all the synthetics to distinguish from their natural counterparts as they have tell-tale growth patterns (striations) and sometimes contain diagnostic inclusions within them. The Verneuil ruby in figure 4.11b has a glossy, glassy look and texture and is internally clean, void of any inclusions. The pink sapphire is also glassy in appearance and internally clean.

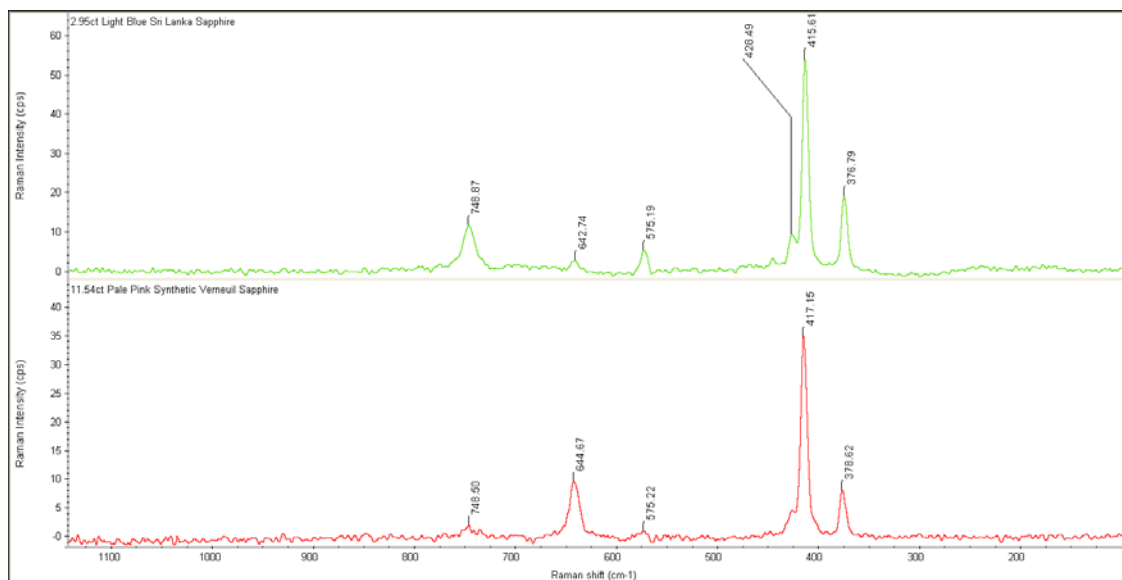


Figure 4.13a: group spectrum of a 2.95ct light blue natural Sri Lankan sapphire and an 11.54ct pink synthetic Verneuil sapphire.



Figure 4.13b: 2.95ct Blue Sri Lanka sapphire

4.3.2.8 Frosted Surfaces of Gemstones

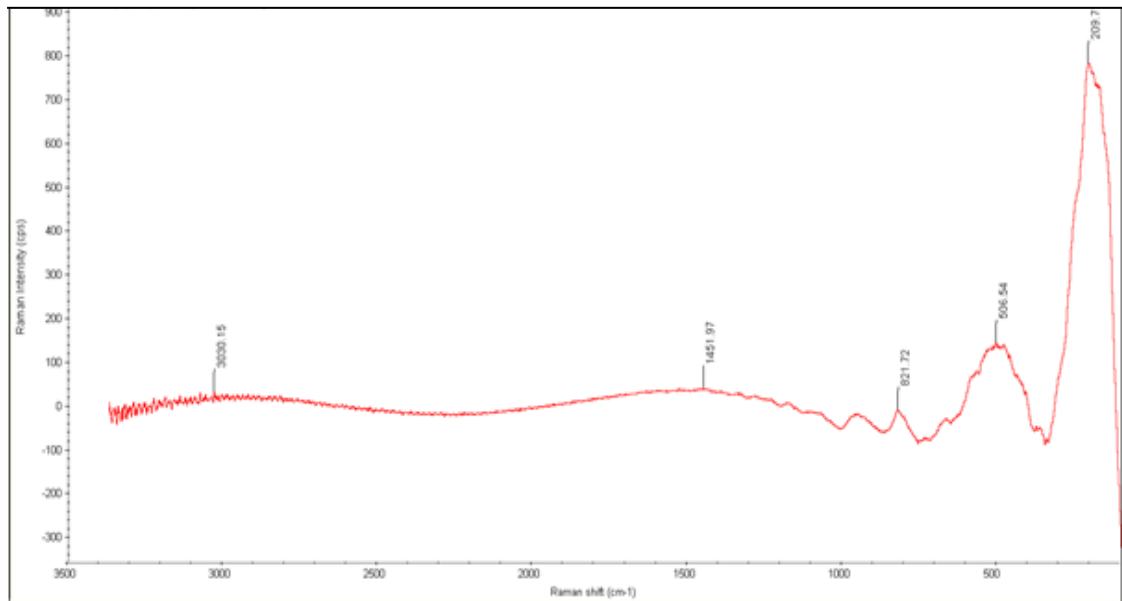
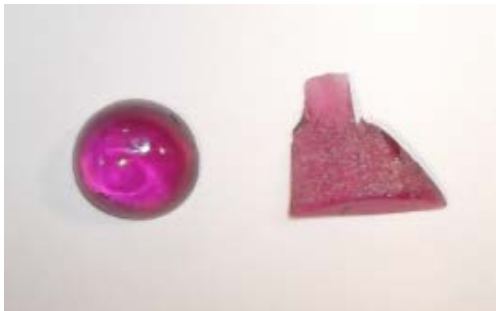


Figure 4.14a: clear surface spectrum of 2.58ct pink red zone refined Inamori Kyocera star ruby



(b)



(c)

Figures 4.14b and 4.14c: 2.58ct pink red zone refined Inamori Kyocera star ruby cabochon and a piece from the original boule showing the frosted (b) and clear (c) surfaces from two different angles

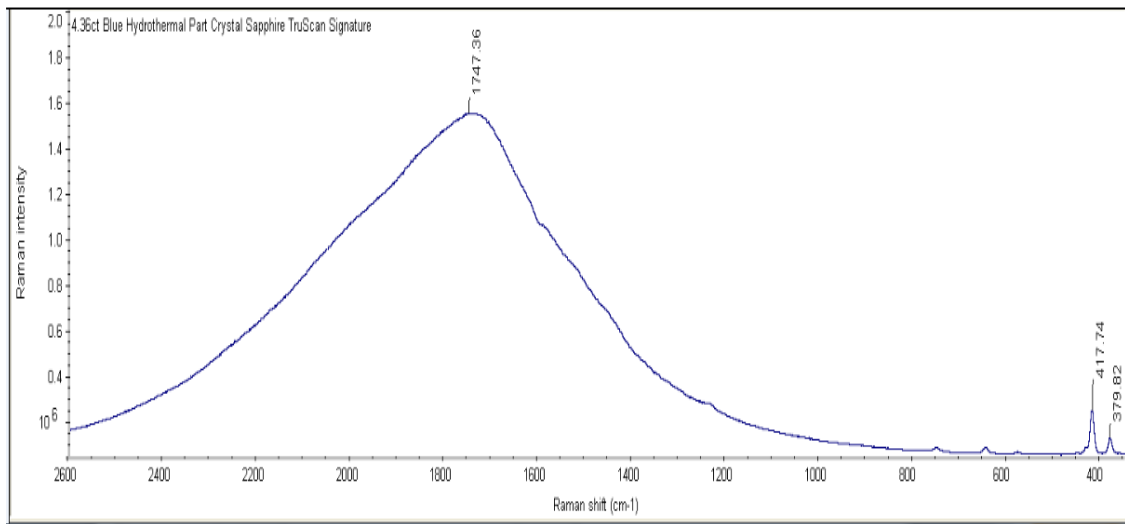


Figure 4.15a: clear surface spectrum of 4.36ct blue hydrothermal part crystal sapphire



(b)



(c)

Figures 4.15b and 4.15c: 4.36ct blue hydrothermal part crystal sapphire with both a smooth (b) and frosted (c) surface

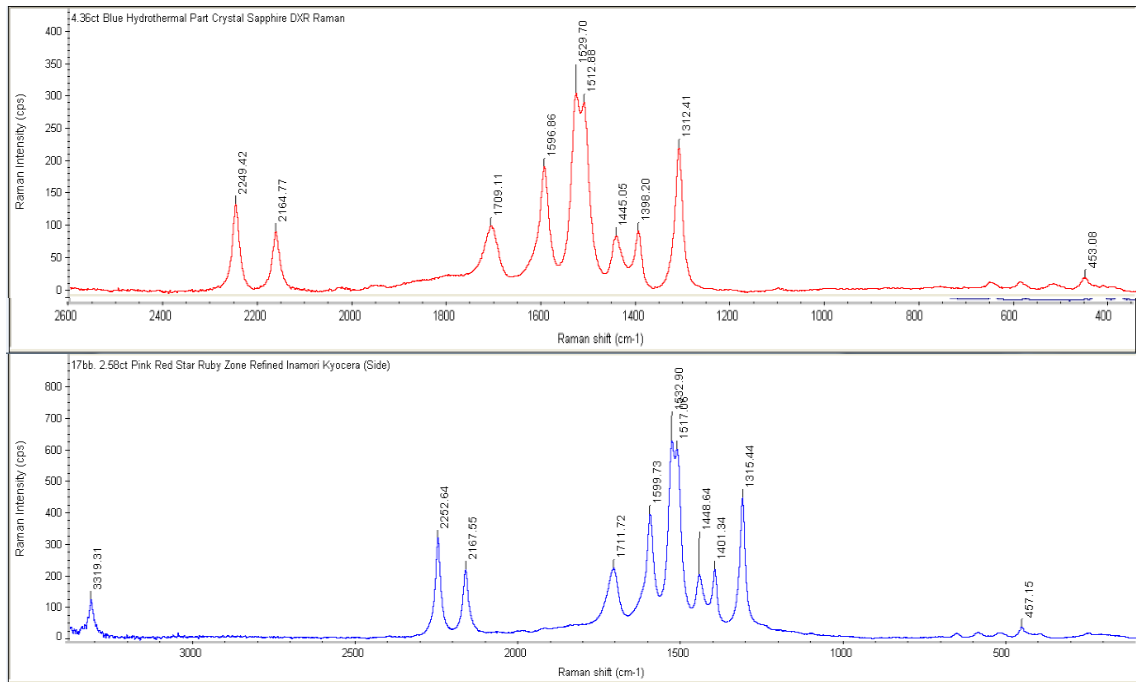


Figure 4.16: DXR Raman comparison between frosted surfaces of a blue 4.36ct hydrothermal part crystal sapphire (above) and a pink red 2.58ct zone refined Inamori Kyocera star ruby (below).

The blue hydrothermal sapphire was cut in a way so that the clear glossy side of the stone could be analysed as well as the frosted side. The same is for the zone refined ruby. The ruby had two pieces in the packet, one was of a cut cabochon with a smooth, shiny surface and the other was a piece of the original rod from which the cabochon was cut. This piece had both a smooth surface on the inside and a frosted surface on the outside as can be seen in figures 4.14b and 4.14c. The Raman bands in the 1200-2400 cm^{-1} region are most likely to have arisen from the frosted surface of the gemstones as seen in figures 4.14b and 4.15c.

4.3.3 TruScan™ Handheld Raman spectroscopy

In order to analyse the rubies and sapphires using the handheld Raman, a method had to be developed of a natural ruby and one of each synthetic production type (flame fusion, pulling, hydrothermal, flux and zone). This was done by following the TruScan SOP outlined in Appendix B for creating a method and then incorporated into the instruments library. Once complete, analysis was performed on the all of the synthetic corundum. Presented below

are the resulting spectra; each figure showing a comparison of the DXR bench top Raman spectrum on top to the TruScan handheld Raman spectrum below.

The spectrum below shows a comparison between the spectrum attained from the DXR and TruScan Raman spectrometers.

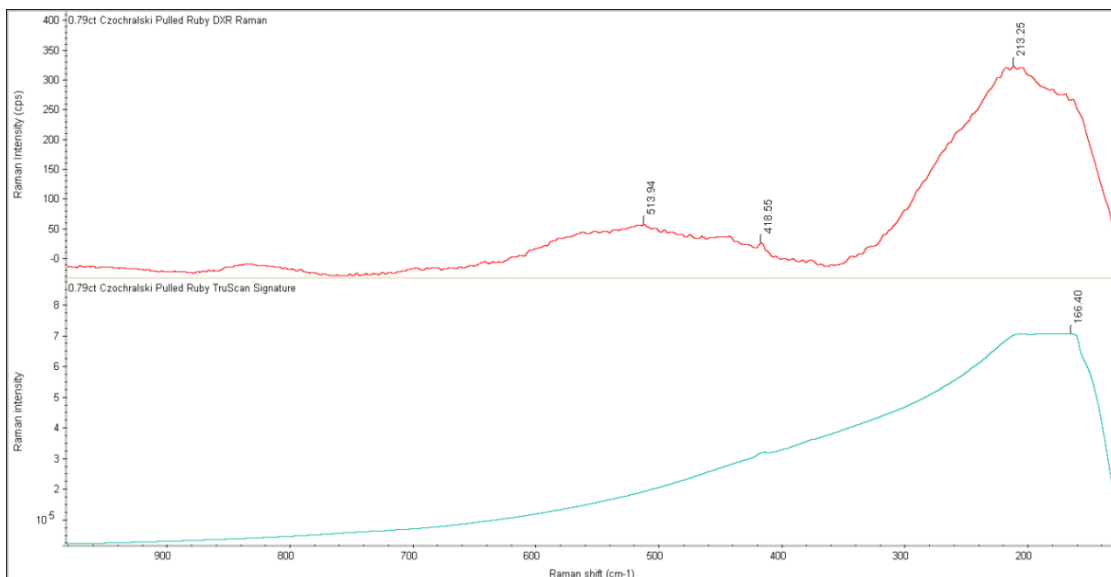


Figure 4.17: spectrum of 0.79ct pulled Czoehralski ruby

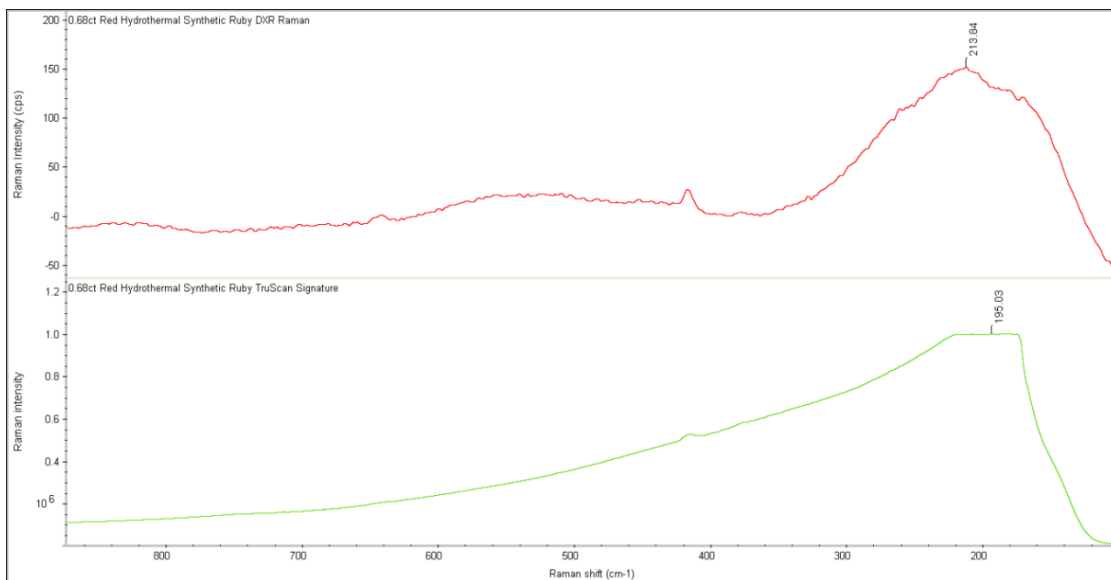


Figure 4.18: 0.68ct Red Hydrothermal Synthetic Ruby comparison spectrum

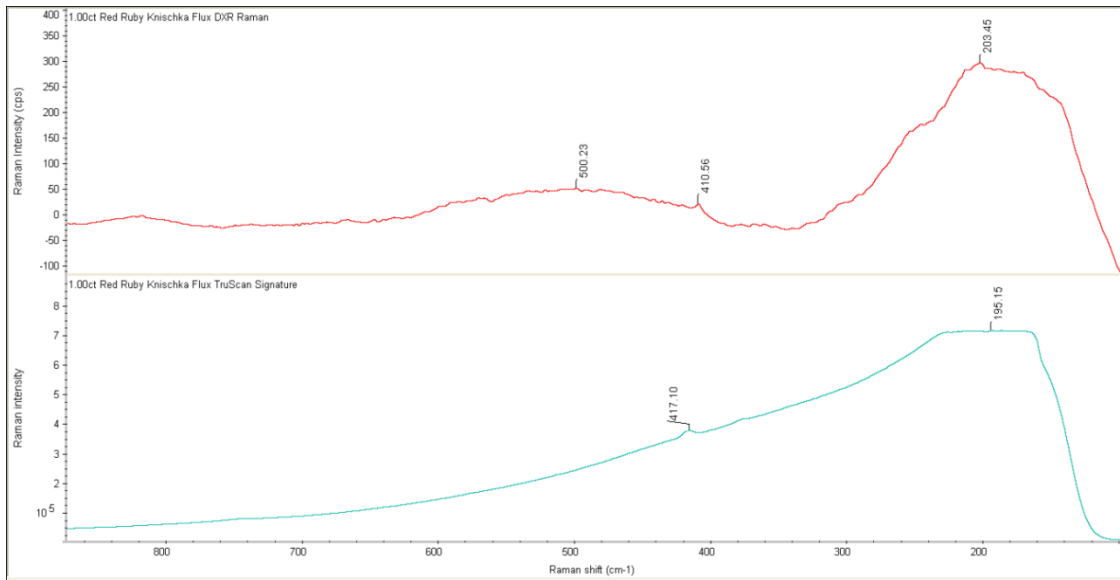


Figure 4.19: 1.00ct Red Ruby Knischka Flux comparison spectrum

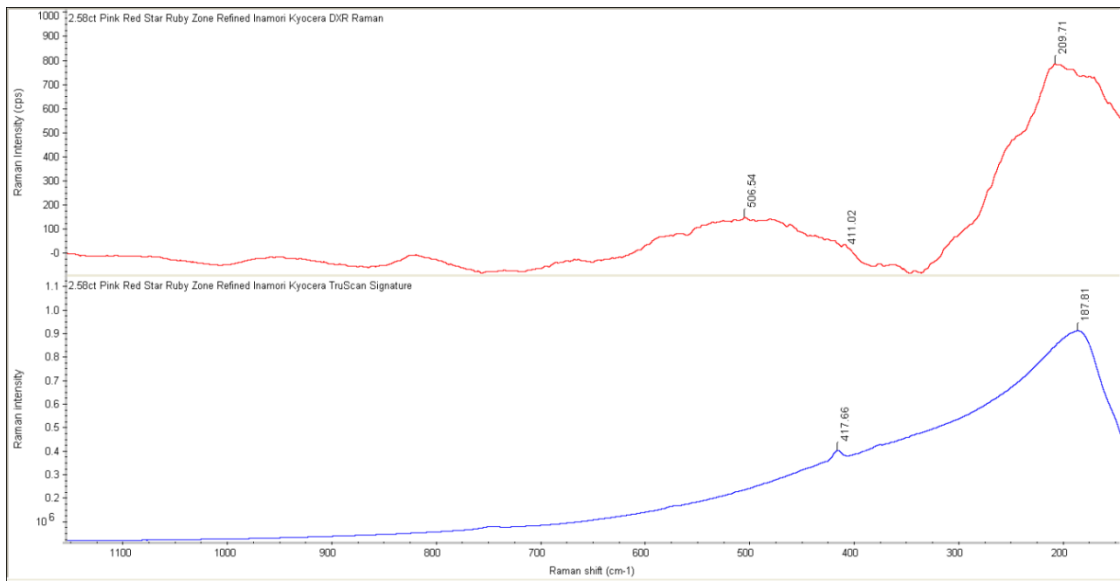


Figure 4.20: 2.58ct Pink Red Star Ruby Zone Refined Inamori Kyocera comparison spectrum

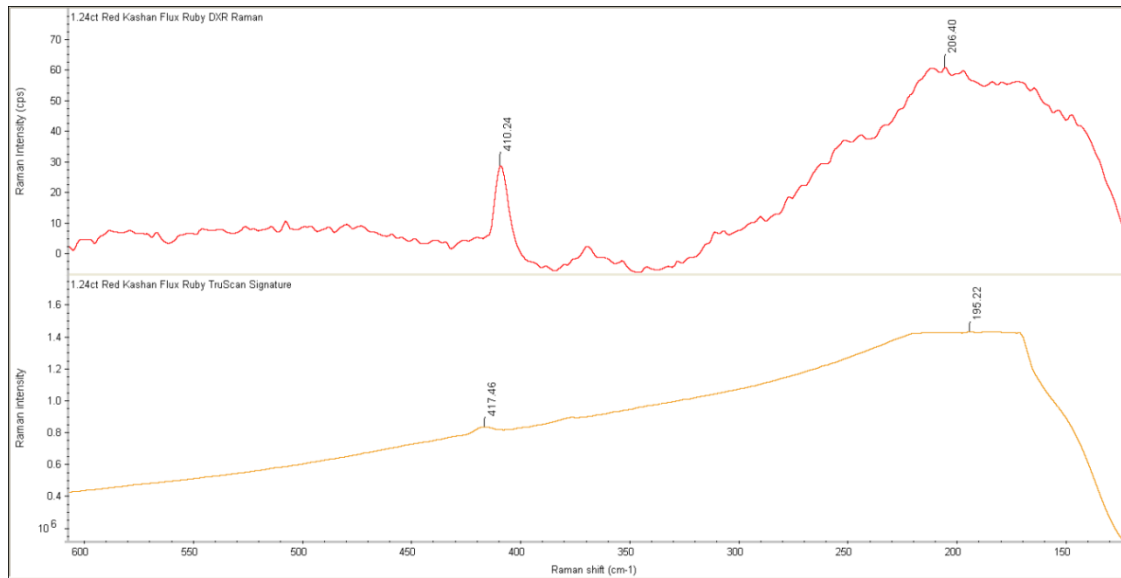


Figure 4.21: 1.24ct Red Kashan Flux Ruby comparison spectrum

Once again, the high intensity of the TruScan does not allow for the peaks to be well defined in the spectrum and as a result some spectral information could be lost or masked.

It was found throughout the study that the TruScan spectra lacked in detail regarding peaks and peak intensities. It is thought that the sheer power of the laser is too strong for the samples and this probably results in a greater intensity being formed in the TruScan spectrum. As viewed in comparison table 3.2, the laser power for the 780nm laser is 14mW and for the 532nm laser is 10mW whilst in comparison, the TruScan laser is an incredible 300mW. When compared, the spectral intensities of the DXR Raman are between 0-400 counts per second (cps) whereas the TruScan intensities are in a much greater range of 10^5 - 10^8 cps. An important factor noted in the difference between the two instruments is that TruScan measures Rayleigh scattering. As mentioned earlier; Rayleigh is the elastic scattering of light which has no use for material identification. It's absorbed and emitted frequencies are equal to one another, resulting in no gain or loss of energy. The Rayleigh peak in the TruScan spectrum is quite broad and has a very strong intensity. It was noted that if the Rayleigh peak was not omitted from the spectrum then the samples peak intensities would remain extremely low; in some cases they would not be seen at all. It is not clear as to why the TruScan software was programmed to include Rayleigh scattering as for the greater part it is generally ignored. In the DXR

Raman; Rayleigh scattering is automatically omitted from the spectrum altogether by the OMNIC software.

4.3.4 SEM/EDX Analysis

4.3.4.1 Ruby

A reading was taken at three separate data points on the table facet of each ruby. The figures for each data point were measured and plotted in the table below.

Table 4.1: Data of each sample spot, taken from three separate areas of each ruby table facet

Data Point	Stone	Al ₂ O ₃	TiO ₂	V ₂ O ₅	Cr ₂ O ₃	MnO	Fe ₂ O ₃	NiO
1	Ruby 1 (2.98)	99.09	0.02	0.00	0.14	0.00	0.70	0.05
2	Ruby 1 (2.98)	99.34	0.01	0.01	0.00	0.00	0.64	0.00
3	Ruby 1 (2.98)	99.12	0.10	0.11	0.00	0.02	0.59	0.06
Av.	Ruby 1 (2.98)	99.18	0.04	0.04	0.05	0.01	0.64	0.04
1	Ruby 2 (Afghan)	99.22	0.00	0.11	0.00	0.00	0.66	0.00
2	Ruby 2 (Afghan)	98.97	0.02	0.13	0.15	0.00	0.69	0.04
3	Ruby 2 (Afghan)	98.75	0.08	0.00	0.21	0.09	0.70	0.15
Av.	Ruby 2 (Afghan)	98.98	0.03	0.08	0.12	0.03	0.68	0.06
1	Ruby 3 (4.63)	99.42	0.00	0.14	0.17	0.18	0.08	0.00
2	Ruby 3 (4.63)	99.60	0.00	0.01	0.26	0.00	0.00	0.03
3	Ruby 3 (4.63)	99.35	0.00	0.00	0.31	0.00	0.13	0.21
Av.	Ruby 3 (4.63)	99.46	0.00	0.05	0.25	0.06	0.07	0.08
1	Ruby 4 (1.76)	99.31	0.00	0.03	0.43	0.00	0.00	0.08
2	Ruby 4 (1.76)	99.26	0.00	0.08	0.43	0.00	0.10	0.13
3	Ruby 4 (1.76)	99.15	0.00	0.07	0.45	0.00	0.00	0.13
Av.	Ruby 4 (1.76)	99.24	0.00	0.06	0.44	0.00	0.03	0.11

NB: Quantities below 0.5%wt are at trace level and quantities below 0.05%wt cannot be guaranteed as present as they are below the detection limit (bdl).

Table 4.2: Overall averages of SEM/EDX analysis results of the 2.98ct Burma, Afghanistan, and 4.63ct and 1.76ct Verneuil rubies respectively

Stone	Al ₂ O ₃	TiO ₂	V ₂ O ₅	Cr ₂ O ₃	MnO	Fe ₂ O ₃	NiO
2.98ct Burma	99.18	<i>bdl</i>	<i>bdl</i>	0.05	0	0.64	<i>bdl</i>
Afghanistan	98.98	<i>bdl</i>	0.08	0.12	<i>bdl</i>	0.68	0.06
4.63ct Verneuil	99.46	0	0.05	0.25	0.06	0.07	0.08
1.76ct Verneuil	99.24	0	0.06	0.44	0	<i>bdl</i>	0.11

NB: Quantities below 0.5%wt are at trace level and quantities below 0.05%wt cannot be guaranteed as present as they are below the detection limit (bdl).

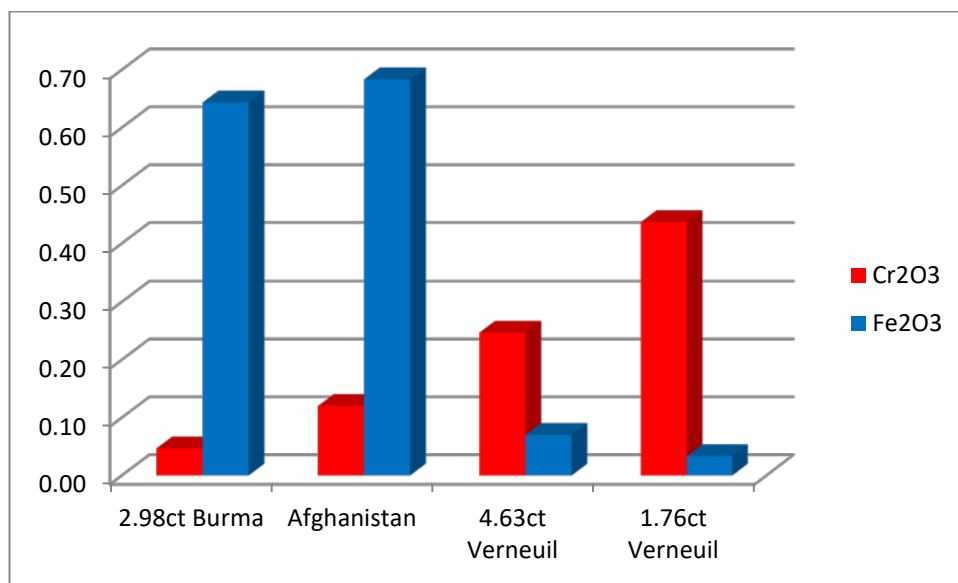


Figure 4.22a: Graph depicting the average difference in concentration of Cr₂O₃ and Fe₂O₃ in natural and synthetic rubies

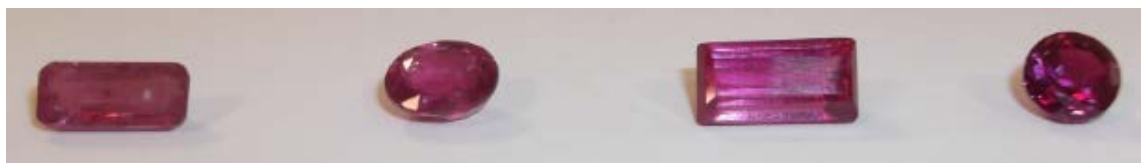


Figure 4.22b: from left to right- 2.98ct Burma, Afghanistan, 4.36ct Verneuil and 1.76ct Verneuil rubies

The graph shows the main differences between the colouring agents in natural and synthetic rubies. As expected, there is a marked difference in the concentrations of iron oxide (Fe_2O_3); more notably a large amount present in natural rubies. There is 0.64%wt and 0.68%wt in the Burmese and Afghanistani rubies respectively; and a minimal 0.07%wt in the 4.63ct Verneuil ruby. Fe_2O_3 in the 1.76ct Verneuil ruby is below the detection limit and therefore cannot be confirmed as being present within the stone. The very presence of large amounts of Fe_2O_3 in the natural stones suggests it has been incorporated into them through surrounding host rocks in the earth as iron ore typically accounts for a large part of the Earth's crust. True to form, the synthetic rubies have an incredible amount of Cr_2O_3 present in their structure. In nature, the formation process only requires an extremely small amount of Cr_2O_3 to be incorporated with the Al_2O_3 to colour the stone red as chromium is an incredibly strong chromophore element. In the synthetic formation process, the Al_2O_3 is bombarded with chromium so much so that the crystal lattice becomes saturated with it and quite commonly substitutes itself for the aluminium. This is why there is such a large volume of chromium present in the verneuil stones. There is 0.05%wt and 0.12%wt in the Burmese and Afghanistani rubies respectively; and a major 0.25%wt in the 4.63ct verneuil ruby and 0.44%wt in the 1.76ct Verneuil ruby respectively. These figures along with the synthetic ruby spectra confirm the strong presence and large substitution of chromium in the stones.

4.3.4.2 Sapphire

Two natural and two synthetic sapphires were analysed. The Raman results showed no significant differences between the chemical bonding of the different sapphires and SEM/EDX between the elemental compositions of the types of stones. After conducting the analysis on these samples it was observed that SEM/EDX cannot differentiate between sapphires of natural and synthetic origin, therefore making this technique limiting for corundum identification analysis; more specifically for blue sapphires.

4.4 Emerald

For analysis purposes of the study, the surfaces of the emeralds were analysed. The 532nm green laser was chosen as previous analysis was not possible with the 780nm laser due to fluorescence issues. It was found that a 25 μ m aperture yielded better, clearer spectra than the 50 μ m aperture for emerald analysis as the larger aperture often resulted in **1CCD overflow* of many of the samples. Using a smaller aperture ensures for a shallower depth of field resulting in a more effective confocal operation. Limiting the aperture size isolates only those rays coming from a narrow region around the microscope focus. Doing so improves the spatial resolution and allows the discrimination of signals from different depths within the sample. Even though the smaller aperture gave better and more results, some of the samples still caused CCD overflow. This is most likely to be due to the deep green colour caused by the dopants; making the stone a strong Raman scatterer.

**1CCD overflow* is caused by too much light hitting the CCD due to the sample being a strong Raman scatterer (producing signals of more than 30,000 counts); or it may occur with long exposure times which can result in saturating one or more pixels of the CCD array. A shorter exposure time, smaller aperture and reduced power laser settings were all applied to try and attain a spectrum but each of these methods conducted individually and collectively was unsuccessful for some of the samples.

4.4.1 Natural Emerald

All the natural emeralds showed clear peaks in both the 1067 cm^{-1} and 685 cm^{-1} region respectively. The Pakistan emerald showed good peaks in the 320 cm^{-1} and 395 cm^{-1} region and the Colombian emerald had just one prominent peak in the 395 cm^{-1} region; however the peaks were not so clear in the Russian emeralds due to a mass of negative peaks masking them.

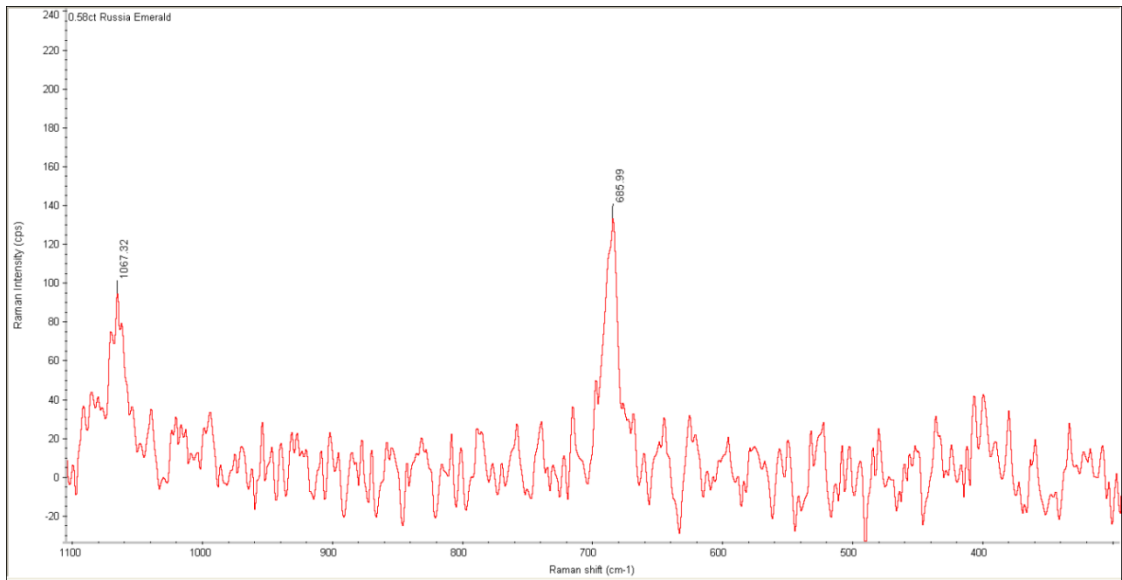


Figure 4.23a: 0.58ct Russia Emerald spectrum



Figure 4.23b: 0.58ct Russia emerald

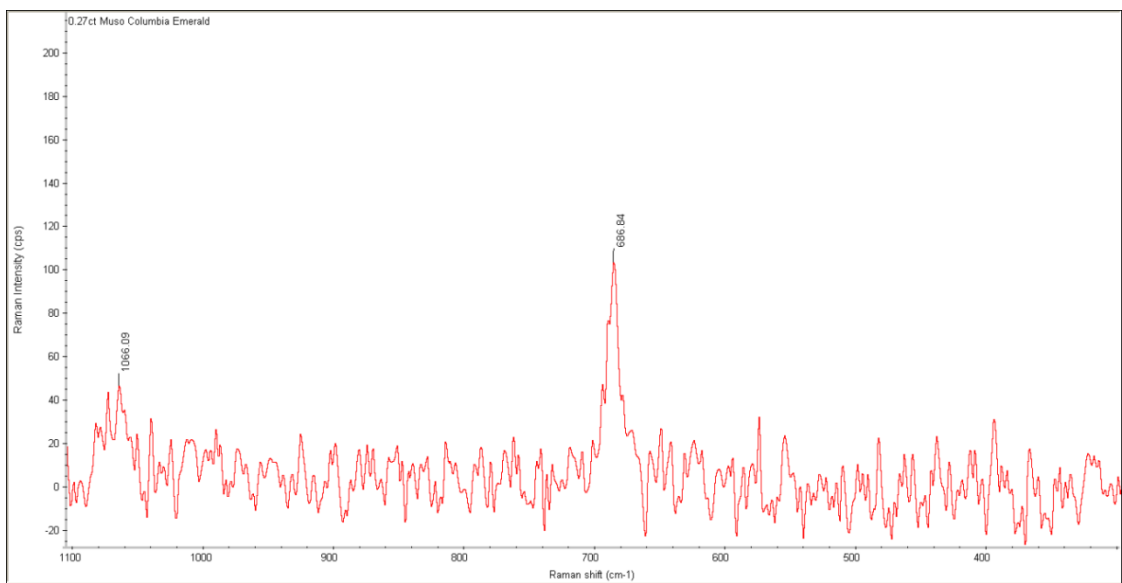


Figure 4.24a: 0.27ct Muzo, Colombia emerald spectrum



Figure 4.24b: 0.27ct Muzo, Colombia emerald with visible solid inclusions

The dark, almost black inclusions are believed to be of carbonaceous matter. This is due to Muzo emeralds forming in thin beds (averaging 2 cm in thickness) of shale and limestone alternating, the shale in predominance. The shale is a dense, black rock, soiling the hands with excess carbonaceous matter, and most of it effervesces with acid from the presence of calcium carbonate. The limestone is likewise black with carbon but differs from the shale in carrying calcium carbonate in excess of silicate material (Olden, 1911).

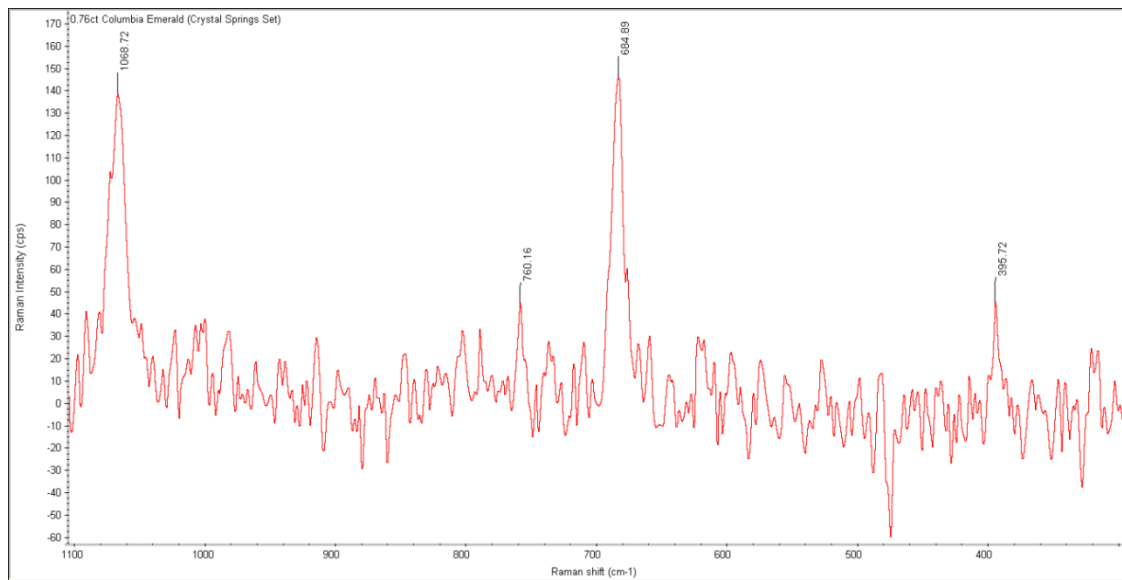


Figure 4.25a: 0.76ct Columbia Emerald spectrum



Figure 4.25b: 0.76ct light green Columbia emerald

There are three major emerald mines in Colombia; the Muzo, Chivor (Somondoco) and Coscuez deposits respectively. The difference in appearance of the emeralds in figures 4.24b and 4.25b respectively is indicative that they may be from different deposits in Colombia. The 0.27ct emerald is labelled as being from Muzo, therefore it can be said that this 0.76ct emerald may be from either the Chivor or Coscuez deposit as it is much lighter in colour and void of any carbonaceous inclusions.

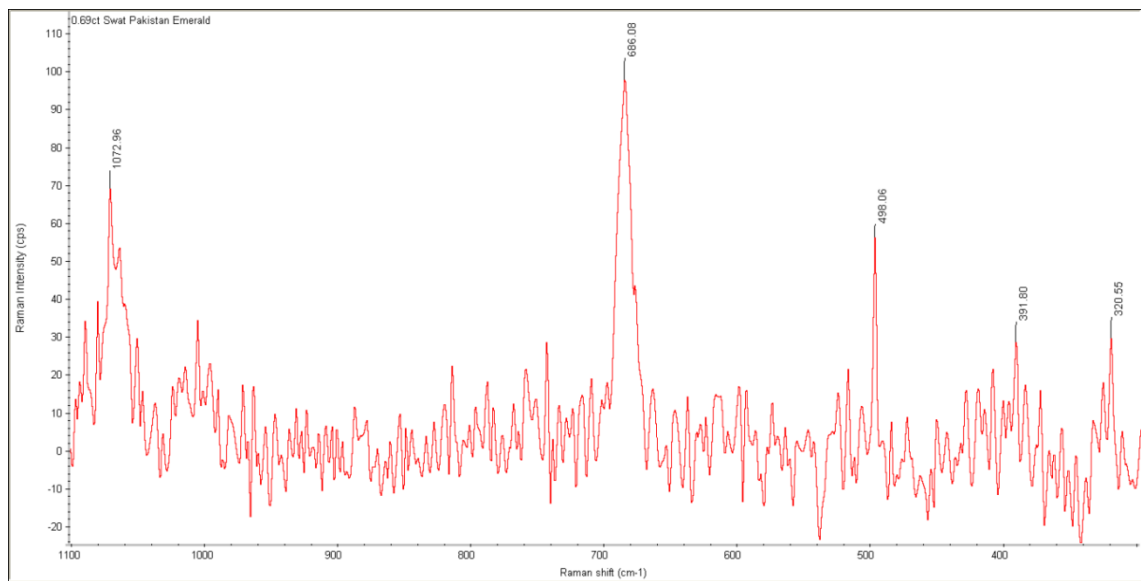


Figure 4.26a: 0.69ct Green Swat, Pakistan Emerald spectrum



Figure 4.26b: 0.69ct light green Swat, Pakistan emerald

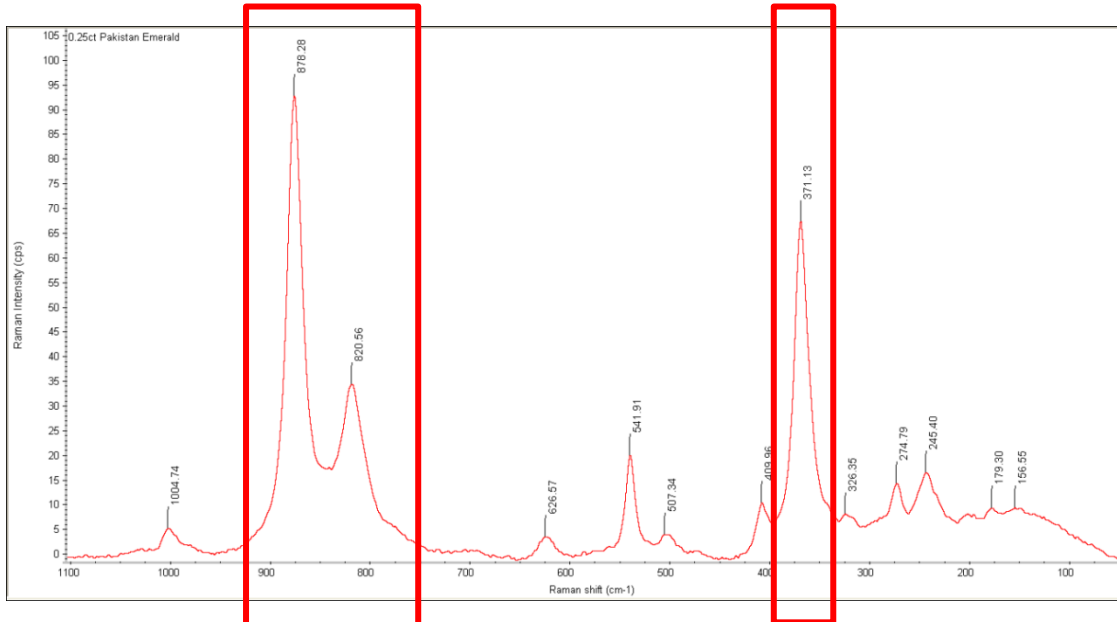


Figure 4.27a: spectrum of a green stone labelled as 0.25ct Pakistan Emerald



Figure 4.27b: dark green stone labelled as a 0.25ct Pakistan Emerald

A significant difference can be seen in the colour of the 0.69ct stone in figure 4.26b to that of the 0.25ct stone in figure 4.27b although they are both labelled as emeralds originating from Pakistan. The Raman spectrum in figure 4.27a confirms that the stone is not an emerald; and the presence of the highlighted characteristic twin peaks at 820cm^{-1} and 878cm^{-1} along with a 371cm^{-1} peak indicates that the stone is likely to be a garnet.

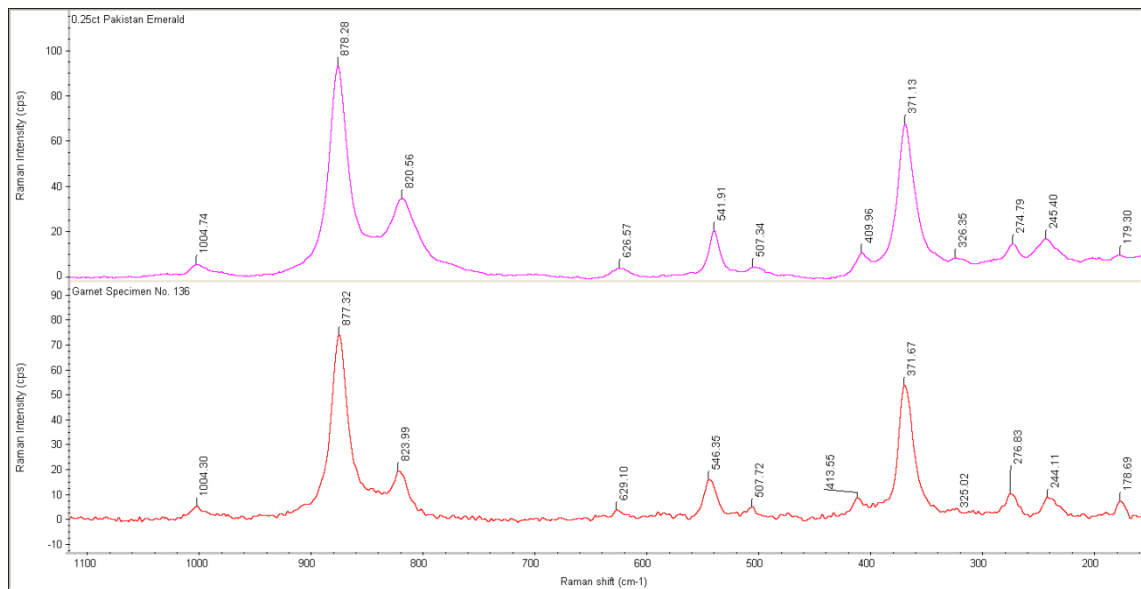


Figure 4.27c: comparison of a 0.25ct green stone labelled as Pakistan emerald (above) and a green grossular garnet (below)

On visual inspection the stone resembled an emerald by possessing the same characteristic included features and green colour; however upon analysis it yielded a completely different spectrum as can be seen in comparison figure 4.27c above. Investigation on online databases and journals did not yield any spectra for the garnet in question therefore the spectrum was taken from previous garnet analyses by Duncan (2010). The spectrum indicated that the stone in question was of the mineral tsavorite, a green grossular species member of the garnet group. The general formula for garnet is $X_3Z_2(SiO_4)_3$ and the chemical formula for tsavorite is $Ca_3(Al,V)_2(SiO_4)_3$, and the cause of the green colour is primarily vanadium (Osanai, 1990). This metamorphic, vanadium-bearing, green grossular garnet was discovered in the late 1960s by Campbell Bridges near Komolo in north-eastern Tanzania. It has since been found elsewhere in Tanzania and Kenya, Madagascar, Antarctica and Pakistan (Smillie, 2010). As mentioned, tsavorite garnet also occurs in Pakistan so it is possible that the stone in question is of Pakistani origin but has been mistaken for the more commonly occurring emerald species.

A 0.23ct two piece set of emeralds from Mellit, Germany were analysed; unfortunately no spectrum was attainable for either of the pieces due to CCD overflow*1 issues.



Figure 4.28: 0.23ct Mellit, Germany two piece emerald set with rough and polished surfaces

4.4.2 Synthetic Emerald

4.4.2.1 Flux Emeralds

Grown by the flux method since the 1940s, the synthesis of Chatham Created emeralds requires an approximate duration time of six months to grow. Although the Chatham Company have not disclosed their growth method, it is believed the emerald crystals are formed by spontaneous nucleation in the flux process.

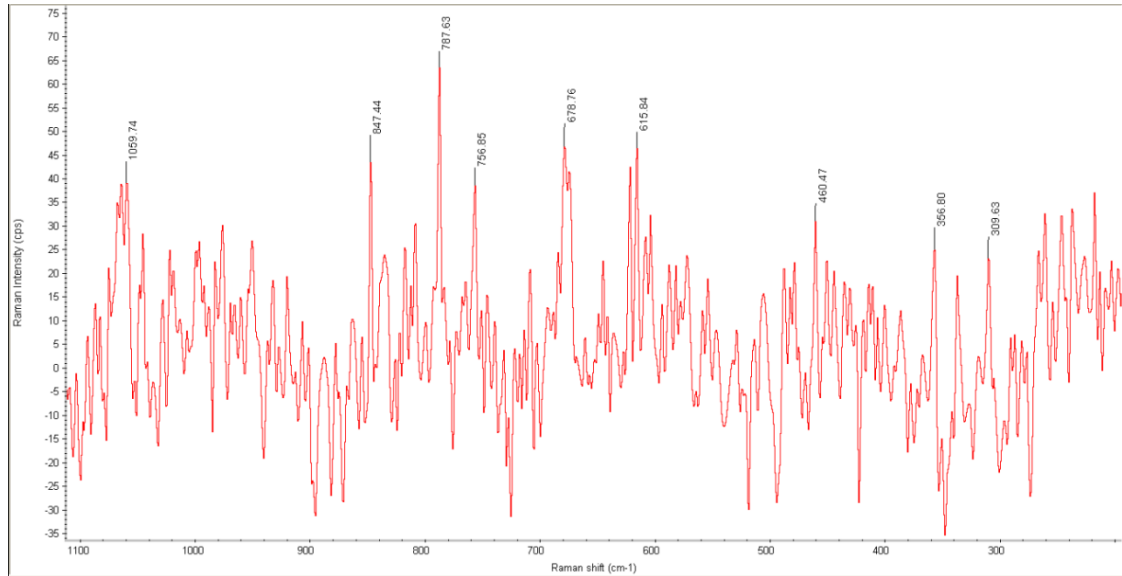


Figure 4.29a: 0.5ct Chatham synthetic flux emerald spectrum

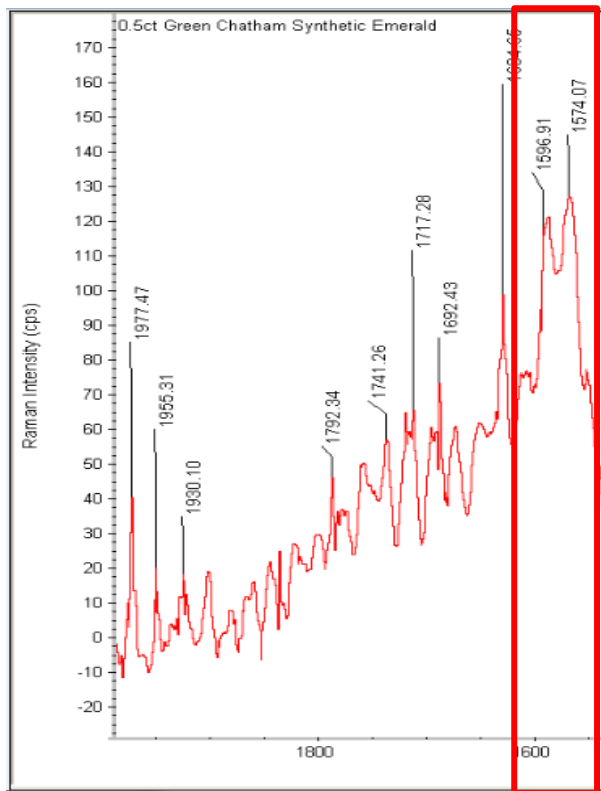


Figure 4.29b: broad twin peak situated in the 1500-1800 cm^{-1} region in the 0.5ct Chatham synthetic flux emerald



Figure 4.29c: 0.5ct Chatham synthetic flux emerald, visibly clear with a glassy appearance

Russian emerald has been grown by the flux method since the early 1980s.

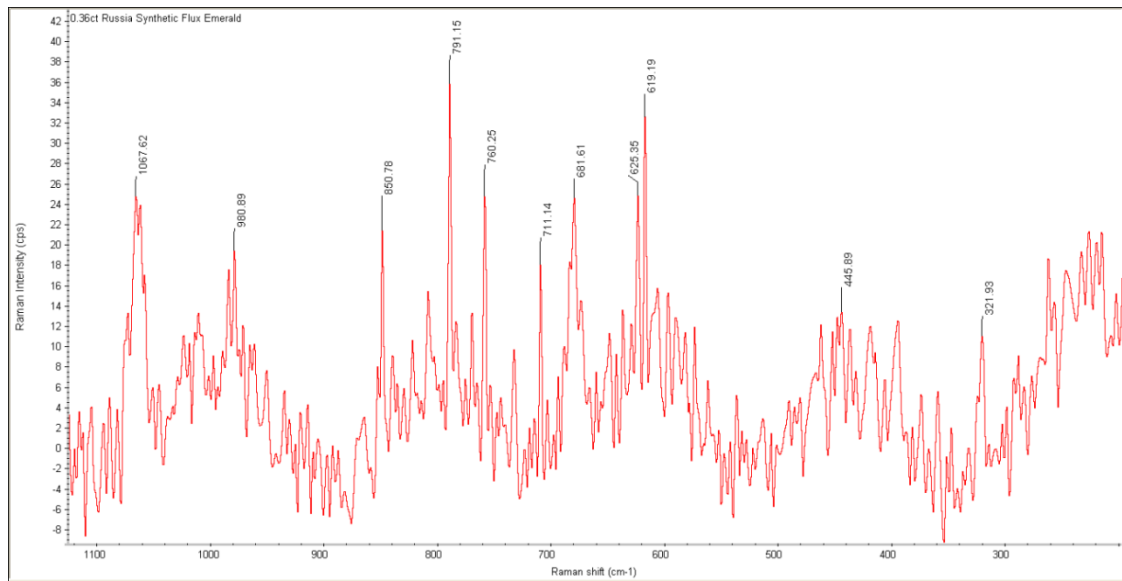


Figure 4.30a: 0.36ct Russian Synthetic Flux Emerald spectrum

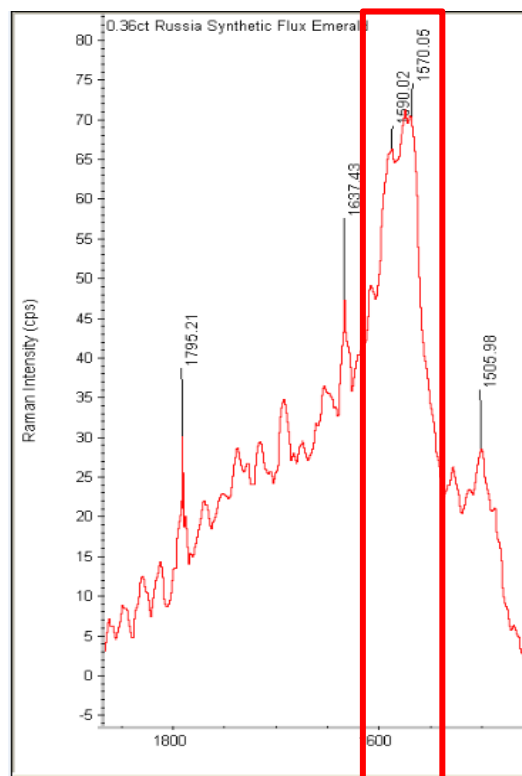


Figure 4.30b: broad twin peak situated in 1500-1800cm⁻¹ region in a 0.36ct Russian synthetic flux emerald



Figure 4.30c: 0.36ct Russian Synthetic Flux Emerald, a visibly clear stone with a glassy appearance

The highlighted twin peaks in both figure 4.29b and 4.30b have only been present in the Chatham and two Russian synthetic flux emeralds. It is a possibility that these peaks may be unique to synthetic flux produced stones.

A 1.17ct Lennix synthetic flux emerald was analysed but no spectrum was obtained due to CCD overflow*¹ issues.

4.4.2.2 Hydrothermal Emeralds

Biron emeralds were hydrothermally grown by an Australian mineral company towards the end of the 1970s. Below is the spectrum of the emerald, by far the cleanest looking spectrum of all the emeralds analysed with minimal negative peaks that do not disrupt the quality of the spectrum. This is indicative that the elemental balance of all the required substances is near impeccable with minimal impurities in the mixture; as Huang *et al* (2010) stated that the amounts of each ingredient were ideal to produce good quality stones.

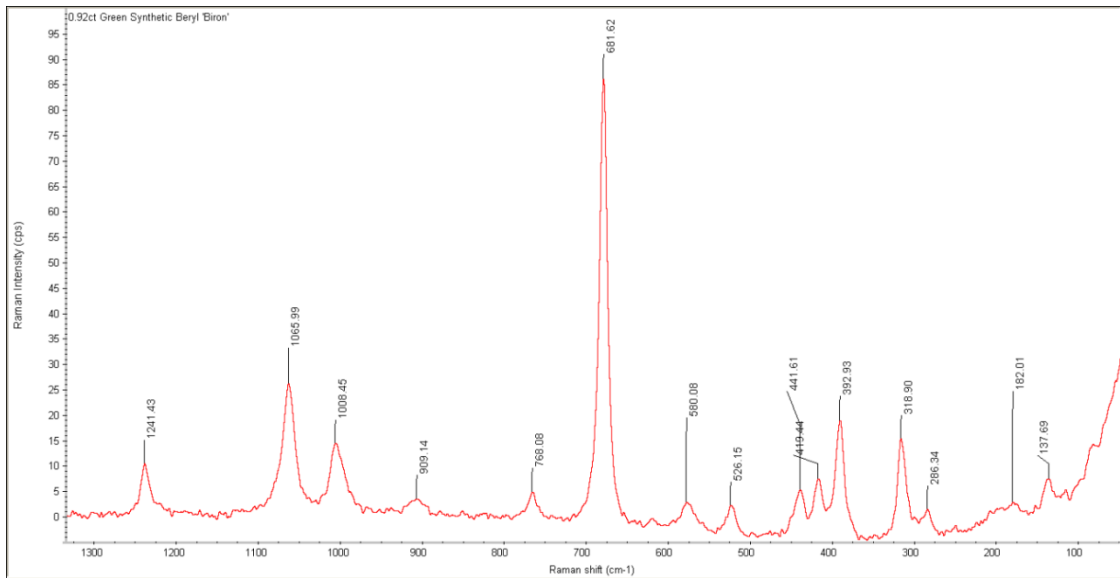


Figure 4.31a: 0.92ct Biron synthetic emerald

Below is the Biron inclusion which was situated on the surface of the stone. The inclusion could not be matched to any minerals that are known to inhabit hydrothermal synthetic emeralds. It is noted that the inclusion is likely to be of some kind of metal which may have become incorporated by separating from the container in which it was made. The most common inclusions in Biron emeralds are known to be gold which indicates that the spectrum beneath could be of that. However, no spectrum was found in literature or online databases for comparison, hence the identity of this inclusion remains inconclusive.

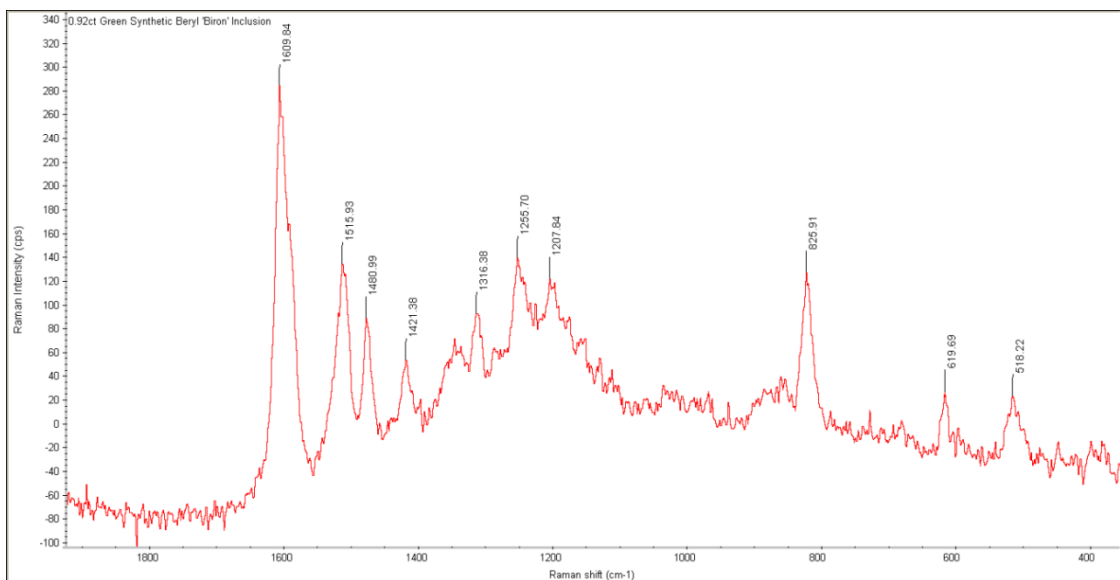


Figure 4.31b: 0.92ct Biron synthetic emerald inclusion

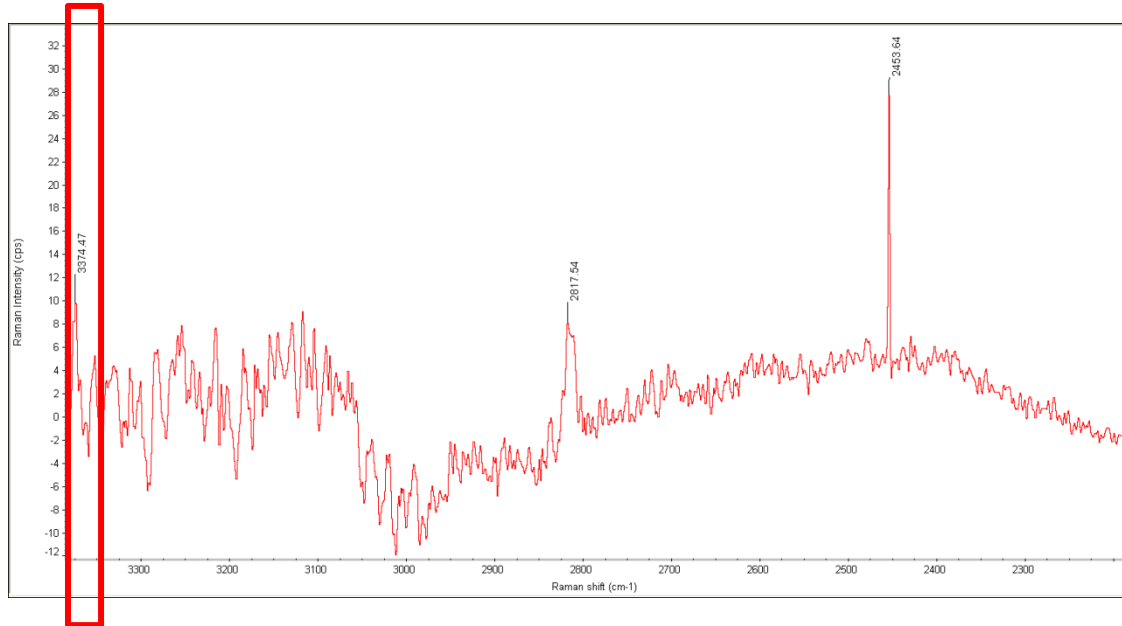


Figure 4.31c: the 2300cm^{-1} to 3400cm^{-1} region in the Biron emerald showing peaks at 2453cm^{-1} , 2817cm^{-1} and 3374cm^{-1} respectively

It is difficult to ascertain what elements the 2453cm^{-1} and 2817cm^{-1} peaks may correspond to as no literature was found which could be used to cross reference this. The highlighted peak at 3374cm^{-1} is sure to correspond to water present in the stone as previous literature by Huong *et al.* (2010) assigns peaks in this region to water. As previously stated, only the surface of the stone was focused on and analysed. Therefore, it can be deduced that there must have been minute water trapped in bubble like inclusions present on or near the surface for such a peak to be highlighted in the Raman spectrum.



Figure 4.31d: 0.92ct synthetic hydrothermal Biron emerald, showing colour zoning

Austrian scientist J. Lechleitner developed a process for coating preformed cut beryl stones in the 1960s (Huong *et al*, 2010). It is believed the stone was natural beryl and overgrown with synthetic emerald by the hydrothermal method. These stones were grown as large, single, high-quality emerald crystals and marketed under the name “Emerita” or “Symeralds” by the Linde Division of the Union Carbide Corporation (Holmes and Crowningshield, 1960).

Lechleitner synthetic emeralds were analysed using the 532nm green laser; unfortunately they produced a great amount of fluorescence resulting in CCD overflow*1. Due to this, no spectra were obtained for these stones.

4.4.2.3 Unknown Origin Emeralds

The emerald spectrum in figure 4.32a below is rather erratic with an array of negative peaks. This type of spectrum was seen in both the Chatham and Russian flux emeralds; which is indicative that this stone is of a flux origin.

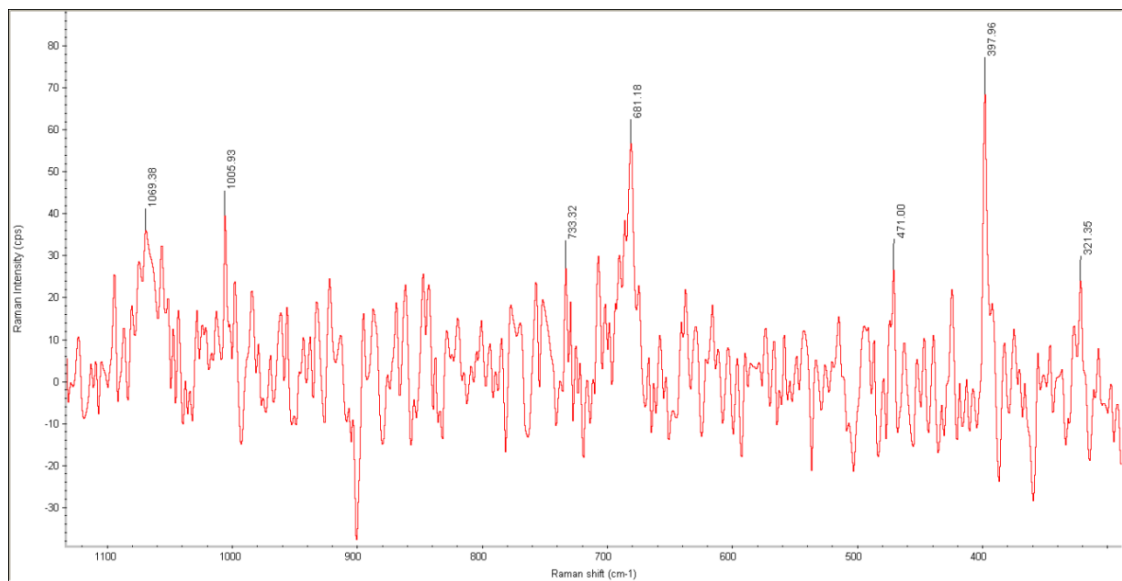


Figure 4.32a: 0.61ct unknown origin emerald spectrum



Figure 4.32b: 0.61ct unknown origin emerald with a glassy appearance, showing solid inclusions

This emerald possesses twin peaks in both the regions of 1068cm^{-1} and 685cm^{-1} , respectively. This type of twinning in two regions has only been seen in the synthetic emeralds, most notably in the flux emeralds which may be indicative of this stones origin.

The spectrum of this 1.02ct emerald below only has one peak at 684cm^{-1} which is one of the main peaks in emeralds. None of the other stones analysed in this study had such a spectrum; therefore origin determination of this stone remains inconclusive.

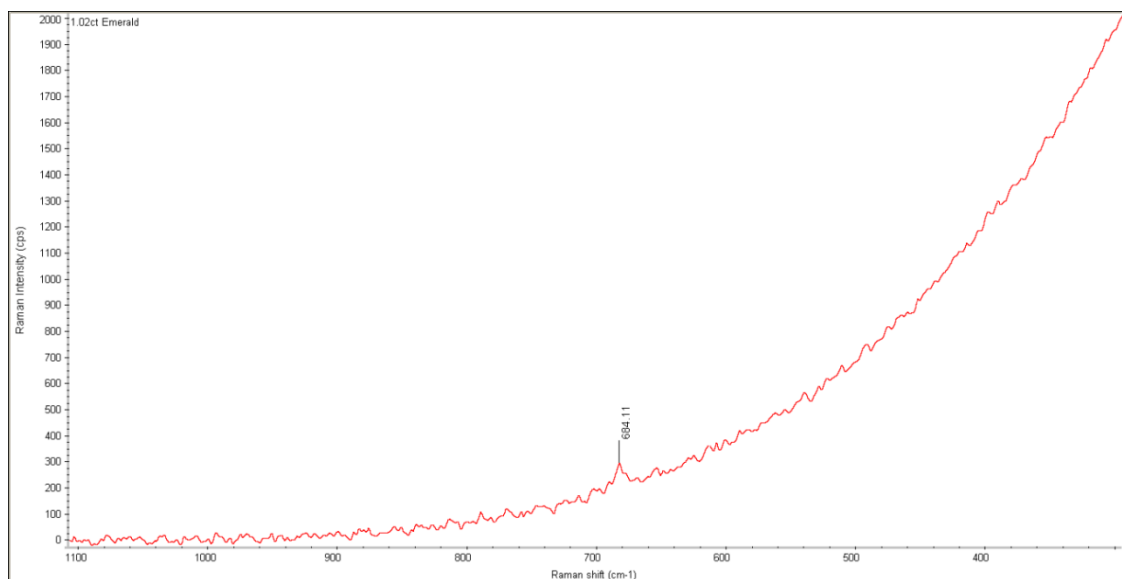


Figure 4.33a: 1.02ct unknown origin emerald spectrum



Figure 4.33b: 1.02ct unknown origin emerald, showing visible dark solid inclusions

Table 4.3: “schist-type”, “non-schist-type”, and synthetic origin determination of emeralds

Natural Emerald		Synthetic Emerald			
Origin/Growth of emerald	Type	“schist-type” (1069-1072cm ⁻¹)	“non-schist-type” (1068-1070cm ⁻¹)	Synthetic type (1067-1068cm ⁻¹)	Inconclusive
0.5ct Chatham				✓	
0.5ct Russia		✓			
0.27ct Colombia	Muso,				✓
0.34ct Swat, Pakistan					✓
0.36ct Russia Flux				✓	
0.40ct Colombia					✓ Twin peak
0.58ct Russia					✓ Twin peak
0.61ct Colombia			✓		
0.61ct Unknown		✓			
0.68ct Colombia			✓		
0.69ct Swat, Pakistan					✓ Twin peak
0.76ct Colombia			✓		
0.86ct Colombia		✓			
0.92ct Biron Hyd.				✓	
1.02ct Unknown					✓ no peak
1.04ct Russia Flux				✓	
1.13ct Columbia					✓
7.43ct Natural Emerald (no info.)			✓		

As mentioned earlier, Huong *et al* (2010) stated schist and non-schist emeralds could be distinguished from one another by analysing their main peak shift which occurs in the 1067-1072 cm^{-1} region. Although the reasoning behind distinguishing emeralds by such means is logical; it is shown by the results in table 4.3 that it is not always possible to apply such a method. The discrepancies shown in the inconclusive column contain what are presumed to be all natural emeralds. The stones highlighted in green all have peak numbers below those that are defined for “schist-type” and “non-schist-type” emeralds. Huong and Häger (2010) assigned this peak region to Si-O vibrations, stating that stones with high silicon content (“non-schist-type”) had low band positions and vice versa. Based on this information, it is possible to conclude that these three stones may be emeralds of the “non-schist-type”. The three stones highlighted in red all have twin peaks with overlapping numbers in the peak defining area. Therefore it is not possible to aptly discriminate the stones on a “schist-type”/“non-schist-type” basis.

4.4.3 TruScan™ Handheld Raman spectroscopy

In order to analyse the emeralds using the handheld Raman spectrometer, a method had to be developed of a natural emerald and one of each synthetic production type (hydrothermal and flux). This was done by following the TruScan SOP outlined in appendix B for creating a method and then incorporated into the machines library. Once complete, analysis was performed on the emeralds. Presented below are the spectra of the emeralds; each figure showing a comparison of the DXR bench top Raman spectrum (above) to the TruScan handheld Raman spectrum (below).

The 7.43ct emerald comparison spectrum shows the differences in peak intensity between the two instruments. The peaks are well defined and prominent in the DXR spectrum, which allows for better interpretation and identification of the emeralds.

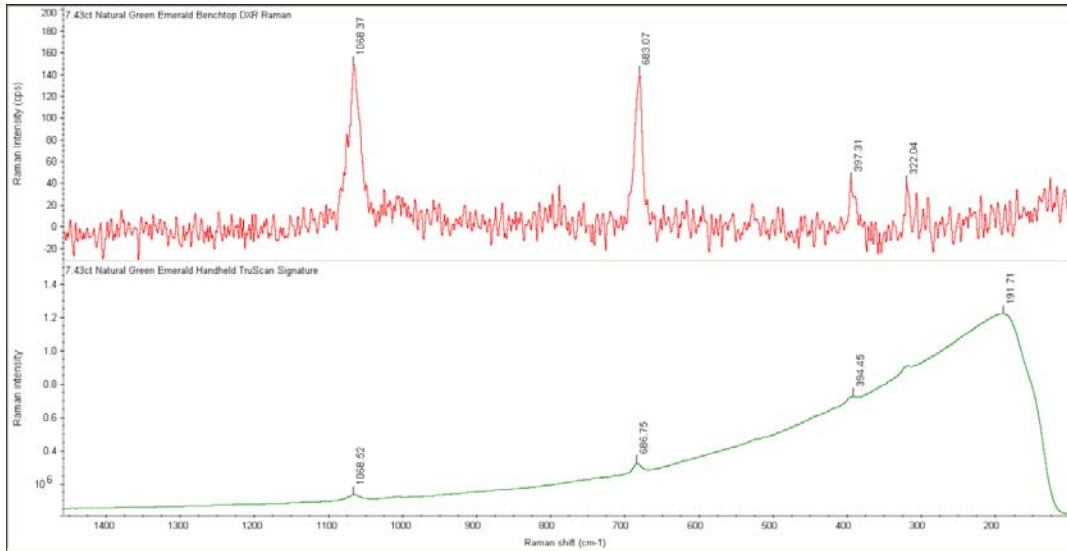


Figure 4.34a: DXR and TruScan comparison spectrum of the 7.43ct unknown origin natural emerald



Figure 4.34b: 7.43ct unknown origin natural emerald with cracks on the surface and light and dark solid inclusions occurring throughout the stone

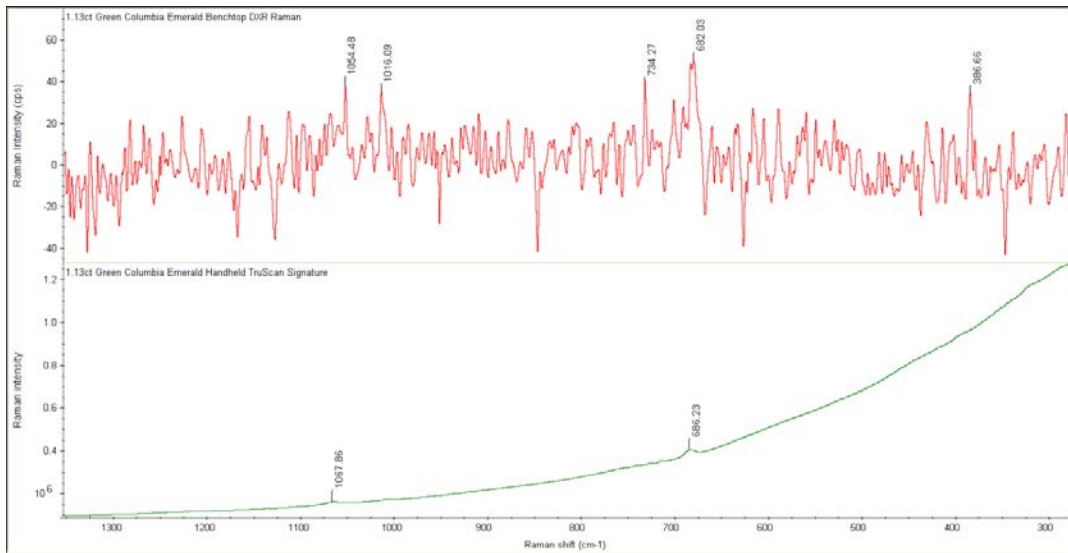


Figure 4.35a: DXR and TruScan comparison spectrum of the 1.13ct Colombia emerald



Figure 4.35b: 1.13ct Colombia emerald

In figure 4.35, it can be seen that the DXR Raman spectrum contains more information regarding the peaks on display. Despite undergoing a data acquisition time of over 30 minutes for each signature in comparison to two minutes using the bench top Raman; the TruScan spectra of the natural emeralds lack a significant amount of data. Likewise, the TruScan also has an extremely high intensity which results in only being able to acquire the main characteristic peaks at 685cm^{-1} and 1067cm^{-1} .

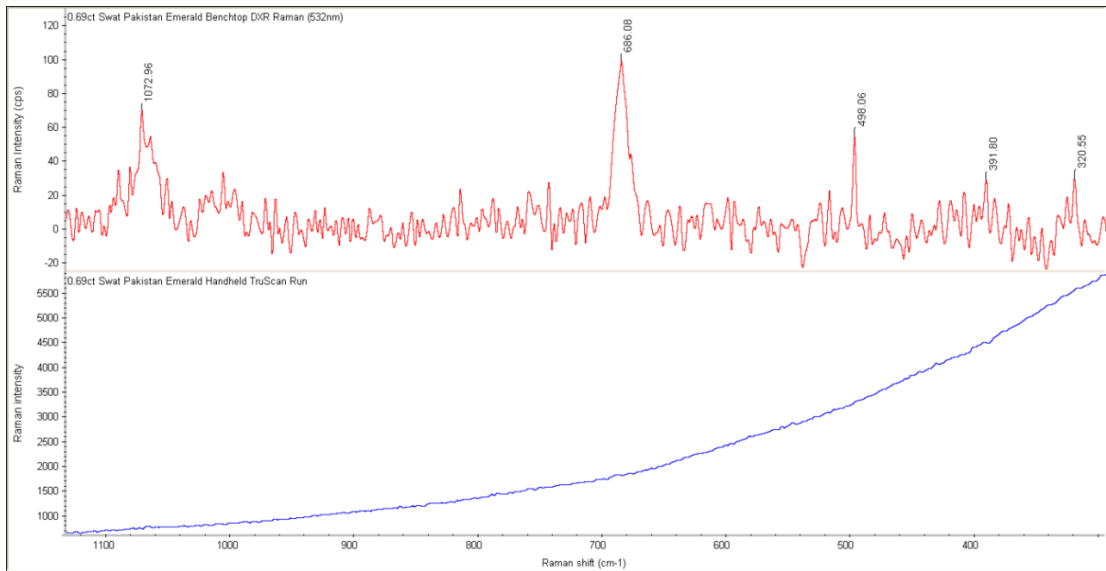


Figure 4.36: DXR and TruScan comparison spectrum of the 0.69ct Swat, Pakistan emerald

The above comparison of the two spectrometers shows how the TruScan's lack of sensitivity and ability to record spectral defining peaks results in a flat line.

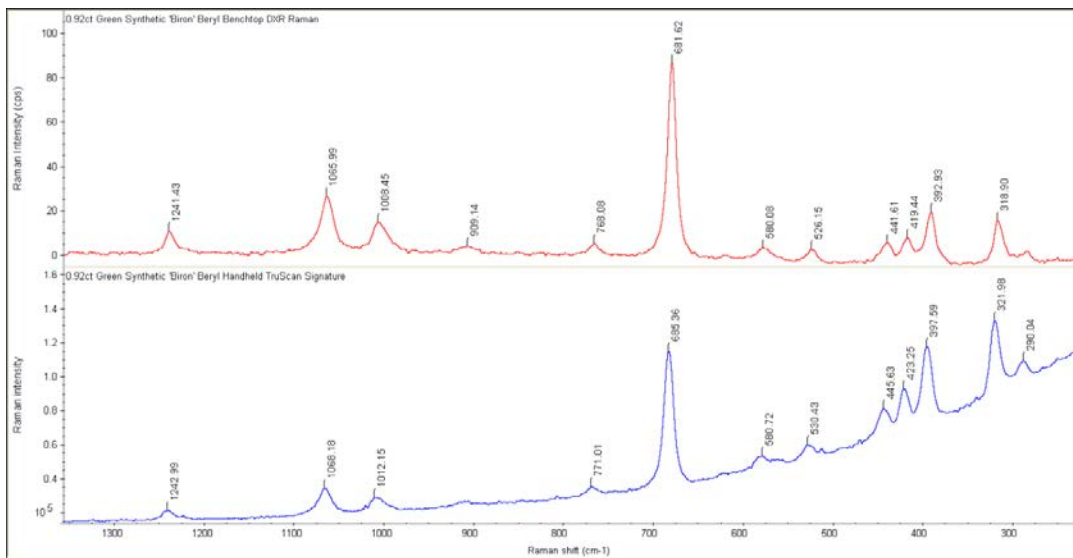


Figure 4.37: DXR and TruScan comparison spectrum of the 0.92ct synthetic hydrothermal Biron emerald

Unlike with the natural emeralds, the TruScan is able to produce an almost identical spectrum for the hydrothermal Biron emerald. The handheld spectrum does not possess the flat baseline like the bench top Raman spectrum but it does have all the peaks required for hydrothermal emerald identification. It is

observed that the same hydrothermal stone had acquired an exceptionally clean and clear spectrum using the bench top Raman instrument.

4.4.4 SEM/EDX Analysis

A reading was taken at three separate data points on the table facet of each emerald. The figures for each data point were measured and plotted in the table below.

Table 4.4: Data of each sample spot, taken from three separate areas of each emerald table facet

Data Point	Stone	Na ₂ O	MgO	Al ₂ O ₃	SiO ₂	TiO ₂	V ₂ O ₅	Cr ₂ O ₃	MnO	Fe ₂ O ₃	CoO	NiO
1	Emerald 1 (0.58)	2.22	2.54	18.67	75.99	0.01	0.01	0.14	0.09	0.25	0.08	0.00
2	Emerald 1 (0.58)	2.16	2.45	18.78	76.13	0.00	0.03	0.06	0.03	0.33	0.00	0.03
3	Emerald 1 (0.58)	2.01	2.25	19.47	75.66	0.17	0.18	0.05	0.02	0.16	0.02	0.00
Av.	Emerald 1 (0.58)	2.13	2.41	18.97	75.93	0.06	0.07	0.08	0.05	0.25	0.03	0.01
1	Emerald 2 (0.69)	2.45	2.55	16.14	76.00	0.03	0.00	1.43	0.00	1.41	0.00	0.00
2	Emerald 2 (0.69)	2.45	2.65	16.13	75.84	0.00	0.00	0.95	0.08	1.80	0.00	0.10
3	Emerald 2 (0.69)	2.28	2.62	16.27	75.40	0.03	0.00	1.36	0.00	1.95	0.04	0.04
Av.	Emerald 2 (0.69)	2.39	2.61	16.18	75.75	0.02	0.00	1.25	0.03	1.72	0.01	0.05
1	Emerald 3 (1.04)	0.07	0.00	21.90	76.87	0.05	0.05	0.79	0.00	0.09	0.18	0.00
2	Emerald 3 (1.04)	0.01	0.00	21.76	76.70	0.00	0.00	1.02	0.05	0.35	0.10	0.00
3	Emerald 3 (1.04)	0.00	0.00	21.78	77.27	0.07	0.07	0.74	0.09	0.00	0.00	0.00
Av.	Emerald 3 (1.04)	0.03	0.00	21.81	76.95	0.04	0.04	0.85	0.05	0.15	0.09	0.00
1	Emerald 4 (0.92)	0.21	0.00	21.34	77.53	0.02	0.17	0.64	0.08	0.00	0.00	0.00
2	Emerald 4 (0.92)	0.23	0.00	21.63	76.91	0.00	0.01	0.85	0.00	0.37	0.00	0.00
3	Emerald 4 (0.92)	0.00	0.00	21.87	77.44	0.00	0.07	0.59	0.00	0.00	0.00	0.00
Av.	Emerald 4 (0.92)	0.15	0.00	21.61	77.29	0.01	0.08	0.69	0.03	0.12	0.00	0.00

NB: Quantities below 0.5%wt are at trace level and quantities below 0.05% cannot be guaranteed as present as they are below the detection limit (bdl).

Table 4.5: Overall averages of SEM/EDX analysis results of 0.58ct Russia, 0.69ct Pakistan, 1.04ct Russian flux and 0.92ct Biron hydrothermal emeralds

Stone	Na ₂ O	MgO	Al ₂ O ₃	SiO ₂	TiO ₂	V ₂ O ₅	Cr ₂ O ₃	MnO	Fe ₂ O ₃	CoO	NiO
0.58ct Russia	2.13	2.41	19.0	75.9	0.06	0.07	0.08	0.05	0.25	0	0
0.69ct Pakistan	2.39	2.61	16.2	75.7	0	0	1.25	bdl	1.72	0	0
1.04ct Russia Flux	0	0	21.8	76.9	0	bdl	0.85	0.05	0.15	0.09	0
0.92ct Biron Hyd.	0.15	0	21.6	77.3	0	0.08	0.69	bdl	0.12	0	0

NB: Quantities below 0.5%wt are at trace level and quantities below 0.05% cannot be guaranteed as present as they are below the detection limit (bdl).

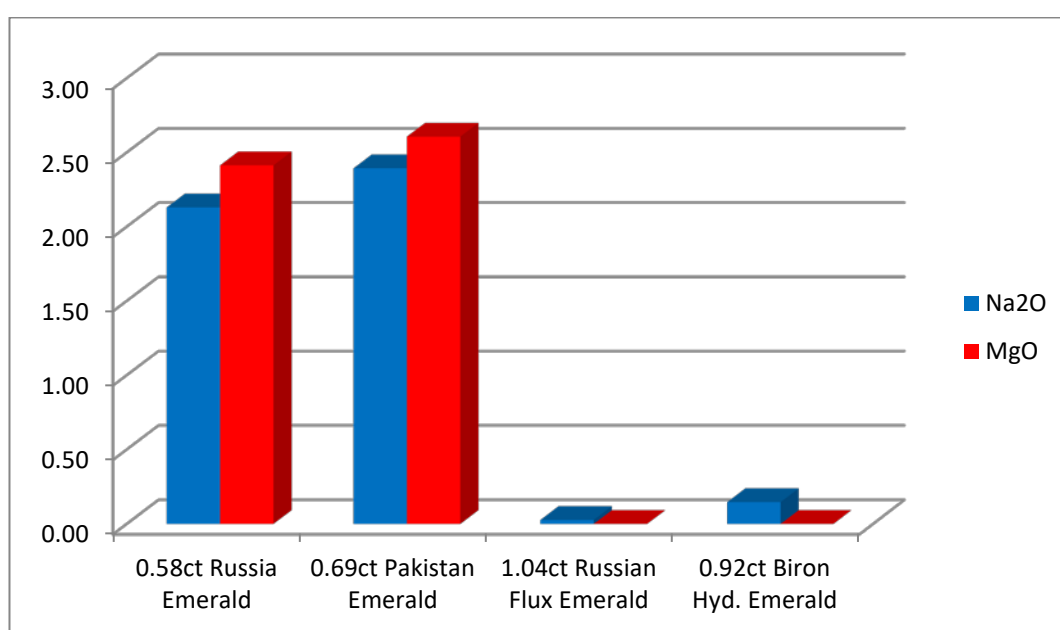


Figure 4.38a: Graph depicting the average difference in concentration of Na₂O and MgO in natural and synthetic emeralds



Figure 4.38b: from left to right: 0.58ct Russian, 0.69ct Pakistan, 1.04ct Russian flux and 0.92ct Biron hydrothermal emeralds

The main differences between the natural and synthetic emeralds were the high presence of sodium and magnesium in the natural emeralds. The sodium and magnesium are most likely to be incorporated into the channel waters of the emeralds from the surrounding host rocks. There was 2.13%wt and 2.41%wt respectively in the 0.58ct Russian emerald and 2.39%wt and 2.61%wt respectively in the 0.69ct Swat, Pakistan emerald. In comparison, both the 1.04ct Russian flux and 0.92ct hydrothermal Biron synthetic emeralds had no MgO present; however the synthetic Biron emerald had a trace amount of Na₂O present. These elements are not present in greater quantities in synthetic emeralds as they are not an integral ingredient for their formation. Both Na₂O and MgO are found in the different types of water in emeralds. The fact that both the Russian and Pakistani natural origin emeralds have both these elements in them indicates that they contain within them two types of water; this being a clear indication of natural formation. As expected the Na₂O in the Biron emerald indicates that there is only one type of water present within the emerald, possibly incorporated into the stone by the nature of the hydrothermal growth process. The amount of water in the natural and hydrothermal emeralds can be calculated by the equation formed by Giuliani *et al.* (1997): H₂O(in wt.%) = [0.84958 x Na₂O(in wt.%)] + 0.8373. Based on this equation and the elemental results obtained for the emeralds; the amount of water in the 0.58ct Russian emerald is 2.65wt%, in the 0.69ct Pakistani emerald is 2.87wt% and in the 0.92ct Biron hydrothermal emerald is 0.96wt% respectively. True to form, there is significantly less water present in the hydrothermal emerald. Again, the lack of either Na₂O or MgO element in the 1.04ct Russian emerald is indicative of a flux origin.

Based on the results of schist and non-schist emerald assignments in Table 4.3; it is advisory that this method should not be used solely as a reliable discriminating argument due to overlapping of the set values. Instead, it should be treated as supplementary identification information to be used in conjunction with inclusion and chemical content information. The overlapping of data values is mainly a result of the abundant variability of the crystal chemistry of beryl crystal structures; whether it is due to locality differentiation in natural emeralds or production methods in synthetic variants.

Identification of synthetic emeralds by Raman spectroscopy is quite a challenging task but is possible by analysing water bands in the regions between 3100cm^{-1} and 3700cm^{-1} . The bands in this region will be able to be used to distinguish between natural (two water peaks), hydrothermal synthetic (one water peak) and flux synthetic (no water peaks) emeralds. Table D2 in Appendix D displays the peaks labelled between the regions of 300cm^{-1} to 1100cm^{-1} . These depict the commonly encountered signature peaks for emerald. Based on the results obtained for this wavenumber region, it is difficult to distinguish the natural from synthetic emeralds as many of the peaks are similar when compared to one another. One visual difference in the spectra is their general shape and form. In the natural emeralds, there are many small negative peaks along a fairly straight baseline which may distort the clarity of the spectra. The peaks at 685cm^{-1} and 1065cm^{-1} tend to be of very strong intensity of approximately 100-150 counts per second (cps). In the spectra of the hydrothermal emeralds, the 685cm^{-1} peak is below 90cps and the 1065cm^{-1} peak is below 30cps respectively. The baseline is exceedingly straight with hardly any distortion based upon the lack of negative peaks. The crisp and clean spectra may be a result of very pure and only necessary elements being incorporated into the growth process. The absence of such negative peaks is also attributable to a low dislocation density of the molecules which would ultimately result in minimal lattice distortion. This is due to optimum conditions and an exceedingly long growth period of up to a year in hydrothermal stones which allow molecules the time to align correctly within the crystal lattice. Although growth periods of flux emeralds are between one to three months, the spectra of these emeralds in figures 4.29a and 4.30a showed the greatest amount of negative peaks, when compared to natural and hydrothermal emeralds. It is possible that the growth timeline is sufficiently long enough to produce the flux emeralds; however is not sufficient to overcome lattice distortion as a result of dislocation density. When analysed with the DXR Raman instrument, these emeralds also showed signs of fluorescence which can be seen by the repetitive wavy pattern of the baseline. The intensity of the flux emerald bands around 685cm^{-1} and 1065cm^{-1} had quite a low intensity of 50cps; the lowest of all the types of stones. A broad band containing a twin peak between the region of 1500cm^{-1} and 1800cm^{-1} was seen only in all of the flux emeralds. It is possible that the peaks seen in this part of the spectrum in

figures 4.29b and 4.30b are unique to only flux emeralds and could possibly be used as a means of flux emerald identification. Generally, the wavy fluorescent baseline coupled with the large volume of negative peaks and very low peak intensities make it quite difficult to analyse and assign true Raman peaks to the flux emeralds.

Overall, the handheld TruScan instrument is unable to produce satisfactory spectra which can be used to define and possibly distinguish between natural emeralds. The high intensity of the instrument results in minute bumps in the baseline which represent the peaks and in some cases there is no information in the spectrum at all. This causes problems in the identification process as there is insufficient information for discrimination and identification of the stones. The instrument does however provide a near identical spectrum for hydrothermal emeralds. This could be due to the lack of impurities within the sample and also due to the purity of all the incorporated elements for emerald growth. As the handheld spectrometer does not possess the full spectral range, it cannot be used to analyse the water regions in emerald; a key distinguishing feature between natural and synthetic hydrothermal and synthetic flux emeralds.

Although only two natural and two synthetic emeralds were analysed, the results for the SEM/EDX analysis are promising for further elemental analysis to be conducted. Consequently, it should be noted that no standards were available during analysis for comparison so these results are to be treated as semi-quantitative only. Due to this issue, it is difficult to determine whether these results are possible discriminants between natural and synthetic stones as not enough is known regarding the natural variation in bulk compositions of emeralds or in the variants of their synthetic counterparts.

4.5 Spinel

In total 20 spinels were analysed of which eight were labelled as natural, seven synthetic and five of unknown origin.

4.5.1 Natural Origin Spinel

This group consists of the eight gemstones which were labelled as being natural spinels and were from known localities of Sri Lanka, Tanzania, Tajikistan and Myanmar (Burma).

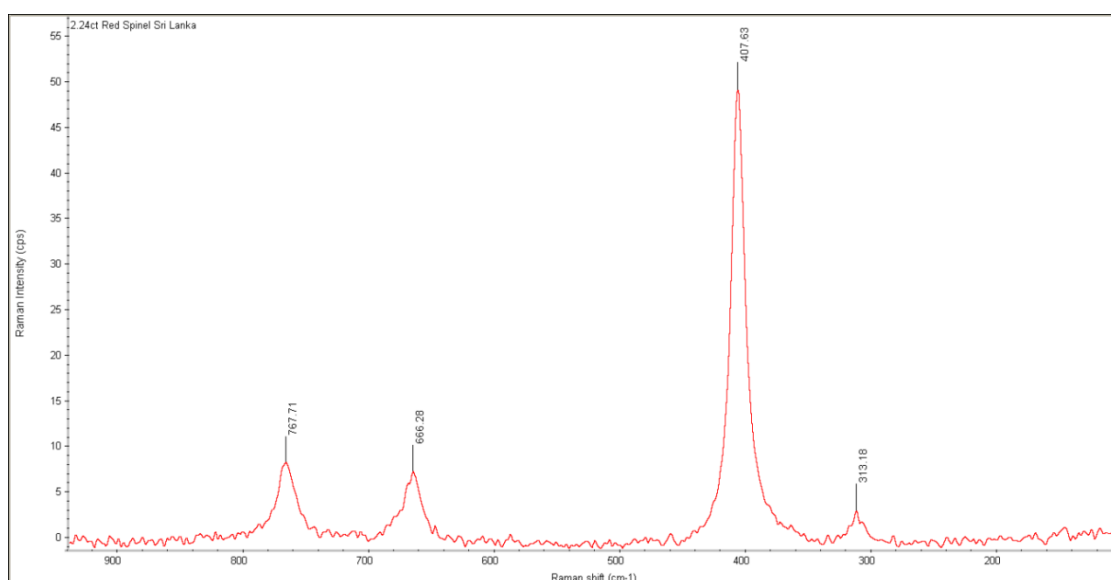


Figure 4.39a: a 2.24ct natural red spinel spectrum from Sri Lanka

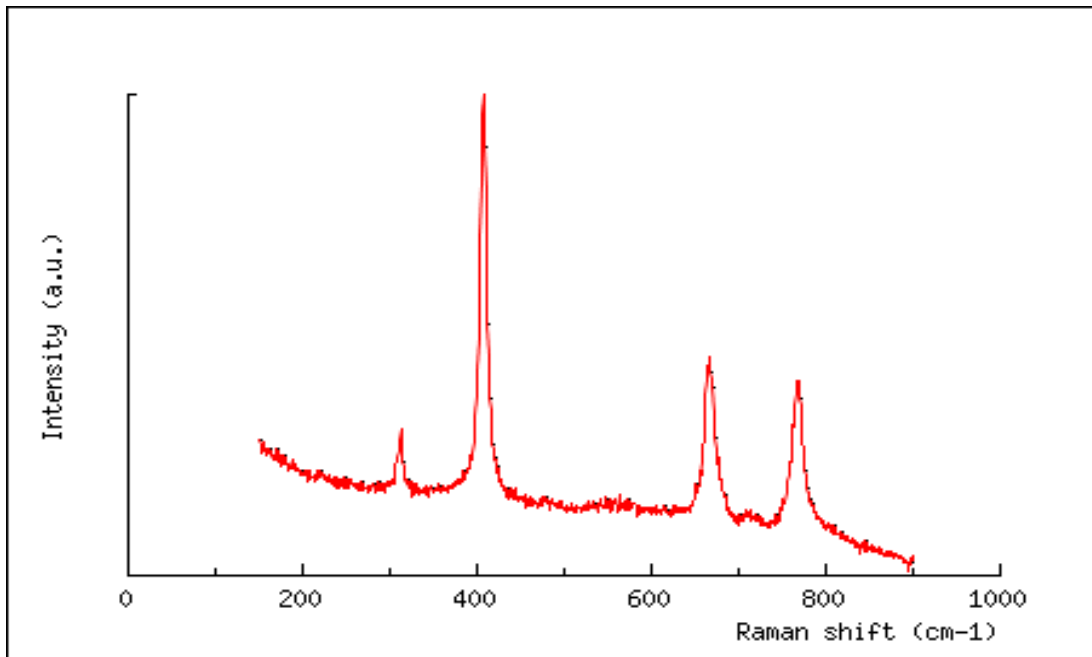


Figure 4.39b: a natural spinel spectrum taken from the Handbook of Minerals Raman Spectra (2012). *NB: the x-axis is reversed to the analytical spectra*



Figure 4.39c: 2.24ct natural red spinel from Sri Lanka

Both figures 4.40a and 4.40b below depict the spectra and correlating photographs of the analysed natural spinels. Despite being different colours due to different metal ions causing the colouration, there is no difference in either spectrum of the spinels to suggest the presence of various metal ions in each stone.

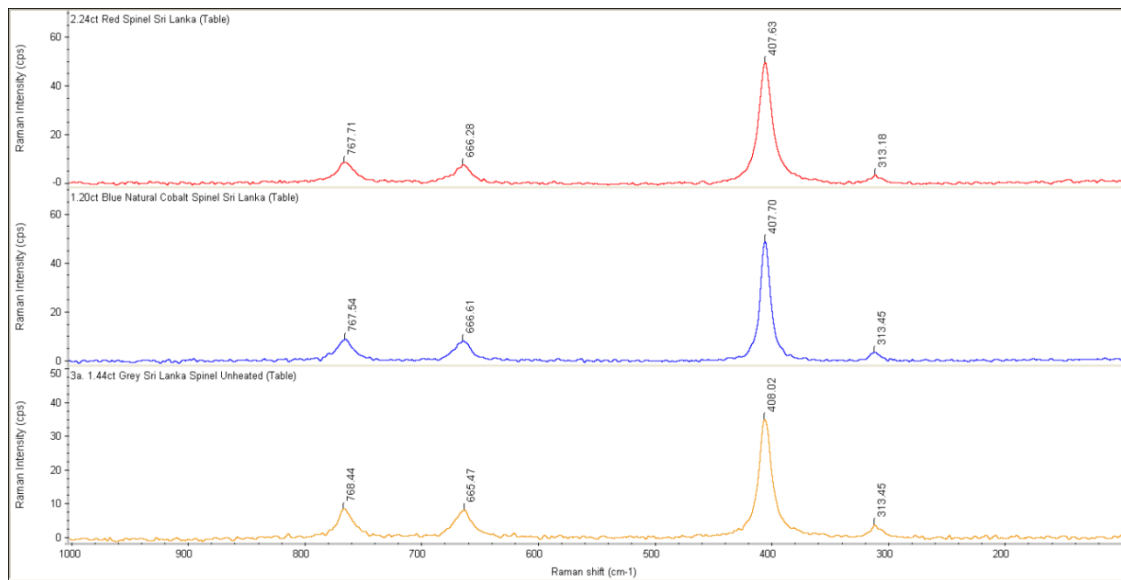


Figure 4.40a: a group spectrum of red, blue and grey spinels of the same origin but of different colours



Figure 4.40b: 2.24ct red, 1.20ct blue and 1.44ct grey spinels of natural origin

4.5.2 Synthetic Origin Spinel

All of the seven synthetic specimens analysed fluoresced on a high magnitude, resulting in unattainable or illegible spectra. Due to this occurrence, no spectral results displaying proper peaks are displayed. The spectrum below depicts a natural blue spinel (red spectrum) and a synthetic blue spinel (blue spectrum). As can be seen, the synthetic spinel sample has fluoresced to a high degree that its true spectrum has been masked.

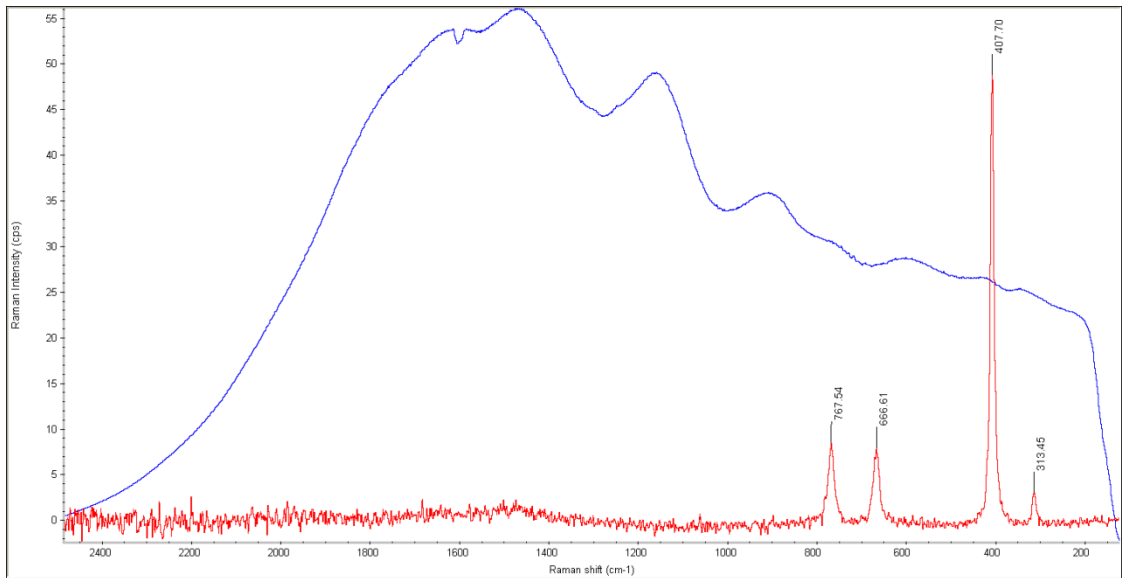


Figure 4.41a: depicting a 1.20ct natural cobalt blue spinel (red spectrum) with defined peaks and a synthetic blue spinel (blue spectrum) exhibiting broad fluorescence in the spectrum



Figure 4.41b: pale blue synthetic spinel

4.5.3 Unknown Origin Spinel

All the stones in this group had no origin information but were initially presumed to be spinel gemstones.

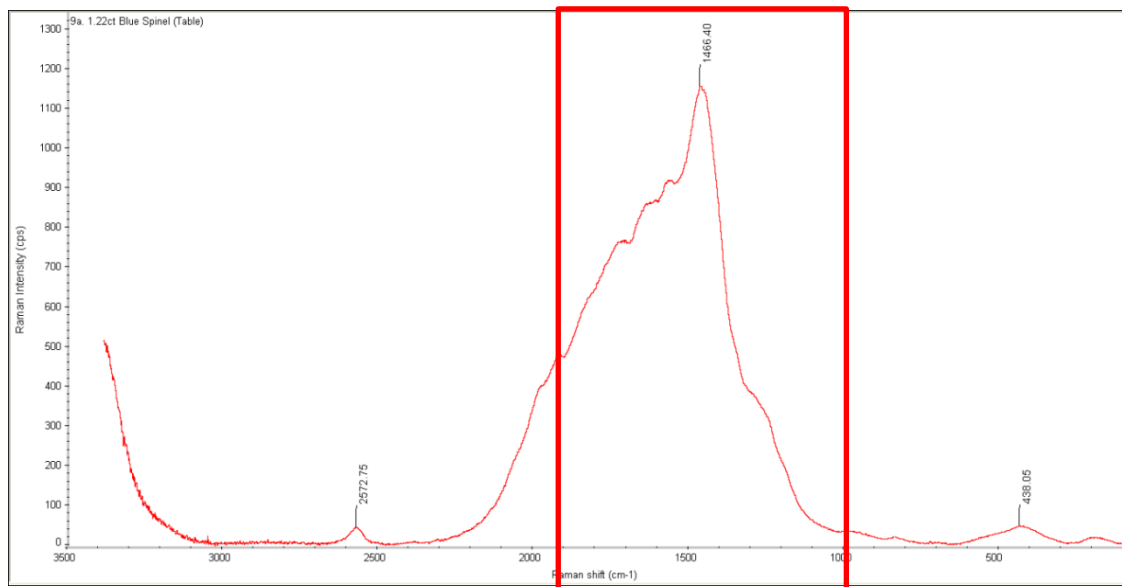


Figure 4.42a: spectrum of a 1.22ct gemstone of unknown origin labelled as spinel

This particular spectrum is of a 1.22ct blue stone purported to be spinel. However, the Raman spectrum shows that the stone is not natural spinel but is that of glass. The highlighted broad and strong intensity peak at 1466cm⁻¹ stretches between 1000cm⁻¹ to 2000cm⁻¹, which is characteristic to this particular material. Below is a glass spectrum for comparison.

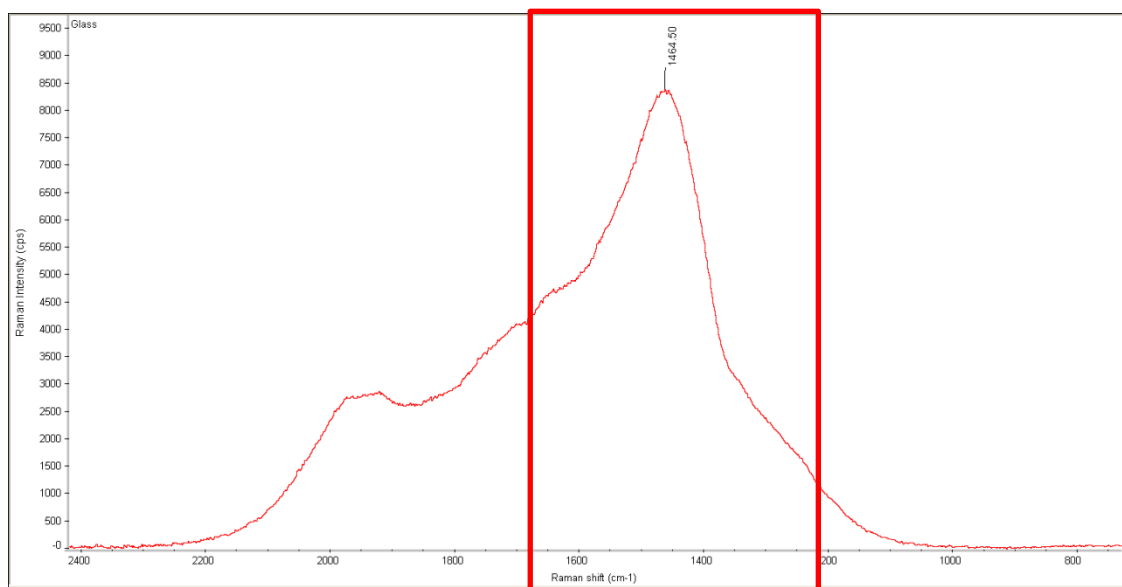


Figure 4.42b: a typical glass spectrum, acquired using a glass vial



Figure 4.42c: 1.22ct gemstone of unknown origin, labelled as spinel

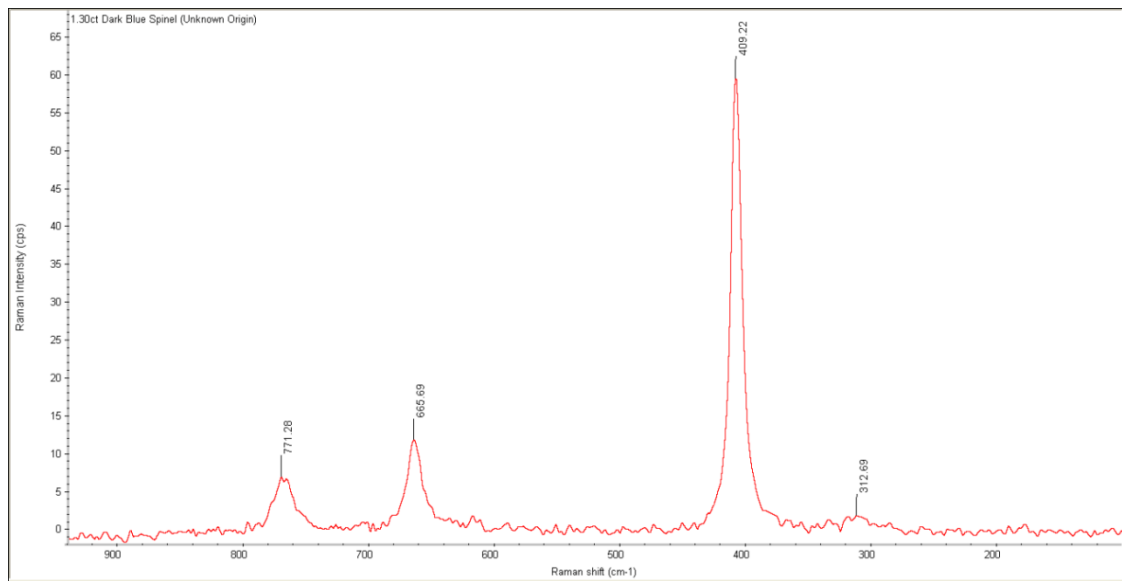


Figure 4.43a: spectrum of a 1.30ct unknown origin dark blue stone, considered to be spinel

The spectrum above confirms that the dark blue unknown origin stone in question is genuine natural spinel based on the distinctive spectral peaks, and also because synthetic spinel fluoresces immensely resulting in either a broad or no spectrum being produced.



Figure 4.43b: 1.30ct unknown origin dark blue stone, considered to be spinel

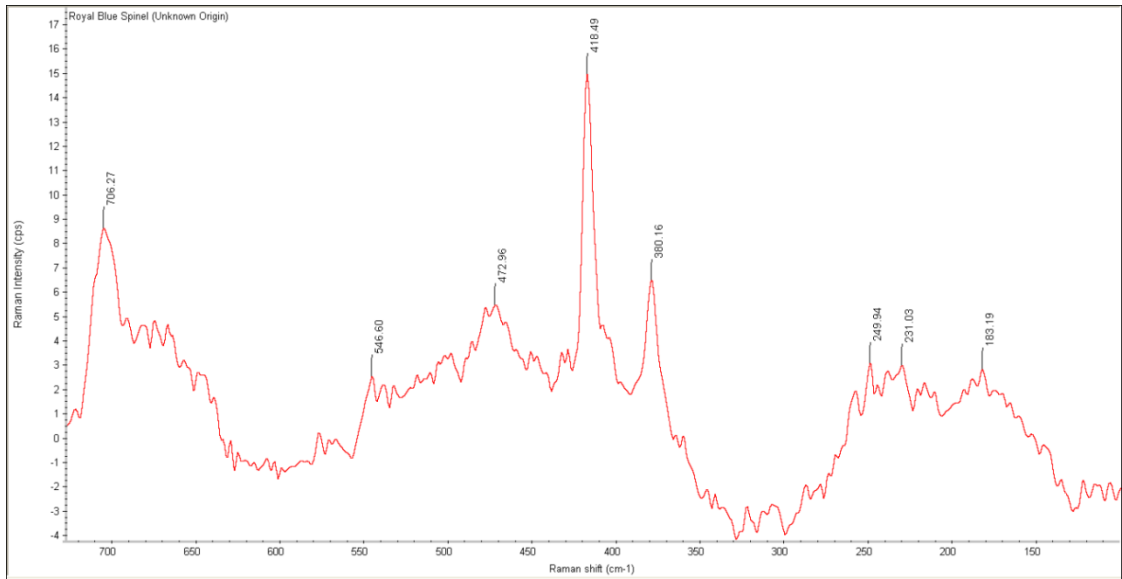


Figure 4.44a: unknown origin royal blue stone, alleged to be spinel

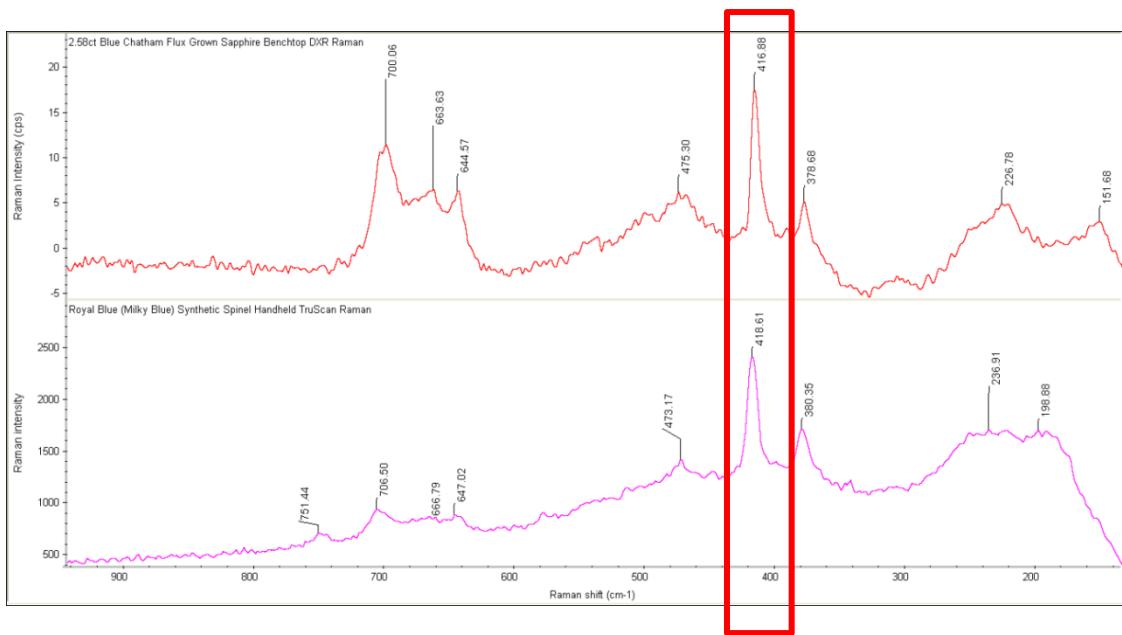


Figure 4.44b: top spectrum of a blue synthetic Chatham flux sapphire and below showing the unknown origin royal blue stone purported to be spinel



Figure 4.45: from left to right: the unknown origin royal blue spinel, 2.58ct Chatham flux sapphire and 2.95ct Sri Lanka sapphire

When analysed, the unknown origin royal blue spinel presented a spectrum that was similar to that of the Chatham flux sapphire which can be seen in figure 4.44b. Upon analysing the peak numbers it was found that the spinel had a 418cm^{-1} characteristic corundum peak in its spectrum as highlighted above, however, the full spectrum did not complement to that of a natural sapphire. Also, the colour and glassy appearance of the stone further confirmed that it was most likely of synthetic origin. Figure 4.45 depicts the spinel in question along with the Chatham flux and natural sapphire. Even the colour of the stone matches that of the synthetic stone; therefore along with the appearance and spectrum result it can be observed that the stone in question is of a synthetic flux origin.

4.5.4 TruScan™ handheld Raman spectroscopy

All the specimens underwent analysis using the handheld instrument. Like with the bench top instrument, the synthetic spinels fluoresced resulting in no spectra being obtained.

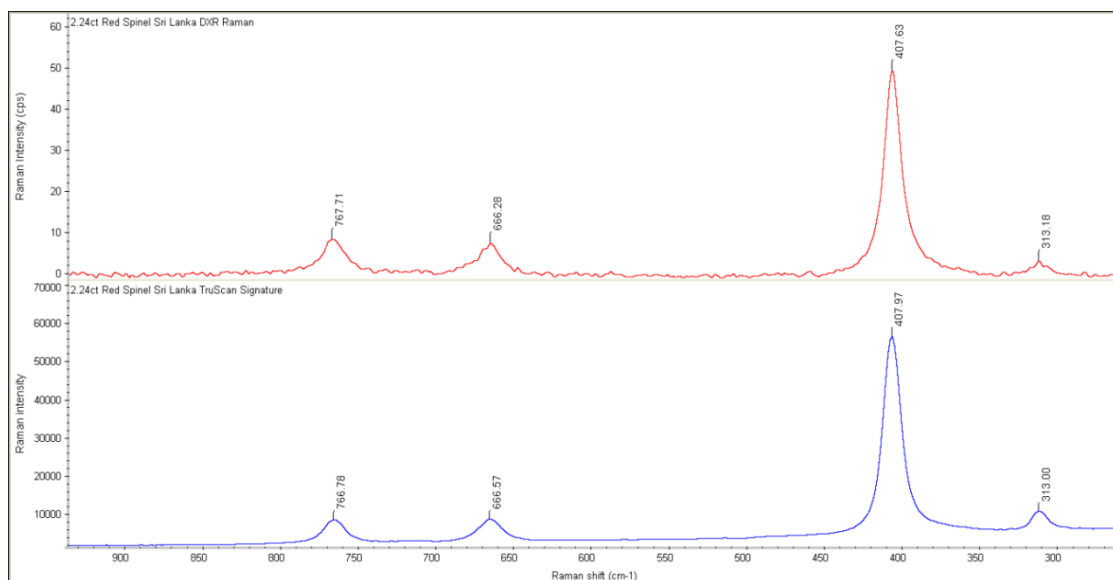


Figure 4.46: Raman spectrum depicting a 2.24ct Spinel of Sri Lankan origin analysed with both the bench top and handheld instrument

The above spectrum represents all of the eight natural spinels which were analysed as all their spectra are cohesive in all properties.

Using bench top Raman spectroscopy to distinguish the natural and synthetic spinels worked very well as all the natural spinel samples gave very clear spectra whereas no spectra were obtained for the synthetic spinels using the 780nm laser. After this result, all the synthetic spinels were analysed again, this time using the 532nm green laser in an attempt to obtain a spectrum, however the same result of fluorescence suppressing and quashing the spectrum occurred.

Reference spectra from a number of online spectral databases were sourced in order to determine if the spectra obtained from the samples were in fact of spinel. Figure 4.39a depicts the spectrum obtained from the DXR bench top Raman using a 780nm laser and figure 4.39b of a Raman spectrum of spinel is from the Handbook of Minerals (2012), shown for comparison purposes. Spinel

of different colours contain different chromophores in order to get their characteristic colours, like chromium for red and iron for blue to name a few. A comparison was done of spinels of different colours to see if their spectra would differ in any way according to the colour they are, but as seen in figure 4.40a that is not the case as all the spectra are the same in the group. The same is also true for spinels from different localities; all having identical spectra. It may be possible to conduct further work on inclusions in order to identify spinel from different geographical and geological origins.

Five of the spinels analysed did not have any labels or accompanying information as to indicate the nature of the samples or where they originated from. The results yielded showed that two of the samples, one green and one royal blue, were synthetic as the spectra were masked by fluorescence. As shown in figure 4.42a the stone thought to be royal blue spinel was actually glass as the characteristic peak at 1466cm^{-1} in the spectrum confirms this. The unknown origin dark blue stone yielded a natural spinel spectrum which can be seen in figure 4.43a. The interesting stone of the batch was a royal blue stone thought to be spinel. When analysed, the stone yielded a completely different spectrum to spinel, as seen in figure 4.44a. The shape of the spectrum, along with the characteristic peak at 418cm^{-1} indicates that the stone is likely to be a royal blue sapphire of synthetic Chatham flux origin.

It can be seen from figure 4.46 that the surface analysis using the handheld instrument produces spinel spectra of great quality which can be used for identification purposes. All the natural spinels worked really well with the TruScan; producing clean, smooth and straight spectra with no negative peaks occurring through any part of the spectrum.

From the results it can be concluded that Raman spectroscopy is able to clearly distinguish natural from synthetic spinels using 532nm and 780nm lasers as synthetics fluoresce profusely during analysis, thus masking the entire spectrum. Where traditional methods are time consuming and unable to plainly distinguish the two types of stone, Raman does that in less than a minute per sample, therefore it is highly desirable for the use of spinel identification. The handheld TruScan spectrometer proved useful in spinel identification as the

same results were obtained as to those from the bench top Raman spectrometer.

5 Conclusion

5.1 DXR Raman spectroscopy

The results achieved through this study demonstrate the competency of the bench top Raman spectrometer as an identification tool when applied to gemstones. Overall it was discovered that Raman spectroscopy is a very useful tool for distinguishing natural from synthetic crystals. In a chapter written by Kiefert *et al* (2001) it was stated that all synthetic stones could not be distinguished from natural stones of the same chemical composition by using Raman spectroscopy, particularly natural ruby from synthetic ruby. This research study has observed that this technique is capable of distinguishing natural and synthetic ruby, and to an extent their different growth production methods. As shown in the results, the Raman spectra obtained were unique for natural and synthetic rubies, despite all the crystals being formed of aluminium oxide. This is because the crystal lattice modes and molecular vibrations are unique to each individual material; even in compounds which are compositionally identical yet have different growth dislocations and imperfections form distinct spectra. The different peaks in the spectra of the synthetic stones to the natural ones could be due to local perturbations as a consequence of structural imperfections occurring during the growth process. These imperfections could be any from a range of interstitial impurities, molecular substitutions, vacancies and dislocations. Intensifying the heat, applying external strain or even interactions of the growth material with the chemical environment could all account for such differences and shifts in the Raman peaks. The study also shows that natural and synthetic emerald and spinel can be distinguished using this technique. The setbacks found in bench top Raman spectroscopy was that it could not differentiate between natural and synthetic sapphires. It is noted that flame fusion is the only growth production method which uses an open flame to melt the materials to form a boule, from which a gemstone is cut. As table 1.1 shows; synthetic aluminium oxide is initially γ -Al₂O₃ but is converted to the natural composition of α -Al₂O₃ when melted at high temperatures. Since the flame fusion method uses the oxy-

hydrogen flame to melt γ - Al_2O_3 at extremely high temperatures it is possible that synthetic Verneuil stones produced by this method may actually have converted into α - Al_2O_3 . If so, this would possibly account for the same peaks seen in the spectra of synthetic Verneuil corundum and natural corundum. The spectra of the synthetics along with showcased well defined peaks allowed for ease of interpretation of the data in order to categorise the gemstones.

There is a possibility that anisotropy in some gemstones can dramatically change peak intensities with changing crystal orientation; making it a possibility for mistakes to be made when comparing experimentally obtained results with standard database data. This is because the relative intensities of Raman peaks are dependent on the orientation between the crystal axes and laser polarisation. As a result it is considered common for peaks to be present at one crystal orientation and absent at another. Therefore the extra 372cm^{-1} peak seen in the synthetic Chatham rubies when orientated on their side is not considered as an unusual occurrence. Also, the database spectra may be acquired using a different wavelength laser so the overall spectral shape and peak intensities of samples may again vary slightly. It is important to pay particular attention to the main peaks present within a samples spectrum as these peaks will always be present regardless of orientation. An example of this is the 418cm^{-1} peak in natural corundum which is always present despite crystal orientation; however one or more of the other corundum peaks may not show at varying orientations.

5.2 Ahura TruScan™ Raman spectroscopy

Currently, the handheld TruScan™ Raman device's main purpose has been raw material identification. Through the results it can be seen that the TruScan™ is capable of gemstone identification; provided the gemstone is in the system's library. As there was no gemstone library, one had to be constructed and incorporated into the current identification system. This was done by acquiring a signature for each type of origin labelled stone (see Appendix B: Part 2: Acquiring a Signature) and then converting it into a method (see Appendix B: Part 3: Creating a Method). Once completed, the remaining stones were processed through runs (see Appendix B: Part 1a: running a

sample) to conclude if TruScan™ was able to determine their origin. It was found that once methods were constructed for each type of stone and added to the library, the handheld Raman was able to identify gemstones according to the type of family they belonged to. However, the handheld Raman instrument is not sensitive enough to determine the origin of a stone, i.e. if natural then its provenance or if synthetic then the type of synthetic production method; and also natural from synthetic gems. The only information it will provide is to confirm what mineral family a stone belongs to. The power of discrimination of the instrument was explored by testing for gemstone identification in different ways. The first method was to analyse a stone by attaching it to a method the operator believed the stone to be. For example; an unknown origin ruby could be attached to a natural or synthetic ruby method. What the TruScan™ will do is give a pass result for either origin regardless of whether the stone is actually natural or synthetic which shows it is unable to distinguish between the two. If the same ruby was analysed by attaching it to the built-in Identification Method; the TruScan™ would present a fail result. What it would then do is provide a discover menu and present the user with a list of items which the sample in question could be. The issue with this is that the list may contain items that are of no relevance or misleading to the user. It was found that due to the lack of peaks present in many of the spectra; the handheld device often displayed identification results of rubies with emeralds together, regardless if the stone in question was definitely a ruby. As the results show; these particular stone types did not yield good spectra with the instrument as they generally had little or no peaks present. When viewed in comparison, the spectra of the handheld instrument are not as defined as the DXR Raman. In fact, due to the nature of the refinement of TruScan™, many spectra have lost vital information through diminution of peak intensity resulting in the lack of peak numbers. An example of this can be seen in figure 4.36 of the 0.69ct Swat, Pakistan emerald where peak numbers in the region between 300cm^{-1} - 1100cm^{-1} are prominent in the DXR Raman spectrum but have been subdued in the TruScan™ spectrum resulting in a flat line with no defining peaks. These missing peaks may be due to the spectral resolution and signal noise of the instrument. Research by Brown (2009) has shown that low spectral resolution or high signal noise can obscure spectral peaks and minimize spectral information. This indicates a lack of

sensitivity in the Raman instrument which can result in having a direct impact upon the quality of the collected spectra.

One of the device features that Ahura Scientific have highlighted is its ability to conduct point-and-shoot analysis. It was found that if the device was not stationary during analysis; but instead being held, then the resulting spectrum contained many negative peaks, thus making the spectrum hazy and ultimately the results may be unreliable.

The TruScan™ manual states that its spectral region lies between 250cm^{-1} and 2895cm^{-1} . It was found that due to the inclusion of Rayleigh scattering, the spectral region begins in a minus wavenumber and defining peaks can be seen in some of the stones analysed.

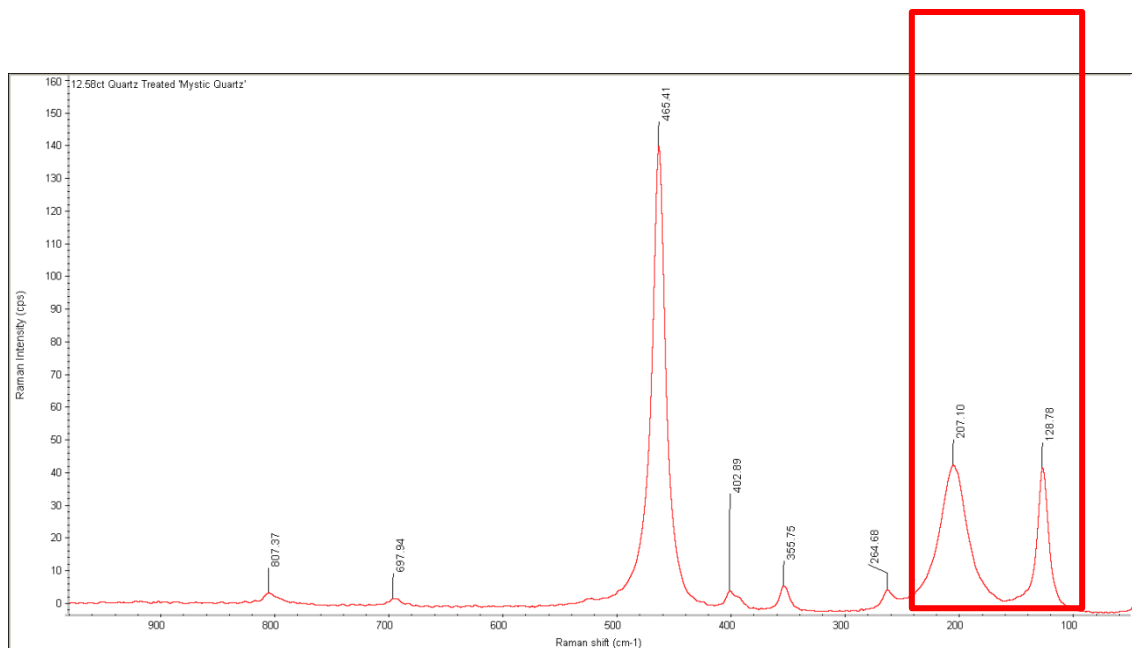


Figure 5.1: handheld spectrum of 12.58ct quartz treated 'mystic quartz'

An example of this was found in the spectra of topaz and quartz gemstones. The highlighted region in figure 5.1 displays characteristic quartz peaks between 100cm^{-1} to 240cm^{-1} which are out with the stated spectral region. It is unclear as to why Ahura Scientific™ have stated that the spectral region begins at 250cm^{-1} when clear defining peaks are obtained below this wavenumber. However this can be seen as a positive result as the experiment has shown that analysis of a wider range of gemstones with characteristic peaks below the stated threshold is possible.

The handheld instrument was put through a series of different light tests in order to establish its optimum conditions. This was done by using it with the laboratory lights off and the blinds open to allow for natural sunlight in the room, with the blinds closed and only in artificial lights and also with both types of light present, with the lights off and with the device covered by a black opaque object. It was observed that the device worked better in dark conditions despite the manual stating that the machine takes light measurements into consideration. When acquiring signatures for methods; covering the instrument with the black object resulted in a significant reduction in acquisition time. This method was used for all the signature acquisitions to speed the process as some processes would take longer than two hours.



Figure 5.2: handheld Raman spectroscope covered with black opaque object

One of the objectives of this study was to determine if a non-scientific person could use this device for identification purposes. The conclusion drawn from the results and of the experience of using this device is that a lay person would find minimal difficulty to operate the instrument in terms of data acquisition as it has been simplified by a point-and-shoot method with no need to manually focus the laser. In respect to that outcome; the same person may find it extremely technically challenging if further interpretation is required as it is confusing to operate the instrument in terms of attaching it to a computer and exporting the material for viewing on a PC. Likewise, if further interpretation of the results is required then a lay person will not know what to do with a spectrum and how to interpret it; resulting in the need for a scientist. Again, the issue lies in the sensitivity of the machine. If a non-scientist wants to use it for general gemstone discrimination and identification then it may be possible to do so; however, as

stated, it is not useful for origin determination. The handheld device would be useful in a scenario where a batch of stones, possibly of the same colour need to be identified. As was seen during analysis of the batch of emeralds; a green stone incorrectly labelled as a natural Pakistani emerald was correctly identified as a green tsavorite garnet. The most common misidentification of coloured stones occurs between ruby and spinel; so identification of these stones would easily be conducted using TruScan on location at a mine site, processing plant or at independent jewellery stores. This type of identification method is primarily useful for miners, traders, sellers and to an extent for consumers too.

Furthermore, Raman scattering can be defined as a sensitive technique which probes local atomic environments within molecules. The properties of these vibrational modes are fundamentally determined by the mass, symmetry and bond type of constituting atoms in the elemental unit; thus making it an excellent method for gemstone identification by providing unique fingerprint spectra.

As the results show; the bench top instrument is capable of not only identifying gemstones from different families and their provenance but can also distinguish between the natural and synthetic ruby and emerald types. The conclusions drawn from these results are confirmed and corroborated by the results provided by SEM/EDX analysis. However, drawbacks in the sensitivity of the handheld Raman spectroscope make it limiting to the depth of identification it can achieve. Raman spectroscopy is currently one of the fastest methods of analysis and one of the very few that have a handheld variation. The non-destructive and versatile nature makes it even more attractive for analysis of materials in virtually any matrix and in any state of matter. The various possibilities and potentials of Raman measurement have been discussed in this study. In addition to the mentioned advantages; the lack of sample preparation allows for direct results of any conducted analysis. Growing interest in this analytical method also stems from easy interpretation thus making it a time-saving and cost-effective technique. In recent years, technical advancement of varying laser wavelengths, sampling conditions, data-processing methods and instrumentation in general have made the technique applicable in various scientific fields.

6 Further work

Kiefert *et al* (2001) stated that the most versatile laser for conducting gemstone work was a 514nm laser which they used to conduct their research. It would be highly desirable to conduct further work in this field of natural and synthetic stones using lasers at different excitation wavelengths in order to compare and contrast results, and to possibly establish what the best type of laser wavelength may be for different types of stone. Establishing the optimum laser wavelength for a particular type of stone will aid in forensic identification as the best possible results will be yielded. Some publications have stated that depending on the type of stone, combined with a specific type of laser wavelength, may produce clearer spectra with more well defined peaks. It has also been stated and should be noted that the laser wavelength does not change the characteristic Raman peaks seen in different stones, but a very slight insignificant shift may occur which does not have any relevance as it occurs by a very small margin. A broader range of stones for analysis would be desirable in order to determine what types of stones work better with what wavelength of laser. The most desirable stones would be those of dark colours as Bruni *et al.* (1999) have observed that Raman spectroscopy is not suited to dark pigments, especially dark green as these colours tend to fluoresce. Previous work by the author showed that emerald spectra were completely unattainable with a 780nm laser due to strong, overpowering fluorescence but were attainable for most emerald stones using a 532nm laser. Also, some synthetic dark blue and green sapphires fluoresced using both laser wavelengths resulting in unattainable spectra. These results confirm the findings by Bruni *et al.* (1999) that this technique is not suited to dark colours, particularly dark green, however with the right laser wavelength legible results are attainable.

It would be worthwhile to undertake a more extensive investigation of crystals from different families and origins, covering a wider range of natural and synthetic stones. This research could not only be conducted using the standard bench top Raman spectrometer but also with the portable hand-held Raman device which would allow for a greater range of stones to be analysed. With the hand-held Raman spectroscope it would be possible to analyse stones that are mounted and set in large, heavy objects that are not easily transportable and

which cannot be analysed using the standard laboratory Raman spectroscope. Using the handheld instrument, it may also be a possibility to take the device to desirable locations such as museums, jewellery stores, exhibitions etc.

Further work would also be desirable for natural and synthetic spinel identification in terms of chemical composition. This would be conducted to determine what percentage of what materials were used to make the synthetics in comparison to the natural stones. The method of choice would be to use SEM/EDX as the instrument showed promising results for corundum and beryl discrimination identification.

7 References

Adams, D.M., Gardner, I.R. (1974) Single-crystal vibrational spectra of beryl and diopside. *Journal of the Chemical Society - Dalton Transactions*, pp. 1502-1505.

Amelinckx, S., van Dyck, D., van Landuyt, J., van Tendeloo, G. (1996) *Handbook of Microscopy: Applications in Materials Science, Solid-state Physics and Chemistry*. VCH Verlagsgesellschaft mbH. Weinheim. Germany.

Amer, M.S. (2010) *Raman Spectroscopy, Fullerenes and Nanotechnology*. RSC Publishing. UK

Arif, M., Fallick, A.E., Moon, C.J. (1996) The Genesis of Emeralds and their Host Rocks from Swat, North-western Pakistan: A Stable Isotope Investigation. *Mineralium Deposita*. **Vol.31**, No.4, pp. 255-268

Bartick, E. (2002) Forensic Analysis by Raman Spectroscopy: An Emerging Technology. *In: 16th Meeting of the International Association of Forensic Sciences [IAFS]*, pp. 2-7

Barcelo, D., Janssens, K., Van Grieken, R. (2004) *Comprehensive Analytical Chemistry: Non-Destructive Microanalysis of Cultural Heritage Materials*. Volume 42. Elsevier B.V. Netherlands

Bersani, D., Lottici, P.P. (2010) Applications of Raman spectroscopy to gemology. *Anal Bioanal Chem*. **Vol.397**, pp. 2631-2646

Biotech Profiles (2008) [Introduction to Raman spectroscopy](#) [Online] Available from www.biotechprofiles.com [Accessed: 01/11/10]

Brown, D.H. (2009) [Comparison of Spectra from a Raman IdentiCheck versus an Ahura® TruScan® Raman Spectrometer](#) [Online] Available from: www.perkinelmer.com [Accessed: 28/12/11]

Bugay, D.E, Smith, P.A.M. (2004) *In: Moffat, A.C., Osselton, M.D., Widdop, B. Clarkes Analysis of Drugs and Poisons*. 3rd Edition. Volume 1. Pharmaceutical Press. UK

Burke, E.A.J. (2001) Raman microspectrometry of fluid inclusions. *Lithos*. **Vol. 55**, pp. 139-158

Canadian Institute of Gemmology (1995) Visual Gemmology-A Basic Approach [Online] Available from: www.cigem.ca/ [Accessed: 18/10/10]

Charoy, B., de Donato, P., Barres, O., Pinto-Coelho, C. (1996) Channel occupancy in an alkali-poor beryl from Serra Branca (Goias, Brazil): Spectroscopic characterization. *American Mineralogist*, **Vol.81**, pp. 395-403

Chem. Europe (2011) Raman spectroscopy [Online] Available from: www.chemeurope.com [Accessed: 07/05/11]

Coates, J. (2000) Interpretation of Infrared Spectra, A Practical Approach. In: Meyers, R.A. (Ed.) *Encyclopaedia of Analytical Chemistry*. John Wiley & Sons Ltd, Chichester, pp. 10815-10837

Das, R.S., Agrawal, Y.K. (2011) Raman spectroscopy: Recent advancements, techniques and applications. *Vibrational Spectroscopy*. **Vol.57, No.2**, pp. 163-176

Degen, I.A. (1997) *Tables of Characteristic Group Frequencies for the Interpretation of Infrared and Raman Spectra*. Acolyte Publications.

Dele, M.L., Dhamelincourt, P., Poirot, J.P., Dereppe, J.M., Moreaux, C. (1997) Use of Spectroscopic Techniques for the Study of Natural and Synthetic Gems: Application to Rubies. *Journal of Raman Spectroscopy*. **Vol. 28**, pp. 673-676

Dove, M.T. (2005) *Introduction to Lattice Dynamics*. Cambridge University Press. UK

Dynys, F.W., Halloran, J.W. (1982) Alpha alumina formation in alum-derived gamma alumina. *Journal of the American Ceramic Society*. **Vol. 65**, pp.442-448

Ebelman, M. (1848) Sur une nouvelle methode pour obtenir des combinaisons cristallisees par la voie seche, et sur ses applications a la reproduction des especes minerales. *Ann. Chimie Phys.* **Vol.22**, pp.213-244

Ebnesajjad, S (2010) *Handbook of Adhesives and Surface Preparation: Technology, Applications and Manufacturing*. William Andrew Inc.

Ebnesajjad, S., Ebnesajjad, C.F. (2006) *Surface Treatment of Materials for Adhesion Bonding*. William Andrew Inc.

Edwards, H.G.M., Chalmers, J.M. (2005) *Raman Spectroscopy in Archaeology and Art History*. The Royal Society of Chemistry. Cambridge. UK

Edwards, H.G.M., de Faria, D.L.A. In: Janssens, K., van Grieken, R. (2004) *Comprehensive Analytical Chemistry: Non-destructive Microanalysis of Cultural Heritage Materials*. Volume 42. Elsevier B.V. The Netherlands

Elwell, D. (1979) *Man-made Gemstones*. Ellis Horwood Ltd. England. UK

Evans Analytical Group (2011) Analytical Techniques [Online] Available from: www.eaglabs.com/techniques/analytical_techniques [Accessed: 04/01/12]

Federal Trade Commission (2007) FTC Amends Its Guides for the Jewellery Industry [Online] Available from: www.ftc.gov [Accessed: 05/05/11]

Ferraro, J.R., Nakamoto, K., Brown, C.W. (2003) *Introductory Raman Spectroscopy*. 2nd Edition. Elsevier Inc.

Fisk, Z., Remeika, J.P. (1989) Growth of single crystals from molten metal fluxes. In: Gschneidner Jr, K.A., Eyring, L. *Handbook on the Physics and Chemistry of Rare Earths*. Elsevier. Amsterdam

Flanigen, E.M., Breck, D.W., Mumbach, N.R., Taylor, A.M. (1967) Characteristics of Synthetic Emeralds. *The American Mineralogist*. **Vol.52**, pp. 744-772

Fritsch, E., Rondeau, B. (2009) *Gemology: The Developing Science of Gems. Elements*. **Vol.5**, pp. 147-152

Gaft, M., Reisfeld, R., Panczer, G. (2005) *Luminescence spectroscopy of Minerals and Materials*. Springer. Germany

Garratt-Reed, A.J., Bell, D.C. (2003) *Energy-dispersive X-ray Analysis in the Electron Microscope*. Garland Science.

Gemmology (2010) The General Procedure in Gemstone Identification and Testing [Online] Available from: www.gemmology.lk/pdf/6729_article_4.pdf [Accessed: 18/10/10]

Gemology Project (2011) Spinel [Online] Available from: www.gemologyproject.com [Accessed: 27/07/11]

Gem Society (2010) International Gem Society Reference Library [Online] Available from: www.gemsociety.org [Accessed: 05/05/11]

Gemstone Buzz (2010) Synthesis and Synthetics [Online] Available from: www.gemstonebuzz.com/synthesis-synthetics [Accessed: 19/10/10]

Gentile, A.L., Cripe, D.M., Andrew, F.H. (1963) The Flame Fusion Synthesis of Emerald. *American Mineralogist*. **Vol.48**, pp. 940-943

Geology (2011) World Diamond Demand [Online] Available from: www.geology.com [Accessed: 30/12/11]

Giuliani, G., France-Lanord, C., Zimmermann, J.L., Cheilletz, A., Arboleda, C., Charoy, B., Coget, P., Fontan, F., Giard, D. (1997) Fluid Composition, dD of H_2O and $d^{18}O$ of Lattice Oxygen in Beryls: Genetic Implications for Brazilian, Colombian and Afghanistani emerald deposits. *International Geology Review*. **Vol.39**, pp. 400-424

Goldstein, J.I., Newbury, E., Echlin, P., Joy, D.C., Fiori, C., Lifshin, E. (1981) *Scanning Electron Microscopy and X-ray Microanalysis*. Plenum Press, New York

Griffith, W.P. (1974) Raman spectroscopy of minerals. In: Farmer, V.C. (Ed.), *The Infrared Spectra of Minerals*. Mineral. Soc. London Monogr., **Vol. 4**, pp. 119-135

Groat, L.A., Giuliani, G., Marshall, D.D., Turner, D. (2008) Emerald Deposits and Occurrences: A Review. *Ore Geology Reviews*. **Vol. 34**, pp. 87-112

Hagemann, A., Lucken, A., Bill, H., Gysler-Sanz, J., Stalder, H.A. (1990) Polarized Raman spectra of beryl and bazzite. *Physics and Chemistry of Minerals*. **Vol.17**, pp. 395-401.

Hänni, H.A. (1982) A contribution to the separability of natural and synthetic emeralds. *Journal of Gemmology*, XVIII, **Vol.2**, pp.138-144.

Hollaender, A., Williams, J.W. (1931) The molecular scattering of light from amorphous and crystalline solids. *Phys. Rev.* **Vol. 38**, pp. 1739-1744

Holmes, R.J., Crowningshield, C.R. (1960) A New Emerald Substitute. *Gems Gemmol.* pp. 11-12

Hope, G.A., Woods, R., Munce, C.G. (2001) Raman microprobe mineral identification. *Minerals Engineering*. **Vol. 14, No. 12**, pp.1565-1577

Horiba Jobin Yvon (2010) Raman Data and Analysis: Raman Spectroscopy for Analysis and Monitoring [Online] Available from: www.horiba.com [Accessed: 05/05/11]

Houghton, R. (2009) *Field Confirmation Testing for Suspicious Substances*. CRC Press. USA

Hughes, R.W. (1997) *Ruby & Sapphire*. RWH Publishing.

Huong, P.V. (1996) New possibilities of Raman micro-spectroscopy. *Vibrational Spectroscopy*. **Vol. 11**, pp.17-28

Huong, L.T.T., Häger, T., Hofmeister, W. (2010) Confocal Micro-Raman Spectroscopy: A Powerful Tool to Identify Natural and Synthetic Emeralds. *Gems & Gemology*. **Vol.46, No.1**, pp. 36-41

Huong, L.T.T., Häger, T. (2010) On some controversially-discussed Raman and IR bands of beryl. *VNU Journal of Science, Earth Sciences*. **Vol.26**, pp.32-41

International Colored Gemstone Association (2012) Price and Prejudice [Online] Available from: www.gemstone.org [Accessed: 03/01/12]

Jellinek, M.H., Fankuchen, I. (1948) The application of X-Ray Diffraction to the study of solid crystals. *Advances in Catalysis*. **Vol. 1**, pp. 257-289

Jenkins, A.L., Larsen, R.A. (2004) Gemstone identification using Raman spectroscopy. *Spectroscopy*. **Vol. 19, No. 4**, pp.20-25

Jickells, S., Nergusz, A (2008) *Clarke's Analytical Forensic Toxicology*. Pharmaceutical Press

Johnson, E.A. (2006) Water in Nominally Anhydrous Crustal Minerals: Speciation, Concentration and Geologic Significance. *Reviews in Mineralogy and Geochemistry*. **Vol.62, No.1**, pp.117-154

Justia Trademarks (2011) Decision Engine-Trademark Details [Online] Available from: <http://trademarks.justia.com/785/75/decision-engine-78575126.html> [Accessed: 17/02/12]

Kiefert, L., Hänni, H.A., Ostertag, T. (2001) *In: Lewis, I.R., Edwards, H.G.M (eds) Handbook of Raman spectroscopy: from the research laboratory to the process line*. Marcel Dekker, New York. pp. 469-490

Kim, C., Bell, M.I., McKeown, D.A. (1995) Vibrational analysis of beryl ($\text{Be}_3\text{Al}_2\text{Si}_6\text{O}_{18}$) and its constituent ring (Si_6O_{18}). *Physica B*, **Vol.205**, pp. 193-208

Können, G.P. (1985) *Polarized Light in Nature*. Cambridge University Press. UK

Marassi, R., Nobili, F. (2009) MEASUREMENT METHODS | Structural and Chemical Properties: Scanning Electron Microscopy. *Encyclopaedia of Electrochemical Power Sources*. pp. 758-768

McMillan, P.F. (1989) Raman spectroscopy in Mineralogy and Geochemistry. *Ann. Rev. Earth Planet. Sci.* **Vol. 17**, pp. 255-283

Miller, R.P., Mercer, R.A. (1965) The High-Temperature Behaviour of Beryl Melts and Glasses. *Mineralogical Magazine*. **Vol.35**, pp. 429-433

Moffat, A.C., Osselton, M.D., Widdop, B. (2004) *Clarke's Analysis of Drugs and Poisons*. 3rd Edition. Volume: 1. Pharmaceutical Press. UK

Montagnac, G (2012) Handbook of Minerals Raman Spectra [Online] Available from: <http://www.ens-lyon.fr/LST/Raman/index.php> [Accessed: 01/01/12]

Morosin, B. (1972) Structure and Thermal Expansion of Beryl. *Acta Crystallographica*, B28. pp. 1899-1903

Moroz, I., Roth, M., Boudeulle, M., Panczer, G. (2000) Raman microspectroscopy and fluorescence of emeralds from various deposits. *Journal of Raman Spectroscopy*. **Vol.31**, pp. 485-490

Museum of Science (1996) Scanning Electron Microscopy [Online] Available from: www.mos.org [Accessed: 12/01/12]

Nassau, K. (2009a) Gemstone Materials. *In: Kirk-Othmer Encyclopaedia of Chemical Technology*. John Wiley & Sons, Inc.

Nassau, K. (2009b) Gemstone Treatment. *In: Kirk-Othmer Encyclopaedia of Chemical Technology*. John Wiley & Sons, Inc.

Non-destructive Testing Resource Centre (2011) Crystal Defects [Online] Available from: www.ndt-ed.org/ [Accessed: 06/05/11]

O'Donoghue, M. (1976) *Synthetic Gem Materials*. Worshipful Company of Goldsmiths. London. UK

- O'Donoghue, M. (1983) *Identifying Man-made Gemstones*. NAG Press Ltd
- O'Donoghue, M. (1997) *Synthetic, Imitation and Treated Gemstones*. Butterworth-Heinemann. UK
- O'Donoghue, M. (2005) *Artificial Gemstones*. NAG Press. UK
- O'Donoghue, M. (2006) *Gems*. 6th Edition. Butterworth-Heinemann. UK
- O'Donoghue, M., Joyner, L. (2002) *Identification of Gemstones*. Butterworth-Heinemann. UK
- Oishi, S. (2003) *In: Byrappa, K., Ohachi, T. Crystal Growth Technology*. William Andrew Inc. New York. USA
- Oishi, S., Teshima, K., Kondo, H. (2004) Flux growth of hexagonal bipyramidal ruby crystals. *Journal of the American Chemical Society*. **Vol. 126**, pp. 4768-4769
- Olden, C (1911) Emeralds: Their Mode of Occurrence and Methods of Mining and Extraction in Colombia, *Transactions of the Institute of Mining and Metallurgy*, **Vol. 21**, pp.193-209
- Olson, D.W. (2001) U.S. GEOLOGICAL SURVEY MINERALS YEARBOOK [Online] Available from: <http://minerals.usgs.gov/minerals/pubs/commodity/gemstones/gemstmyb01.pdf> [Accessed: 02/01/12]
- Osanai, Y., Ueno, T., Tsuchiya, N., Takahashi, Y., Tainosho, Y. , Shiraishi, K. (1990) Finding of vanadium-bearing garnet from the Sør Rondane Mountains, East Antarctica, *Antarctic Rec. (Japan)* **Vol.34**, pp.279–291
- Pamplin, B.R. (1980) *Crystal Growth*. Pergamon Press. UK
- Pardieu, V. (2005) Lead Glass Filled/Repaired Rubies [Online] Available from: www.aigslaboratory.com [Accessed: 19/05/11]

Pelletier, M.J. (1999) *Analytical Applications of Raman Spectroscopy*. Oxford: Wiley Blackwell Science Ltd.

Princeton Instruments (2010) Raman Spectroscopy Basics [Online] Available from: www.piacton.com [Accessed: 01/11/10]

Raman, C.V. (1922) Molecular Diffraction of Light. *Nature*. **Vol. 110**, pp. 505-506

Raman, C.V., Krishnan, K.S. (1928) A new type of secondary radiation. *Nature*. **Vol. 121**, pp. 501-502

Ramaura Cultured Ruby (1998) What's The Difference [Online] Available from: www.ramaura.com [Accessed: 02/11/2010]

Rare and Precious Gems (2010) Investment Summary: Coloured Diamonds and Precious Gems [Online] Available from: www.rareandpreciousgems.com [Accessed: 21/02/12]

Read, P.G. (2005) *Gemmology*. 3rd Edition. Elsevier Butterworth-Heinemann. UK

Robert Gordon University (2010) X-Ray Analysis using the Scanning Electron Microscope [Online] Available from: http://www2.rgu.ac.uk/life_semweb/xray.html [Accessed: 09/01/12]

Scheel, H.J., Fukuda, T. (2003) *Crystal Growth Technology*. William Andrew Inc. Norwich. New York

Schrader, H.W. (1983) Contribution to the study of the distinction of natural and synthetic emeralds. *Journal of Gemmology*, XVIII, **Vol.6**, pp. 530-543

Schwarz, D., Schmetzer, K. (2002) The Definition of Emerald. *ExtraLapis English*. **Vol.2**, pp. 74-78

Shah, R. (2010) *The use of Raman spectroscopy to analyse inclusion bodies in gemstones in order to establish provenance*. Unpublished BSc Honours Thesis, Edinburgh Napier University

Shelementiev, Y., Serov, R. (2011) Synthetic Emeralds. MSU Gemmological Centre of Moscow University: Annual CIBJO Congress Emerald Day Conference.

Shigley, J.E. (2000) Treated and synthetic gem materials. *Current Science*. **Vol. 79, No. 11**, pp. 1566-1571

Smillie, I. (2010) *Blood on the Stone: Greed, Corruption and War in the Global Diamond Trade*. Anthem Press. UK.

Smith, W.E. (2008) Practical Understanding and use of Surface Enhanced Raman Scattering/Surface Enhanced Resonance Raman Scattering in Chemical and Biological Analysis. *Chem. Soc. Rev.* **Vol. 37**, pp. 955-964

Smith, G.D., Clark, R.J.H. (2004) Raman microscopy in archaeological science. *Journal of Archaeological Science*. **Vol. 31**, pp. 1137-1160

Smith, W.E., Dent, G. (2005) *Modern Raman Spectroscopy: A Practical Approach*. John Wiley & Sons Ltd. London

Sodo, A., Nardone, M., Ajo, D., Pozza, G., Bicchieri, M. (2003) Optical and structural properties of gemmological materials used in works of art and handicraft. *Journal of Cultural Heritage*. **Vol. 4**, pp. 317s-320s

Spectroscopy Europe Asia (2010) Thermo's Acquisition of Ahura Finalised [Online] Available from: <http://www.spectroscopyeurope.com/news/company-news/2409-thermos-acquisition-of-ahura-finalised> [Accessed: 23/11/11]

Sprawls, P (1995) *Physical Principles of Medical Imaging* (2nd Edition). Medical Physics Publishing Corporation.

Staatz, M.H., Griffiths, W.R., Barnett, P.R. (1965) Differences in the minor element composition of beryl in various environments. *The American Mineralogist*, **Vol.50**, pp. 1783-1795.

Stockton, C.M. (1984) The chemical distinction of natural from synthetic emeralds. *Gems & Gemmology*. **Vol.20**, No.3, pp. 141-145.

Sunagawa, I. (2005) *Crystals: Growth, Morphology and Perfection*. Cambridge University Press, UK

Thermo Fisher Scientific Inc. (2012) TruScan [Online] Available from: <http://www.ahurascientific.com/material-verification/products/truscan/index.php> [Accessed: 06/01/12]

Thermo Fisher Scientific Inc. (2011) Raman Spectroscopy [Online] Available from: www.thermo.com [Accessed: 01/11/10]

Thomas, A. (2008) *Gemstones: Properties, Identification and Use*. New Holland Publishers Ltd. UK

Thomas, S., Stephen, R. (2009) *Rubber Nanocomposites: Preparation, Properties and Applications*. John Wiley and Sons.

United Nations Statistics Division (2011) Classifications Registry [Online] Available from: www.unstats.un.org [Accessed: 01/01/12]

United States Geological Survey (2011) Mineral Commodity Summaries [Online] Available from: <http://minerals.usgs.gov/minerals/pubs/mcs/2011/mcs2011.pdf> [Accessed: 29/12/11]

United States Geological Survey (2002) Synthetic and Simulant [Online] Available from: www.minerals.usgs.gov/minerals/pubs/commodity/gemstones/sp14-95/synthetic.html [Accessed: 04/01/11]

University of California Riverside (1996) **Central Facility for Advanced Microscopy and Microanalysis**: Introduction to Energy Dispersive X-ray

Spectrometry (EDS) [Online] Available from:
<http://micron.ucr.edu/public/manuals/EDS-intro.pdf> [Accessed: 13/02/12]

University of Cambridge (2007) Raman Spectroscopy [Online] Available from: www.doitpoms.ac.uk/tlplib/raman/raman_scattering.php. [Accessed: 02/05/11]

University of Notre Dame (2012) Techniques for Metal Analysis at CEST [Online] Available from: <http://www.nd.edu/~cest/news/inorgmetals.pdf> [Accessed: 09/01/12]

The University of Texas at Austin (2011) Gems and Gem Minerals [Online] Available from: www.geo.utexas.edu [Accessed: 06/05/11]

University of Texas at Austin (2011) Spinel [Online] Available from: www.geo.utexas.edu [Accessed: 27/07/11]

Whittaker, A.G., Mount, A.R., Heal, M.R. (2000) *Physical Chemistry*. USA: BIOS Scientific Publishers Ltd.

The World Jewellery Confederation (2010) Gemstones, Organic Substances & Artificial Products — Terminology & Classification [Online] Available from: www.cibjo.org [Accessed: 19/02/11]

Wood, D.L., Nassau, K. (1967) Infrared Spectra of Foreign Molecules in Beryl. *Journal of Chemical Physics*. **Vol.47**, pp. 2220-2228

Appendix A

Bench top DXR Raman spectroscopy Standard Operating Procedure

The following SOP was devised by Shah (2010) during previous research studies:

1. Turn the Raman instrument and computer on
2. Start up the OMNIC software
3. Turn the lamp on (flip switch on from standby (0) to run (I); situated by the side of the instrument)
4. Go to 'Collect' in the toolbar, click on 'Experiment Setup', then 'Bench' and turn the laser from Off to On
5. Open the doors under the microscope
6. Place the mounted sample underneath the laser aperture, set at 50 μ m pinhole
7. Focus the laser on the sample surface using both the coarse and fine adjustment knobs of the microscope*
8. Close the sampling area doors
9. Collect the sample by clicking on the 'Collect Sample' button in the toolbar
10. Enter a name for the sample in the dialogue box
11. Click 'Start Collection' to start collecting the data on the sample
12. To save the spectrum, click on the 'File' menu and then click on "Save As"
13. Enter a name for the sample spectrum
14. Save the sample spectrum as both the default file Spectra (*.SPA) and a TIFF (*.TIF) file**

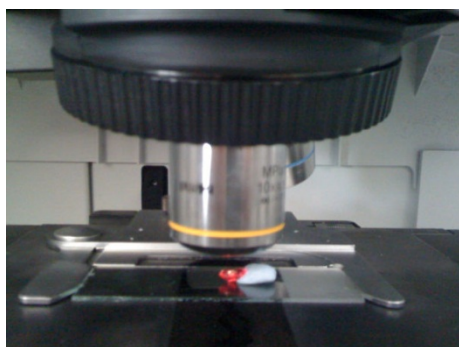


Figure A1: mounted gemstone sample placed on the stage under the laser

*Take extreme caution in making sure the sample does not come into contact with the microscope lens as this may result in damage to the instrument.

**Saving data as a TIFF (*.TIF) file allows for the data to be viewed on a computer without OMNIC software.

Appendix B

Ahura TruScan™ Standard Operating Procedure (SOP)

A standard operating procedure was developed from the outset to enable quick and repetitive sample analysis. Conforming to the same sampling structure and method ensured the acquisition of non-biased, reliable results.

Part 1a: Running a sample

1. Press on the power “” button
2. Press “login” to start up the instrument; as prompted onscreen
3. *1Select administrator username “Jack_admin” using the enter “↵” key
4. Enter password “k”
5. Select appropriate attachment for the laser/nose aperture:
 - small (barrel) or large (pointed) laser diameter nose cone
 - vial holder
 - pill holderensuring both the test sample and unit are clean
6. Refer to page 23 of the TruScan™ manual: Best Practices for Making Measurements.

NB: the barrel shaped nose cone yields optimum results for gemstone analysis.

7. Mount the gemstone, table side up, securely onto the end of the nose cone using sellotape®
8. Select “Run”
9. Select “Method”
10. Enter a sample ID
11. Select “Go” and wait for analysis
12. A “Pass” or “Fail” dialogue box will appear on the screen
13. If given a fail result then go to “Discover” and to “positive matches found”
14. Click on an item within the list to view the spectrum comparison to the library

**1 once logged in using the “jack_admin” username, it is possible to create your own account whereby any ‘runs’ performed will show under your username. Doing this will make it easier to find your ‘runs’ on the TruScan™ system if there are multiple people using the device.*

Part 1b: Viewing and saving a run in the bench top DXR Raman Omnic system

1. In the Main Menu, go to “Tools” and then to “Review Runs”:
 - *NB:* A list of runs will appear; the small icon next to the run name indicates whether the run is a pass or fail. Each run is titled with the username, date and time for identification purposes:



=Pass



= Fail

2. Insert the CF Memory card into the CF slot
3. Highlight the run to be examined, the “Review Runs” menu will appear
4. Highlight “Export to Card”. A confirmation dialogue box will appear once the run has been exported.
5. Eject the memory card and place into the USB stick (red and grey colour side up: opposite to how it is inserted into the TruScan™ device)
6. Insert the USB stick into the PC hard drive; the “Removable Disk E/F” will automatically open up
7. Transfer the exported runs onto the PC by saving them to a folder

Part 2: Acquiring a Signature

1. Go to:
 - “Tools”
 - “Signature”
 - “Acquire” → once the signature acquisition screen appears, a bar across the bottom of the screen will say “Initializing” then change to “minutes left” displaying the amount of time left for acquiring a sample spectrum. The data quality will increase with increasing acquisition time from low (red), to medium (yellow), to high (green). As the bar moves into the green coloured region the spectrum should be of good quality to use.
2. Once the signature is acquired go to “Inactive” and “View spectrum” to check spectrum quality and then the “Esc” key to exit.

NB: Take a note of the signature number so the spectrum can be correctly identified and named when transferred to the computer or alternatively rename the spectrum on the device before exporting it.

Part 3: Creating a Method

A method is an analytical task which the TruScan™ system uses to determine whether or not a test sample's identity can be verified. Each method defines the name of the material involved, its spectral signature and any supplementary information that is available.

1. Connect the CF-Ethernet Adapter to the CF slot in the instrument.
2. Connect the red Cross-over Cable to the CF-Ethernet Adapter and to the computer hard drive.
3. On the instrument go to the "Inactive" signature list and go to "activate as" (*NB: you will have the option to activate the signature using the generic name or you can rename it*)
4. Open "New Internet Shortcut" located on the computer desktop.
5. Go to username "Jack_admin" and enter password "k" to log in.
6. Click on "Method Management" then "Add New Method" and give the method (the tested sample) a name.
7. Go to the "Status" dialogue box and click on enabled
8. Scroll through the dialogue box located below and move the "unattached signature" over to the "signatures in method" dialogue box, click on "save changes" and exit the programme. The signature is now active as a method so it is ok to remove all leads from the computer and instrument.

Part 4: Exporting a Signature spectrum from the handheld TruScan™ Raman to the bench top DXR Raman and PC

1. Insert the memory card into the CF Slot
2. Go to "Signatures" and to the "Inactive" list and choose the appropriate

signature then “Export” it to the memory card

3. Remove the memory card; place into the USB stick and plug it into the computer
4. Open “Omnics” located on the computer desktop
5. Go to:
 - “My Computer”
 - “Removable Disk E”
 - There will be two icons present for one signature. The signature will be the generic number or the title given when renamed on the device and in the format PKCS#7 Certificates (*NB: do not select the file which has the word “dark” in the title as the file’s spectrum is incorrect and not of use; it can be deleted*).
 - Right click on file → Open with → “OpenOmnicsFiles”

The spectrum should now be visible in the Omnics application.

6. To save the file to the computer; copy and paste the signature icon to a folder of choice; rename the file as desired.

Appendix C

Scanning Electron Microscopy coupled with Energy Dispersive X-Ray Spectroscopy (SEM/EDX): Standard Operating Procedure (SOP)

The following SOP was devised to enable repetitive sample analysis for reliable results:

1. Mount the stones using plasticine directly onto a holder as seen in figure C1.



Figure C1: Two of each stone; rubies, sapphires and emeralds mounted on the chamber holder using a grey Plasticine® substance.

NB: make a note of the position of each stone, as once the holder is placed into the chamber the picture on screen is black and white.

2. Once the stones are firmly mounted, place the holder onto the stage in the chamber and secure the door
3. Manually adjust the Z height of the stage up and down till required height is achieved
4. Using a 10x magnification, locate a position on the table facet of the stone focussing on a flat surface using the control box
5. Once the desired location is acquired, use a 50x magnification to view the surface, making sure the camera is focussed on an area free from impurities and grooves
6. Conduct analysis by controlling the data acquisition time for 90 seconds using the Vista™ software

7. Repeat steps 4 to 6 for at least 3 data points on each sample in order to counter heterogeneity and to acquire an average result for each element analysed in each stone

Appendix D

Main vibrations in natural and synthetic major commercial gemstones

Table D1: Main vibrations in natural and synthetic corundum types

Stone	Type	Main Vibrations (cm ⁻¹)						
Ruby Al ₂ O ₃	Natural	w190	w223	s378	vs417	m575	mw645	m750
	Chatham Flux		vw208		s410	vw506		
	Ramaura Flux		vw207		w481			
	Knischka Flux		vw200		mw400	vw500		
	Kashan Flux		vw200		mw400	vw500		
	Verneuil Flame Fusion		vw211		m418	vw521		
	Lechleitner Hydrothermal		vw210		mw410	vw501		
	Czochralski Pulled		vw213		mw410	vw513		
	Seiko Zone		vw209			vw506		
Sapphire Al ₂ O ₃	Natural	w187	w240	s338	vs416	mw574	mw640	m748
	Chatham Flux	w151	w226	s378	vs416		mw645	m700
					w475		mw663	
	Verneuil Flame Fusion			s378	vs417	mw575	mw644	m745
	Lechleitner Hydrothermal			s370	vs410		mw637	m745
	Czochralski Pulled			s378	vs417	mw575	mw644	m750
Seiko Zone			s378	vs416				

vs = very strong; s = strong; m = medium; mw = medium weak; w = weak; vw = very weak (peak intensities). Raman shifts reproducible to ±5

Table D2: Main vibrations in natural and synthetic emerald types

Stone	Type	Main Vibrations (cm ⁻¹)											
Emerald <i>Be₃Al₂(SiO₃)₆</i>	Natural		<i>mw</i> 320 <i>mw</i> 395	<i>vw</i> 498		<i>vs</i> 685	<i>mw</i> 760			<i>vs</i> 1067			<i>mw</i> 3598 <i>w</i> 3608
	Flux		<i>w</i> 321	<i>w</i> 445		<i>w</i> 625 <i>m</i> 681	<i>s</i> 760 <i>s</i> 795	<i>s</i> 850	<i>mw</i> 980	<i>s</i> 1059 <i>s</i> 1067		<i>vs</i> 1570 <i>vs</i> 1590	
	Hydrothermal	<i>w</i> 286	<i>s</i> 318 <i>s</i> 392	<i>mw</i> 419 <i>mw</i> 441	<i>w</i> 526 <i>w</i> 580	<i>vs</i> 682	<i>mw</i> 768		<i>w</i> 909	<i>s</i> 1008 <i>vs</i> 1065	<i>mw</i> 1241		<i>mw</i> 3374

vs = very strong; *s* = strong; *m* = medium; *mw* = medium weak; *w* = weak; *vw* = very weak (peak intensities). Raman shifts reproducible to ±5

Table D3: Main vibrations in natural spinel

Stone	Type	Main Vibrations (cm ⁻¹)			
Spinel <i>MgAl₂O₄</i>	Natural	<i>m</i> 313	<i>vs</i> 407	<i>s</i> 666	<i>s</i> 768

vs = very strong; *s* = strong; *m* = medium; *mw* = medium weak; *w* = weak; *vw* = very weak (peak intensities). Raman shifts reproducible to ±5